PROGRAMA DE PÓS-GRADUAÇÃO EM CIÊNCIAS BIOLÓGICAS:FISIOLOGIA
INSTITUTO DE CIÊNCIAS BÁSICAS DA SAÚDE
UNIVERSIDADE FEDERAL DO RIO GRANDE DO SUL - UFRGS

TESE de Doutorado

Caracterização da Função Cardiovascular em Modelo Murino de Mucopolissacaridose tipo II

Aluna
Angela Maria Vicente Tavares

Orientação
Prof. Dr. Guilherme Baldo

Porto Alegre, dezembro de 2022

INSTITUIÇÕES E FONTES FINANCIADORAS *- Este trabalho foi desenvolvido no Centro de Terapia Gênica do Centro de Pesquisa Experimental do Hospital de Clínicas de Porto Alegre (HCPA) e Laboratório de Pesquisa Cardiovascular do Depto de Fisiologia da UFRGS. O estudo foi financiado pelo Fundo de Incentivo à Pesquisa e Eventos do HCPA (FIPE), CAPES e CNPq. Todos os experimentos apresentados nesta tese estão incluídos no projeto de pesquisa aprovado pelo Comitê de Ética e Pesquisa do Grupo de Pesquisa e Pós-Graduação do Hospital de Clínicas de Porto Alegre, sob o registro nº 17-0584.*

AGRADECIMENTOS

Certa vez escrevi: “A única coisa que não nos pode ser tomado é o conhecimento...” Realmente, não pode. Mas descobrimos que ele pode ser colocado em dúvida e até desacreditado.

Vivemos em tempos tão difíceis! Tempos em que a ciência e a vida são colocadas à prova; em que a dúvida que gera o medo, se torna o medo que gera a dúvida que estimula a ignorância e, portanto, nos fragiliza de forma impiedosa e nos coloca em perigo iminente todos os dias. Fazer ciência é compromisso de fé, é promessa de muito trabalho, resiliência e parceria, pois ninguém faz um doutorado sozinho, mas a muitas mãos.

Certamente, este trabalho, como outros tantos, foi incapaz de demostrar o enorme esforço de todos os envolvidos para que pudéssemos contribuir com a ciência, de forma inequívoca. E que fique registrado que nada disso é possível sem a figura do orientador. Eu agradeço demais ao Guilherme, não apenas por proporcionar o que, de fato, nos permite fazer ciência, mas pela sua maneira de conduzir os processos. Isso não passa somente pela sua capacidade de proporcionar as ferramentas e o material necessário para pesquisa, mas também pelo cuidado que ele tem com as pessoas.

Em meio a todo este caos, esta foi a figura deste orientador, comprometido, disponível, sempre muito atento e empenhado em fazer com que tudo aconteça da melhor forma e com muita qualidade. Agradeço a ele e a todos que contribuíram para os trabalhos colocados nesta tese.

Muito obrigada!

SUMÁRIO

LISTA DE ABREVIATURAS

Arginina	Arg
Átrio Ventricular	AV
Cardiomiócito	CM
Cardiomiopatia Dilatada	CMD
Catepsinas	Cts
Catepsina B	CtsB
Catepsina D	CtsD
Catepsina K	CtsK
Catepsina L	CtsL
Catepsina S	CtsS
Célula endotelial	CE
Células musculares lisas vasculares	VSMC
Débito Cardíaco	DC
Dermatan Sulfato	DS
Dilatação da raiz aórtica	ARD
Doenças de Depósito Lisossomal	DLs
Enzima Iduronato-L-sulfatase	IDS
Enzima lisossomal α-l-iduronidase	IDUA
Espécies Reativas de Oxigênio	ROS
Estresse Crônico Leve	CMS
Estresse Oxidativo	EO
Fibrose Intersticial Miocárdica	MIF
Fosfato de Dinucleotideo de Nicotinamida e Adenina	NADPH
Fração de encurtamento	FrEnC
Fração de ejeção	FE
Glicosaminoglicanos	GAGs
Glutamina	Gln
Heparan Sulfato	HS
Hipertrofia Ventricular Esquerda	HVE
IC com Fração de Ejeção preservada	ICFEp
IC com Fração de Ejeção reduzida	ICFEr

Insuficiência Cardíaca	IC
Leucina	Leu
Matriz Extracelular	ECM
Metaloproteinases de Matriz	MMPs
Miofibroblasto	MioFB
Mucopolissacaridose Tipo I	MPS I
Mucopolissacaridose Tipo II	MPS II
N-acetilglucosamina	GlcNAc
Óxido Nítrico	NO
Proteoglicanos de HS	HSPGs
Receptores de manose-6-fosfato	M6PR
Regurgitação aórtica	RA
Regurgitação Mitral	RM
Terapia de reposição enzimática	TRE
Transplante de células-tronco hematopoiéticas	TCTH
Ventrículo Esquerdo	VE

RESUMO

A mucopolissacaridose tipo II (MPS II) ou síndrome de Hunter é uma doença genética ligada ao X, causada por mutações no gene *IDS* que codifica a enzima Iduronato-2-sulfatase (IDS). A enzima IDS é responsável pela degradação dos glicosaminoglicanos (GAGs) lisossomais, heparan sulfato (HS) e dermatan sulfato (DS). A deficiência da enzima leva ao acúmulo progressivo de GAGs nos diversos tipos celulares, afetando a estrutura e a função de múltiplos órgãos e tecidos. Os desfechos cardiovasculares são comumente observados em pacientes com MPS II, sendo uma das principais causas de morbimortalidade entre estes pacientes. Tendo em vista as várias alterações cardíacas apresentadas e o fato de que as terapias existentes possuem baixa eficácia sobre os danos resultantes da doença no sistema cardiovascular, a caracterização dessas modificações em modelos animais tem grande relevância. O modelo animal murino de MPS II reproduz o fenótipo mais grave da doença, o que corresponde à forma neuronopata da MPS II. Os camundongos MPS II (knockout para enzima IDS) têm sido amplamente utilizados para avaliar a ocorrência de distúrbios em órgãos e tecidos afetados pela deficiência da enzima, como doenças neurológicas e esqueléticas. Entretanto, as alterações cardiovasculares e sua progressão, nestes animais, não são totalmente conhecidas. Portanto, o objetivo deste trabalho foi caracterizar as alterações cardiovasculares presentes no modelo animal de MPS II em diferentes momentos, explorando possíveis mecanismos fisiopatológicos. Para tanto, foram realizadas análises bioquímicas, histológicas e funcionais do músculo cardíaco e principais valvas e artérias. Foram encontradas anormalidades funcionais nos tempos avaliados, 6, 8 e 10 meses de idade que incluíram dilatação cardíaca e aórtica e também redução do débito cardíaco e da Fração de Ejeção. Análises histológicas mostraram quebra de elastina na artéria aorta, desarranjo das fibras musculares e presença de vacúolos no tecido cardíaco. As análises bioquímicas mostraram ainda que a atividade de catepsina B, uma protease lisossomal, bem como outras catepsinas, estavam aumentadas no tecido cardíaco. Os resultados deste trabalho levaram a conclusão de que os desfechos cardiovasculares da MPS II podem ser observados a partir dos 6 meses de idade e são progressivos. Além disso, o modelo mimetiza os desfechos cardiovasculares da MPS II, semelhantes ao observado em seres humanos portadores da doença.

Palavras-chave: mucopolissacaridose tipo II, dilatação de raiz de aorta, fração de ejeção, doenças cardiovasculares, glicosaminoglicanos.

ABSTRACT

Mucopolysaccharidosis type II (MPS II), or Hunter syndrome is an X-linked genetic disorder caused by mutations in the IDS gene, that codifies the Iduronate-2-sulfatase enzyme (IDS). The cause of MPS II is the IDS enzyme deficiency, involved in the degradation of glycosaminoglycans (GAGs) heparan and dermatan sulfate. This deficiency leads to progressive GAGs accumulation in different cell types, affecting multiple organs and tissues. Cardiovascular outcomes are commonly observed in patients with MPS II, being one of the main causes of morbidity and mortality in adults. In view of the various cardiac alterations presented in MPS II and the fact that existing therapies have low efficacy on the damage resulting from the disease in the cardiovascular system, the characterization of these modifications in animal models is of great relevance. MPS II (IDS knockout) mice have been widely used to assess the occurrence of disorders in organs and tissues affected by IDS enzyme deficiency, such as neurological and skeletal diseases, however, the follow up of the cardiovascular manifestations progression in these animals still is not fully known. Therefore, the goal of this study was to characterize the cardiovascular abnormalities in the MPS II mouse model at different time points. Biochemical, histological, and functional analyzes of the cardiac muscle and main valves and arteries were performed. Functional abnormalities were found at 6, 8 and 10 months of age in MPS II mice, which included cardiac and aortic dilatation, reduced cardiac output, and decreased ejection fraction. Histological analyzes showed a breakdown of elastin in the aorta artery, disarrangement of fibers and presence of vacuoles in the cardiac tissue. Biochemical analyzes showed that cathepsin B, a lysosomal protease, was increased in the cytosolic compartment outside cardiomyocyte lysosomes. In conclusion, we have demonstrated that the deleterious cardiovascular outcomes can be observed from 6 months of age and are progressive. In addition, the animal model used was mimetic to the effects and outcomes of MPS II observed in humans with regard to cardiovascular changes.

Keywords: mucopolysaccharidosis type II, aortic root dilation, ejection fraction, cardiovascular diseases, glycosaminoglycans.

1. **INTRODUÇÃO**

1.1 As Doenças Cardiovasculares e o Remodelamento Cardíaco

1.1.1 As doenças Cardíacas e a Disfunção Lisossomal

Um sistema cardiovascular incompetente, independentemente da causa, tem consequências deletérias importantes para o organismo. O miocárdio pode sofrer alterações intrínsecas, como distúrbios elétricos e comprometimentos estruturais e funcionais, ambos provocando adaptações patológicas, que podem evoluir para insuficiência cardíaca (IC). No último quarto de século, houve um enorme progresso na pesquisa genética que definiu muitas das causas moleculares das cardiomiopatias. Mais de mil mutações foram identificadas em muitos genes com ontologias variadas, indicando diversas moléculas e vias de sinalização que podem causar cardiomiopatias hipertrófica, dilatada, restritiva ou arritmogênicas (Elliott et al. 2008).

O rearranjo ou remodelamento frente a um insulto cardíaco é uma resposta do órgão perante a necessidade de manutenção do débito cardíaco (DC), frente as adaptações hemodinâmicas secundárias a eventos celulares e moleculares, uma vez que a perda da capacidade de bomba no miocárdio implica em redução do fluxo de oxigênio, necessário ao organismo como um todo (Braunwald 2013). Neste sentido, vários são os mecanismos patogênicos que levam ao remodelamento cardíaco, entre os quais se incluem a estimulação neuro-humoral excessiva, ciclo anormal do cálcio dos miócitos, apoptose acelerada, ativação de citocinas inflamatórias, estresse oxidativo, ativação proteolítica, autofagia, proliferação excessiva ou inadequada da matriz extracelular (MEC) e fibrose intersticial miocárdica (MIF) (Konstam et al. 2011).

No contexto celular, a manutenção do equilíbrio dinâmico e homeostático deste ambiente faz parte das funções constitutivas das organelas celulares. Devido a sua característica ubíqua, alterações na estrutura dos lisossomos, por exemplo, levam ao desenvolvimento de muitas doenças, incluindo as doenças cardiovasculares (Chi, Riching, e Song 2020). De fato, alterações na função lisossomal da célula muscular cardíaca são notadamente associadas à maioria das doenças cardíacas e a patogênese da IC (Wang e Robbins 2014). É válido notar ainda que as alterações lisossomais, não necessariamente, são apenas descritivas

de sua estrutura, pois doenças genéticas que afetam o seu conteúdo também demonstram ser interveniente na sua capacidade funcional (Gatica e Klionsky 2017). Isto posto, também foi observado que, sob certas condições, a alta atividade lisossomal também é deletéria. A hiperativação da função do lisossomo tem sido implicada em diversas complicações cardiovasculares. Um exemplo disso está vinculado a função das catepsinas (Cts) lisossômicas. As Cts lisossômicas são um subgrupo de proteases de cisteína composto por 11 membros (catepsina B, C, F, H, K, L, O, S, V, X e W). Elas contribuem com outras hidrolases ácidas na degradação lisossomal de substratos celulares. Sob certas condições patológicas, tanto o nível de expressão, quanto a localização subcelular dessas Cts podem mudar, tornando-as morbígeras. O aumento da expressão das Cts têm sido associado a uma variedade de condições e de doenças como estresse, remodelamento cardíaco e IC (Blondelle et al. 2015; Lutgens et al. 2007). A expressão de CtsS e CtsK foi aumentada no miocárdio de roedores hipertensos e em humanos com IC induzida por hipertensão (Cheng et al. 2006). CtsD elevada foi encontrada no plasma de pacientes após infarto do miocárdio (IM) (Naseem et al. 2005). Em um estudo de ensaio clínico, a CtsB sérica mais alta, foi associada a um risco aumentado de um desfecho composto de eventos cardiovasculares específicos ou mortalidade por todas as causas em 4.372 pacientes com doença coronariana estável (Wuopio et al. 2018). Estudos realizados pelo nosso grupo mostraram aumento da atividade colagenolítica da CtsB, com consequente redução do colágeno na aorta e no tecido cardíaco em modelo murino de mucopolissacaridose tipo I (MPS I) (E.A. Gonzalez et al. 2018). Uma vez que essa protease é liberada especificamente por macrófagos, em condições patológicas, atuando na redução do colágeno, sugerimos que este mecanismo poderia estar envolvido na perda da capacidade funcional observada nestes animais (Baldo et al. 2017; E.A. Gonzalez et al. 2018; Schuh et al. 2020). Sabidamente, os macrófagos residentes compõem uma variedade de órgãos e tecidos, onde são determinantes críticos do comportamento celular. No coração, uma população de macrófagos tem um efeito notável na patogênese das doenças cardiovasculares (Bajpai et al. 2018). Vários estudos sustentam que a CtsB tem um papel no remodelamento da MEC e na patogênese da doença cardiovascular em pacientes com cardiomiopatia isquêmica e dilatada (CMD) (Schenke-Layland et al. 2009). A presença de macrófagos *per se* é indicativa de mudança no ambiente, onde um aumento no pH

ácido pericelular pode resultar na realocação dos lisossomos. O pH pericelular ácido também aumenta a secreção de CtsB no espaço extracelular. Além disso, a liberação de CtsB na MEC induz a ativação de metaloproteinase de matriz (MMP-9), a qual contribui para o remodelamento da MEC (Radosinska, Barancik, e Vrbjar 2017; Riaz et al. 2020). De fato, a CtsB secretada pode contribuir para a degradação da MEC no coração e artéria aorta de animais com MPS I, o que pode levar a um quadro de IC. Apesar do caráter progressivo da doença cardiovascular encontrado nos animais MPS I, observamos que a fração de ejeção (FE) destes animais, aos 6 meses de idade, ainda estava preservada, embora outros parâmetros indicassem perda de contratilidade e dilatação da câmara ventricular esquerda, indicando dilatação cardíaca (Baldo et al. 2017; E.A. Gonzalez et al. 2018).

1.2 As Doenças de Depósito Lisossomal - DLs

1.2.1 O papel dos lisossomos na maquinaria celular

Os lisossomos são geralmente considerados como o compartimento final das vias endocíticas, onde a carga capturada está sujeita à degradação via hidrolases ácidas (Luzio, Pryor, e Bright 2007). Os lisossomos são organelas em constante estado dinâmico, responsáveis pela quebra e reciclagem de várias macromoléculas celulares, como ácidos nucléicos, lipídios, proteínas e carboidratos, e uma variedade de substratos complexos, incluindo glicosaminoglicanos e esfingolipídios, trazidas do ambiente extracelular e capturadas por meio de mecanismos de endocitose, fagocitose e autofagia (Doherty e McMahon 2009; Ravikumar et al. 2009). A função catabólica dos lisossomos é realizada por meio da ação conjunta de aproximadamente 60 hidrolases ácidas distintas, que pertencem a diferentes famílias de proteínas, como glicosidases, sulfatases, peptidases, fosfatases, lipases e nucleases (Bajaj et al. 2019). As substâncias são entregues ao lisossomo para degradação, via fusão com endossomos tardios (material extracelular) ou autofagossomos (material intracelular), além da membrana plasmática, o que lhes confere um papel central na comunicação célula-célula e célula-matriz extracelular, resposta à infecção e consequente manutenção da homeostase celular, um processo que é mediado por

SNARE (receptor de proteína ativadora do fator N-etilmaleimida solúvel) e proteínas Rab (proteínas de tráfego e fusão). Eles funcionam como centros metabólicos que controlam a detecção de nutrientes, homeostase de aminoácidos e íons e sinalização de cálcio (Platt et al. 2018).

O lisossomo têm função essencial no processo de autofagia que regula os mecanismos fisiológicos e patológicos do sistema cardiovascular. Durante o processo de autofagia, os componentes citoplasmáticos direcionados para degradação são envolvidos por uma membrana em rápida expansão chamada fagóforo. A expansão e maturação do fagóforo levam ao sequestro da carga dentro de vesículas de membrana dupla (autofagossomos) que finalmente se fundem com o lisossomo. Uma vez que a fusão é concluída, a membrana autofagossômica interna é degradada dentro do lisossomo, onde lipases e hidrolases ácidas, incluindo catepsinas B, D e L (CtsB, CtsD e CtsL) degradam a carga, gerando moléculas essenciais, como os aminoácidos, que podem ser transportados de volta ao citosol para serem reciclados pela célula (Gatica et al. 2022).

A proteína transmembrana lisossomal multi-spanning SLC38A9 parece ser o transportador central responsável pela reciclagem de aminoácidos do lúmen lisossomal para o citosol (J. Jung, Genau, e Behrends 2015; Rebsamen et al. 2015; Wang et al. 2015b). SLC38A9 detecta arginina (Arg), que desempenha um papel modulador no efluxo lisossomal de glutamina (Gln) e leucina (Leu) e outros aminoácidos essenciais para o citosol. O efluxo de aminoácidos dependente de SLC38A9, a qual é detectada pela mTORC1, ativada pelos próprios aminoácidos, gerando um feedback negativo que finalmente inibe a autofagia (Gatica et al. 2022). A MTORC1 é uma serina/treonina quinase que auxilia na regulação da homeostase celular, em resposta a muitos estímulos, como estado nutricional e nível de energia (J. Jung et al. 2015). A autofagia é essencial para o sistema cardiovascular, pois sua função de degradar proteínas mal dobradas e organelas danificadas contribui de sobremaneira para o desenvolvimento cardíaco normal (Gatica et al. 2022).

1.2.2 Deficiência da função lisossomal

As DLs são erros hereditários (inatos) do metabolismo que afetam a função do lisossomo. Os DLs compreendem um grupo de aproximadamente 70 distúrbios monogênicos do catabolismo lisossomal, a maioria dos quais são

herdados como traços autossômicos recessivos, embora três sejam ligados ao X. Esses distúrbios são causados por mutações em genes que codificam proteínas lisossômicas, tais como glicosidases lisossomais, proteases, proteínas integrais de membrana, transportadores, modificadores ou ativadores de enzimas. Mutações em genes que codificam proteínas lisossômicas afetam estas proteínas, resultando em mau funcionamento lisossômico e acúmulo gradual de substratos dentro do lisossomo (Marques & Saftig 2019; Parenti et al. 2021).

Aproximadamente 1.300 genes estão envolvidos na função lisossomal; muitos distúrbios monogênicos foram descritos, incluindo 50 deficiências enzimáticas, que podem ser subclassificadas de acordo com o tipo bioquímico de material armazenado. De fato, os distúrbios de deficiência enzimática podem ser agrupados de acordo com o material armazenado e incluem esfingolipidoses, gliproteinoses, mucopolissacaridoses e doença de armazenamento de glicogênio (Platt et al. 2018). O acúmulo de substratos dentro dos lisossomos pode iniciar uma cascata de efeitos secundários, levando a danos celular irreversíveis, morte celular e consequente disfunção e degeneração do órgão-alvo (Parenti, Medina, e Ballabio 2021; Platt et al. 2018).

As DLs são tradicionalmente classificadas de acordo com as propriedades químicas do substrato acumulado. Individualmente, cada um desses distúrbios é raro. No entanto, sua prevalência cumulativa é relativamente alta, quando comparada com outros grupos de doenças raras. A prevalência é estimada em aproximadamente 1 em 8.000 nascidos vivos (Parenti et al. 2021). Várias DLs possuem um protocolo clínico específico e a identificação e tratamento precoces têm impacto direto no seu prognóstico, o que estimula os gestores de saúde a inclusão das DLs mais prevalentes na avaliação-diagnóstica de triagem neonatal (Platt et al. 2018).

1.2.3 As Mucopolissacaridoses - MPS

As MPS são um conjunto heterogêneo de doenças monogênicas de depósito lisossomal caracterizadas pela deficiência total ou parcial de enzimas envolvidas em rotas de degradação de grandes moléculas de açúcares como os GAGs. A depender da deficiência enzimática relacionada à degradação de GAGs, diferentes compostos não-degradados acumulam-se no interior dos lisossomos. Os GAGs

têm papel fundamental na maquinaria celular e, seu acúmulo nos lisossomos leva a alterações em funções críticas celulares, observadas em vários órgãos e sistemas (Fecarotta et al. 2020). Esse acúmulo altera a composição das membranas, com impacto direto no tráfico e fusão de vesículas, alterações na autofagia, perturbações da função mitocondrial e estresse oxidativo, com consequente desregulação de vias de sinalização, o que impacta diretamente na função do organismo (Figura 1) (Parenti et al. 2021).

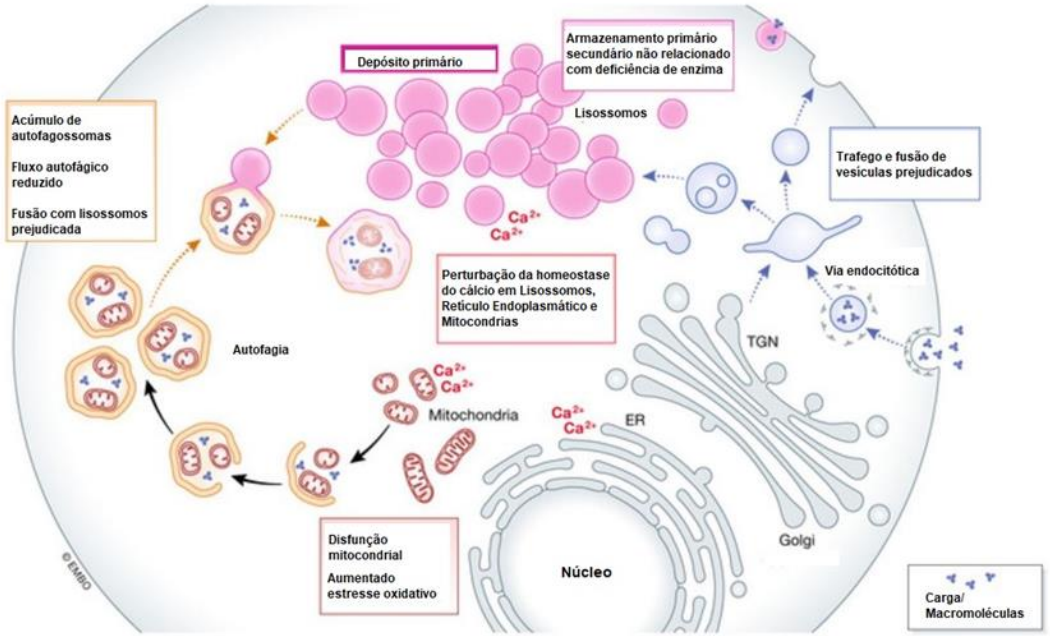

Figura 1: Mecanismo fisiopatológico geral das MPS - Alterações celulares decorrentes do acúmulo de glicosaminoglicanos nas mucopolissacaridoses. *Adaptado de Parenti G, 2021* (Parenti et al. 2021).

O acúmulo de GAGs observado nas MPS pode afetar diferencialmente múltiplos tecidos e órgãos, especialmente nos sítios específicos de atuação destas macromoléculas, sendo considerado a principal causa de sintomas graves, resultando na perda de independência e morte prematura dos pacientes (Fecarotta et al. 2020).

Um exemplo disso é a MPS III, onde o principal GAG acumulado é o heparan sulfato (HS), o qual possui papel fundamental para as funções cerebrais. Por esta razão, o fenótipo de pacientes com MPS III é majoritariamente neurológico. Outras MPS, como a MPS I e II acumulam além do HS, o dermatan sulfato (DS), gerando, além do fenótipo neurológico, alterações mais pronunciadas em outros órgãos, como o miocárdio e a vasculatura (Cross et al. 2022; Fecarotta et al. 2020).

Por acumularem os mesmos GAGs, ambas as doenças apresentam semelhanças e diferenças metabólicas e clínicas importantes. Tanto na MPS I, quanto na MPS II, os pacientes compartilham manifestações fenotípicas características, incluindo alteração da estatura, hérnias inguinais e umbilicais, hidrocefalia, perda auditiva, características faciais grosseiras, abdome protuberante com hepatoesplenomegalia, alterações cardiovasculares e envolvimento neurológico (Hampe et al. 2021). Por outro lado, acredita-se que algumas das dissemelhanças entre MPS I e MPS II possam ser atribuídas às diferenças entre as porções expostas dos GAGs, parcialmente degradados, nessas duas condições, com potencial de ativar diferentes processos celulares (Gaffke et al., 2020).

A idade de início dos sintomas geralmente é determinada pela quantidade da atividade enzimática residual, que é governada pelas mutações genéticas específicas (Platt et al. 2018). As manifestações compartilhadas por MPS I e II geralmente se desenvolvem mais cedo em crianças com MPS I, com fenótipo grave, em comparação à MPS II (Hampe et al. 2021). As principais características de cada tipo de MPS podem ser conferidas de forma resumida na tabela 1.

Tabela 1. Características principais das mucopolissacaridoses.

MPS	Enzima	GAG Acumulado	Gene	Sinais Clínicos
I	Alfa-L-iduronidase	Dermatan e Heparan Sulfato	IDUA	Transtorno cognitivo, degeneração da retina, opacidade da córnea, miocardiopatia, organomegalia.
II	Iduronato-L-sulfatase	Dermatan e Heparan Sulfato	IDS	Transtorno cognitivo, face dismórfica, miocardiopatia, organomegalia.
III*	Heparan-N-sulfatase Alfa-N-acetilglucosaminidase Alfa-glucosamina-N-acetiltransferase N-acetilglucosamina-6-sulfatase	Heparan Sulfato	SGSH NAGLU HGSNAT GNS	Retardo mental, deterioração cognitiva progressiva, hiperatividade, disfunção motora.
IV*	Galactosamina-6-sulfato-sulfatase Beta-galactosidase	Queratan e condoitrin sulfato Queratan sulfato	GALNS GLB1	Displasia esquelética, disfunção motora, hiperflexibilidade articular, opacidade da córnea. Não apresentam transtorno cognitivo.

VI	N-acetilgalactosamina-4-sulfatase (ou Arilsulfatase-6)	Condroitin sulfato, dermatan sulfato	ARSB	Displasia esquelética, disfunção motora, cifose, defeito cardíaco, opacidade da córnea. Não apresentam transtorno cognitivo.
VII	Beta-glucoronidase	Dermatan e Heparan sulfato	GUSB	Hidropsia fetal, hepatomegalia, displasia esquelética, opacidade da córnea, retardo mental.
IX	Hialuronidase	Ácido hialurônico	HYAL1	Alterações articulares, baixa estatura.

Abreviaturas: GAG- glicosaminoglicano. * A Mucopolissacaridose III possui 4 subtipos (A-D) e a IV possui 2 subtipos (A e B). *Adaptado de Suarez-Guerreiro JL, 2016.*

1.3 A Mucopolissacaridose Tipo II

1.3.1 Aspectos Gerais

Diferente da maioria dos outros distúrbios de armazenamento lisossomal que possuem herança autossômica recessiva, a MPS II é uma doença genética ligada ao sexo, herdada em um padrão ligado ao X. Esta doença se manifesta predominantemente em homens, com alguns casos esporádicos relatados em mulheres portadoras. A MPS II é causada pela deficiência da enzima Iduronato-2-sulfatase (IDS), responsável pela degradação dos GAGs lisossomais (Hampe et al. 2021). A deficiência da enzima IDS e, consequente diminuição da sua atividade, resulta no acúmulo intracelular e extracelular dos GAGs HS e DS, o que causa hipertrofia lisossomal e um aumento no número de lisossomos nas células (Hampe et al. 2021; Hashmi e Gupta 2022). Os GAGs estão presentes em todo o organismo, pois são uma parte essencial da matriz extracelular (MEC). A falta de turnover de GAGs na MEC afeta as funções celulares, como adesão celular, endocitose, tráfego intracelular de diferentes moléculas, equilíbrio iônico intracelular e inflamação (Hampe et al. 2021).

Segundo Semyachkina e colaboradores, as variações genéticas resultam em diferentes fenótipos da MPS II, dos quais, os dois fenótipos principais são “grave” e “atenuado”. Pelo fato dos pacientes com a forma grave sofrerem alterações neurológicas, o fenótipo grave também é chamado de neuronopata, o que confere a forma atenuada a descrição de não-neuronopata (Semyachkina et al. 2019). Embora a forma mais atenuada não apresente retardo mental, as

alterações somáticas estão presentes e são progressivas, pois a expectativa de vida pode chegar até a idade adulta. Infelizmente, a maior parte dos pacientes, cerca de 60%, possui o fenótipo grave, para os quais as mutações mais prevalentes incluem deleção total do gene, bem como certas mutações que levam a códons de parada prematuros ou alterações em sítio de *splicing* (p.R443X, p.G374sp) (Brusius-Facchin et al. 2013; Froissart et al. 2002).

Na forma mais grave da doença, as alterações no sistema nervoso podem incluir retardo no desenvolvimento motor, prejuízo cognitivo e hidrocefalia, além do retardo mental progressivo. Assim como em outras MPS, entre os sintomas somáticos estão características faciais grosseiras, infecções respiratórias, opacidade de córnea e perda de audição, deformidades esqueléticas, hepatoesplenomegalia, rigidez articular, hérnias umbilicais e inguinais e cardiomiopatia (Menkovic et al. 2019). Isto posto, reconhecidamente, a MPS II é o mais variável e abrangente dos tipos de MPS, o que coloca em questão o termo “doença atenuada”, pois pacientes com doença neurocognitiva menos grave (não neuronopata) podem ainda exibir sintomas somáticos graves. Segundo Hampe e colaboradores, o fato da doença envolver um amplo espectro de características cognitivas e somáticas, distinguir em dois fenótipos separados pode não ser precisa (Hampe et al. 2021). Sendo assim, o fenótipo dos pacientes com MPS II pode ser variável e com manifestações clínicas diferentes, cujos sintomas iniciam logo após o nascimento e a progressão é rápida. Segundo Khan e colaboradores, embora os sintomas ocorram precocemente, as características clínicas da MPS II geralmente se tornam aparentes entre dois e quatro anos de idade (Khan et al. 2017). Os pacientes mais gravemente afetados sobrevivem apenas até a segunda década de vida, enquanto os pacientes menos gravemente afetados podem sobreviver até a quinta ou sexta década de vida (Ramírez-Hernández et al. 2022).

Embora a maioria dos desfechos cardiovasculares possam ocorrer, primariamente, por ação direta do acúmulo de GAGs, distúrbios que ocorrem em outros órgãos podem contribuir de sobremaneira para o comprometimento cardíaco. Um exemplo disso é o desfecho cardíaco provocado pela apneia obstrutiva do sono, a qual faz parte de distúrbios relacionados ao sistema ventilatório, cujas manifestações são frequentes em todos os tipos de MPS. As causas subjacentes são diversas e compreendem anormalidades respiratórias e do sistema nervoso central (SNC). Distúrbios respiratórios do sono, como apneia

obstrutiva do sono e hipoventilação noturna, podem surgir em pacientes com obstrução das vias aéreas superiores e/ou com alterações na mecânica respiratória. A apneia do tipo central (considerada decorrente de disfunção do centro respiratório na medula) foi descrita, principalmente, em paciente com MPS II (Rapoport e Mitchell 2017). A apneia obstrutiva do sono, de forma geral, já é um fator de risco importante para a progressão da IC, o que torna plausível sugerir que os pacientes com MPS II evoluam para quadros mais graves de IC, quando apresentam disfunção em outros sítios, como o trato respiratório (Berger et al. 2013; Tulebayeva, Sharipova, e Boranbayeva 2020).

1.3.2 A Enzima Iduronato-2-sulfatase - IDS

A enzima IDS é codificada pelo gene *IDS*, localizado no braço longo do cromossomo X (locus - Xq28); consiste em 9 exons e tem um comprimento de 28,3kb. A IDS é a primeira enzima envolvida no catabolismo de HS e DS e normalmente hidrolisa os grupos 2-sulfato das unidades L-iduronato 2-sulfato destes GAGs (Maccari et al. 2022). Como parte da degradação de GAGs lisossomais, a função biológica da IDS é hidrolisar grupos sulfato ligados ao oxigênio (O) na posição C-2 da extremidade não redutora terminal de resíduos de ácido L-idurônico (IdoA) em DS e HS (Mohamed et al. 2020). A IDS faz parte de um conjunto de enzimas, cujas ações ocorrem sequencialmente, portanto, qualquer alteração na atividade de uma delas resulta no comprometimento do processo de degradação lisossomal dos GAGs (Fecarotta et al. 2020).

A redução da atividade da enzima é resultado de diferentes mutações encontradas no gene IDS, que pode causar os sinais clínicos apresentados em pacientes com MPS II. Enzimas defeituosas podem ser geradas por variantes *nonsense, frameshift, missense* e outras mutações genéticas, que podem levar a manifestações patogênicas (Kosuga et al. 2016). Um total de seiscentas e trinta e sete mutações no gene IDS foram descritas e identificadas no *Human Gene Mutation Database* envolvendo 322 *missense/nonsense*, 59 mutações de *splicing*, 1118 pequenas deleções, 49 pequenas inserções, 14 pequenos *indels*, 51 deleções grosseiras, 4 inserções/duplicações brutas e 20 rearranjos complexos (https://www.hgmd.cf.ac.uk/ac/gene.php?gene=IDS), segundo dados acessados em 05 de novembro de 2022.

1.3.3 Aspectos Gerais dos Glicosaminoglicanos

Mucopolissacarídeos ou glicosaminoglicanos (GAGs) são moléculas de açúcar de cadeia longa que consistem em unidades repetidas de dissacarídeos. Os GAGs diferem quanto ao tipo de hexosamina e açúcar não nitrogenado, pelo grau de sulfatação e posição em que são sulfatados, bem como o tipo de ligação glicosídica inter e intradissacarídica. São encontrados na superfície celular da maioria dos tecidos e na MEC. Podendo ainda apresentar-se livres ou ligados a proteínas (Farrugia et al. 2018).

A MEC cardiovascular é uma malha complexa de proteínas e açúcares estruturais e não estruturais, subdivididos em glicoproteínas, proteoglicanos e glicosaminoglicanos presentes em miócitos cardíacos e células vasculares (Rienks et al. 2014). A falta de renovação de GAGs na MEC afeta funções celulares, como adesão celular, endocitose, tráfego intracelular de diferentes moléculas e equilíbrio iônico intracelular (Hampe et al. 2021). Além disso, as porções de GAGs estão entre os principais componentes de MEC conhecidos por apoiar, proteger e desencadear a atividade de moléculas informativas, incluindo fatores de crescimento, citocinas e outros garantidores da homeostase do tecido. Alterações dos componentes da MEC como consequência de patologias, lesões teciduais ou envelhecimento podem, assim, afetar a integridade tecidual dos órgãos, como coração e vasos (Huynh et al. 2012).

1.3.4 O Heparan Sulfato - HS

O HS é um GAG formado por um polissacarídeo linear sulfatado que consiste em uma estrutura simples de dissacarídeos repetidos, N-acetilglucosamina (GlcNAc) e ácido glicurônico ou ácido idurônico. O HS também funciona como um componente de proteoglicanos (proteoglicanos de HS, HSPGs) (Li e Kusche-Gullberg 2016a; Minami et al. 2022). Grandes cadeias de HS são primeiro degradadas em fragmentos menores por uma endo-β-glicuronidase (heparanase), seguida por uma degradação sequencial perfeitamente ordenada, com uma unidade de monossacarídeo por vez, a partir da extremidade não redutora (Dreyfuss et al. 2009; Wu et al. 2021).

O HS é amplamente expresso na membrana celular e na MEC, participando efetivamente dos processos biológicos que incluem adesão célula-célula e transdução de vias de sinalização intracelular (Song et al. 2022). O extenso remodelamento que ocorre na MEC, durante a progressão da doença cardíaca de diferentes etiologias tem sido estudado e uma avaliação do remodelamento pós-infarto do miocárdio (IM) em ratos que receberam terapia de transferência gênica com fator de crescimento endotelial vascular, imediatamente após o insulto, mostrou aumento do HS, e uma clara regulação negativa da heparanase (Mataveli et al. 2009).

Um estudo que mostrou o efeito do estresse crônico leve (CMS) em componentes não fibrilares da MEC do tecido miocárdico mostrou que o HS em tecido ventricular esquerdo aumentou nos corações do grupo CMS em 35,3%, em comparação com os camundongos controle. Além disso, as alterações no perfil de GAGs miocárdicos estavam associadas ao aumento da expressão de mRNA do marcador inflamatório interleucina 6 (IL-6) e da espessura da parede miocárdica (Luong et al. 2021). De fato, o HS foi identificado como um importante regulador da inflamação cardíaca e da fibrose, modulando a sinalização intracelular através da ligação a moléculas sinalizadoras com suas cadeias polissacarídicas.

Por ser expresso na MEC, o HS é um componente crítico do tecido fibrótico, intimamente associado à expressão de colágeno dos fibroblastos cardíacos. Esses resultados enfatizaram o papel potencial do HS na fibrose cardíaca, como por exemplo na cardiomiopatia dilatada (CMD), um tipo de cardiomiopatia caracterizada pela dilatação das cavidades ventriculares e função sistólica prejudicada (Song et al. 2022). O HS também tem papel relevante na vasculatura; um estudo que utilizou enzimas para degradar seletivamente os componentes do glicocálice da superfície de células endoteliais aórticas mostrou que a depleção de HS bloqueou a produção de óxido nítrico (NO) induzida por cisalhamento (Pahakis et al., 2007). Assim, HS também pode ser considerado crítico na regulação da proliferação de células musculares lisas vasculares (VSMC) e determinação do tamanho do vaso (Adhikari N, 2010).

1.3.5 O Dermatan Sulfato – DS

As cadeias de DS consistem em unidades dissacarídicas alternadas,

compostas por resíduos de N-acetil-D-galactosamina (GalNAc) e ácido L-idurônico (IdoA) com 50-200 repetições, construídas por glicosiltransferases e epimerase específicas. O DS é formado pela epimerização de qualquer um dos resíduos de ácido glicurônico em ácido idurônico (Silbert e Sugumaran 2002). As características do DS, como comprimento da cadeia, colocação do ácido idurônico e posição do grupo de sulfatação, são variáveis, o que torna a estrutura do DS complexa. As funções fisiológicas do DS ocorrem por meio da sua interação com moléculas efetoras, como fatores de crescimento, fatores de crescimento de fibroblastos (FGFs) e colágeno.

Os papéis cruciais do DS têm sido demonstrados no desenvolvimento tecidual da cútis, vasos sanguíneos e osso através da construção da MEC e sinalização celular. Embora o DS e os proteoglicanos-DS (DSPGs) desempenhem um papel indispensável em vários eventos biológicos, eles também têm sido implicados em vários distúrbios como tumorigênese, infecções e doenças cardiovasculares (Mizumoto e Yamada 2022; Trownbridge e Gallo 2002). Alguns estudos experimentais sustentam o papel do DS no remodelamento cardíaco após IM, demonstrado pelo aumento da expressão de DS em cicatrizes miocárdicas de cães e ratos (Rienks et al. 2014). Em um estudo realizado pelo nosso grupo de pesquisa mostramos que o DS estava aumentado no tecido cardíaco de camundongos MPS I (Schuh et al. 2020).

1.3.6 Alterações Cardiovasculares nas MPS

Nas mucopolissacaridoses, mesmo que as mutações genéticas observadas não sejam específicas do sistema cardiovascular, direta ou indiretamente, este sistema pode ser comprometido (Cohn et al. 2000). Anomalias cardíacas tem sido relatadas em todos os tipos e subtipos de MPS, com exceção da MPS IX, com potencial risco de causar morte súbita, devido a distúrbios arritmogênicos, morte por oclusão coronariana (infarto) e IC (Poswar et al. 2019). Entre as manifestações cardiovasculares encontradas nas MPS estão a dilatação da câmara ventricular esquerda, hipertrofia cardíaca patológica, disfunção valvar (espessamento dos folhetos valvares e calcificação, podendo levar a estenose ou regurgitação) e dilatação da aorta (Braunlin et al. 2011; Lin et al. 2016). De fato, a dilatação da raiz da aorta é comum em pacientes com todos os tipos de MPS. Estudos mostram que

a incidência geral de dilatação da raiz aórtica (ARD) é estimada em até 40% em pacientes com MPS (Bolourchi, Renella, e Wang 2016; Poswar et al. 2019). Lin e colaboradores observaram que a dilatação da raiz da aorta (escore z> 2) foi de 47% em todos os pacientes, incluindo 66% daqueles com MPS IV, 45% daqueles com MPS VI, 28% daqueles com MPS III, 51% daqueles com MPS II, e 27% daqueles com MPS I em pacientes de Taiwan (Khan et al. 2017; Lin et al. 2021). Segundo Boffi e colaboradores, os desfechos de pior prognósticos são observados nas MPS I, II e VI. O início precoce da cardiomiopatia dilatada em pacientes com MPS é considerado uma marca registrada da forma agressiva da doença e do grau de gravidade do comprometimento cardíaco. No entanto, é interessante destacar que quando a cardiomiopatia é secundária à doença valvar, o curso clínico é diferente e menos grave e, nesses pacientes, as terapias farmacológicas podem prevenir ou reduzir o risco de IC (Boffi, Russo, e Limongelli 2018).

1.3.7 Alterações Cardiovasculares nas MPS II

Os distúrbios cardiovasculares surgem silenciosamente e contribuem significativamente para a morbimortalidade dos pacientes com MPS II. Uma coorte de pacientes italianos que avaliou a incidência global e o comprometimento do coração mostrou que 68% dos pacientes com MPS II apresentavam algum dano cardíaco (Sestito et al., 2022). No sistema cardiovascular, o acúmulo de GAGs ocorre progressivamente no músculo cardíaco, lúmen da artéria aorta e válvulas cardíacas. Um estudo recente mostrou que 63% dos pacientes com MPS II apresentaram doença cardíaca valvar. Um acúmulo anormal de GAGs, constituintes primários das válvulas cardíacas, resulta em válvulas espessas, o que, invariavelmente, leva à doença cardíaca valvar (regurgitação, prolapso e/ou estenose), principalmente das valvas mitral e aórtica que, frequentemente, podem requerer substituição (Hashmi e Gupta 2022).

Embora o percentual de pacientes com doença valvar seja alto, é importante observar que, reiteradas vezes, nos estudos cardiológicos da MPS II, tendo ou não como base a disfunção valvar, os pacientes também apresentam outras morbidades do sistema cardiovascular, como hipertrofia ventricular esquerda (HVE) e hipertensão, cujo desfecho é uma diminuição geral da eficiência cardíaca (Hashmi e Gupta 2022; Lin et al. 2016). O espessamento do septo interventricular

e a hipertrofia progressiva do ventrículo esquerdo podem levar à perda da função cardíaca, afetando a expectativa de vida dos pacientes e causando sua morte prematura (Costa et al. 2017).

Um estudo que avaliou os desfechos cardíacos em pacientes com diferentes DLs mostrou que, dos 7 pacientes diagnosticados com MPS II, 6 apresentavam sopro cardíaco, dos quais 4 tinham aumento da espessura septal; outros 4 apresentavam prolapso de mitral, dentre os quais, 2 apresentavam hipertrofia septal assimétrica (Lin et al., 2016).

O exame clínico de indivíduos com MPS costuma ser difícil devido às limitações físicas e, às vezes, intelectuais do paciente. Neste contexto, a ausência de sopros precordiais não exclui a presença de doença cardíaca. Portanto, a ecocardiografia e a eletrocardiografia são técnicas diagnósticas fundamentais para avaliação do tecido de condução, função das válvulas, dimensões e função ventricular (Braunlin et al., 2011).

Processos arritmogênicos também estão presente em paciente com MPS II (Sestito et al. 2022). Os distúrbios de condução podem ser variados; taquicardia sintomática, bradicardia assintomática, extrassístoles, batimentos ectópicos supraventriculares, fibrilação atrial e bloqueio AV de segundo grau, para o qual há indicação de implantação de marca-passo (Ayuna et al. 2020; Sestito et al. 2022). Autópsias realizadas em pacientes com MPS II mostraram a presença de grandes células vacuoladas no sistema de condução, assim como em valvas e artérias cardíacas e sistêmicas (Ayuna et al. 2020; Nagashima et al. 1976).

Recentemente, Lin e colaboradores publicaram um trabalho que avaliou 48 pacientes com MPS II; 24 pacientes neuronopáticos e 24 não neuronopáticos. Este estudo mostrou que a maioria desses pacientes, 85% (41) apresentava anormalidades cardíacas. As avaliações ecocardiográficas dos 48 pacientes revelaram que 77% (37) apresentavam valvulopatias, 35% (17) apresentavam estenose valvar e 65% (31), regurgitação. As anormalidades valvares mais prevalentes foram regurgitação mitral (RM) (54%), seguida de regurgitação aórtica (RA) (35%). Ainda, 27% (13) dos pacientes tiveram prolapso da válvula mitral, 46% (22) apresentaram septo interventricular espessado e 8% (4) hipertrofia septal assimétrica. A disfunção diastólica, avaliada pela razão reversa entre velocidade de enchimento ventricular precoce e tardia (atrial) (razão E / A <1) foi identificada em 17% (8) pacientes. Entretanto, a disfunção sistólica, avaliada pela fração de

ejeção (FE) foi encontrada em apenas 2% (1) dos pacientes. Ainda, 21% (10), 8% (4) e 6% (3) dos pacientes, respectivamente, apresentavam hipertrofia concêntrica e remodelamento, associados a um maior risco de eventos cardiovasculares subsequentes, em comparação com os outros 31 pacientes (65%) com geometria normal do VE. Não foi encontrada diferença nos parâmetros de função cardíaca entre as formas grave e leve da MPS II. Além disso, a existência e a gravidade da hipertrofia cardíaca e das valvulopatias, nesses pacientes, pioraram com o aumento da idade, corroborando com o caráter progressivo dessa doença (Lin et al. 2021).

Neste sentido, é importante destacar que, a depender do grau de comprometimento do sistema cardiovascular, quando progride para um quadro mais grave, a IC pode ser considerada de difícil manejo e com a possibilidade de intervir apenas com tratamentos paliativos (Braunlin et al. 2011).

1.4 Tratamentos para as MPS

1.4.1 Tratamentos e Intervenções Disponíveis

Existem dois tratamentos disponíveis para a MPS II, o transplante de células-tronco hematopoiéticas (TCTH) e a terapia de reposição enzimática (TRE). O TCTH fornece reposição enzimática contínua por meio de células enxertadas. Na MPS I, o TCTH tem sido usado como uma opção eficaz para mitigar os resultados neurológicos centrais adversos e também parece atenuar a doença arterial coronariana, mas os benefícios em MPS II ainda não são consensuais (Boelens et al. 2013; Guffon et al. 2009; Kubaski, Osago, et al. 2017; Peters e Krivit 2000). O tratamento com TRE melhora muitos aspectos das MPS, mas não consegue atingir o sistema nervoso, pois a enzima não ultrapassa a barreira hematoencefálica.

A capacidade da TRE em tratar distúrbios cardiovasculares, como a doença coronariana, é questionável. Morte súbita e inesperada, com evidência de estenose da artéria coronária ou infarto do miocárdio, foi relatada em pacientes com MPS I e II, após 1–2 anos de TRE (Lin et al. 2005; Sohn et al. 2012). Além disso, algumas alterações cardiovasculares, como a dilatação da aorta e espessamento das valvas cardíacas, tampouco possuem melhora após o tratamento com TRE, sendo importante que a patogênese da doença no sistema cardiovascular seja melhor

entendida, para que tratamentos alternativos e/ou complementares possam ser desenvolvidos (Braunlin et al. 2011).

Atualmente, as TREs são enzimas recombinantes que hidrolisam os ésteres 2-sulfato de resíduos terminais de sulfato de iduronato de DS e HS. A TRE, propriamente dita, é uma infusão intravenosa semanal que aproveita o receptor de manose-6-fosfato na superfície celular e lisossomal. A TER pode apresentar reações relacionadas à infusão, como urticária, pirexia e cefaleia. Do ponto de vista cardiovascular, pode causar cianose, arritmia, taquicardia, hipertensão ou hipotensão. A maioria das reações adversas são leves a moderadas, no entanto, a idursulfase pode provocar reações anafiláticas, as quais foram observadas em alguns pacientes durante as infusões. Intervenções cardiovasculares são cada vez mais comuns em pacientes com MPS, principalmente para substituição da válvula aórtica e mitral. À medida em que os pacientes com MPS tem aumento de sobrevida, a necessidade de intervenções cardiovasculares também ocorre com mais frequência, com alguns pacientes necessitando de múltiplas intervenções na idade adulta. A triagem cardíaca regular é necessária nesses pacientes porque os sintomas podem não ocorrer ou podem não ser percebidos (Muenzer et al. 2006; Sohn et al. 2013).

Entre os procedimentos cirúrgicos disponíveis realizados em pacientes com MPS estão a troca valvar mitral, aórtica e pulmonar, revascularização do miocárdio, fechamento de comunicação interventricular, ressecção de apêndice atrial gigante, aortoventriculoplastia de Konno com alargamento da raiz da aorta e transplante cardíaco (Cross et al. 2022).

1.4.2 Outros tratamentos

Vários outros tratamentos têm sido desenvolvidos de forma promissora. A terapia farmacológica com chaperonas especificamente projetadas para se ligar ao sítio ativo da proteína lisossomal inativa tem objetivo de fazer com que ela se dobre na conformação apropriada, melhorando assim sua estabilidade e atividade enzimática da proteína lisossomal (Valenzano et al. 2011). A terapia gênica envolve a injeção de um vetor que carrega uma cópia saudável do gene *IDS* e permite a expressão dentro das células em vários tecidos (Tomatsu et al. 2016). Ainda, a terapia de redução de substrato (SRT), cujo objetivo é prevenir o armazenamento,

reduzindo a biossíntese e, assim, diminuindo os GAGs acumulados, sem corrigir o defeito enzimático original (Coutinho, Santos, e Alves 2016a).

1.4.3 O Processo Delphi

Recentemente o Comitê Terapêutico do Colégio Americano de Medicina Genética e Genômica (*American College of Medical Genetics and Genomics - ACMG*) conduziu um estudo com o objetivo de gerar diretrizes de prática clínica para o tratamento da MPS II.

A partir da análise dos dados da literatura e classificação criteriosa das evidências, foi gerado um relatório detalhado e consistente no qual foram colocadas as recomendações sobre as melhores práticas para o tratamento da doença. Além disso, foram incluídos pontos de consenso e áreas onde o consenso não pôde ser obtido devido à falta de evidências de qualidade. (McBride, Berry, e Braverman 2020).

1.5 O modelo animal de MPS II

O modelo animal murino de MPS II foi criado a partir da inserção de um gene de resistência à neomicina em células-tronco embrionárias de camundongo, retirando parte do *exon 4* e o *exon 5* do gene da *IDS* murina. Resumidamente, foi feita uma interrupção direcionada do *locus* I2S de camundongo (deletados éxon 4 e parte do éxon 5) foi realizada por recombinação homóloga com um vetor de substituição contendo o gene de resistência à neomicina. Fêmeas heterozigotas para o alelo ligado ao X (IdS+/j) foram obtidas de Joseph Muenzer (Universidade da Carolina do Norte, Chapel Hill, NC, EUA) e foram cruzadas com camundongos de tipo selvagem C57BL/6 (Taconic, Germantown, NY, EUA), gerando machos de tipo selvagem (IdS+/0) e fêmeas (IdS+/+), bem como machos IdS-KO hemizigóticos afetados (IdSj/0) e fêmeas portadoras (IdS+/j). Todos os descendentes foram genotipados por análise de reação em cadeia da polimerase de DNA de corte da cauda. Todos os camundongos usados neste estudo eram machos identificados como camundongos IdS-KO hemizigóticos (j/0) ou irmãos de ninhada de tipo selvagem (WT) (+/0) (Garcia et al. 2007). Em tese, os animais MPSII (IdS-KO)

reproduzem o fenótipo mais grave da MPS II, com atividade nula da enzima IDS. Estudos prévios do grupo confirmam que estes animais reproduzem a forma neuronopata (grave) da MPS II. A forma grave observada nestes animais se caracteriza, além da atividade enzimática nula, pelas alterações nos testes de campo aberto e de campo aberto de repetição, a partir dos 6 meses de idade, sugerindo que exista um comprometimento progressivo das funções cerebrais neste modelo (Azambuja et al. 2018). Estudos posteriores do grupo confirmaram que os animais possuem neuroinflamação, com proliferação de células GFAP positivas e aumento dos níveis de interleucina-1-beta no tecido cerebral (Azambuja et al. 2020). Outros estudos demonstraram que esse modelo animal também apresenta alterações ósseas, como alteração no volume e densidade óssea (Garcia et al. 2007). Estes achados fisiopatológicos permitem que vias de sinalização alteradas sejam identificadas, e novos tratamentos sejam testados neste modelo, para posterior teste em pacientes. No entanto, não existe descrição na literatura sobre o desenvolvimento e progressão de alterações cardiovasculares nesse modelo murino. Nosso grupo tem avaliado a progressão dos distúrbios cardiovasculares e no modelo murino da MPS I, a qual também ocorre de forma progressiva, com início da perda de função cardíaca aos 6 meses de idade, embora alterações histológicas já pudessem ser observadas mais precocemente (Baldo et al. 2017; E.A. Gonzalez et al. 2018). Neste modelo, os desfechos cardiovasculares encontrados foram progressivos. Doença valvar, vacuolização, infiltração de GAGs e, consequente, espessamento de valvas cardíacas, quebras de elastina por ação de colagenases e catepsina B por estimulação da infiltração de GAGs e aumento de secreção de macrófagos na aorta, entre outros achados que, invariavelmente causam prejuízo e levam a perda da capacidade funcional do sistema cardiovascular (Baldo et al. 2012, 2017; Gonzalez et al. 2017, 2018, 2021. Por se tratar de doenças semelhantes, as quais acumulam os mesmos glicosaminoglicanos, é possível que os mecanismos responsáveis pelas alterações cardíacas na MPS II sejam similares aqueles observados na MPS I. No entanto, a investigação da ocorrência destas alterações, sua progressão e possíveis processos fisiopatológicos envolvidos no modelo murino de MPS II não foram realizadas até o momento.

2. JUSTIFICATIVA

Tendo em vista as várias alterações cardíacas apresentadas pelos indivíduos com MPS II e o fato de que as terapias existentes possuem baixa eficácia sobre os danos resultantes da doença no sistema cardiovascular, a caracterização dessas modificações em modelos animais tem grande relevância, não somente para o estudo do comportamento do órgão frente à doença e suas particularidades intrínsecas às formas apresentadas, mas para observar a evolução da doença, perante novas propostas terapêuticas. Neste contexto, vários estudos têm sido conduzidos com o objetivo de caracterizar a MPS II em modelos animais, entretanto, estes estudos não têm sido consistentes no aspecto cardiovascular, o que sugere a necessidade de maior atenção sobre os desfechos bioquímicos e funcionais da MPS II no sistema cardiovascular.

Ao analisar os animais em diferentes tempos, nós observamos que o envelhecimento poderia ser um viés de confusão para a avaliação da MPS II, uma vez que este é fator de risco para as doenças cardiovasculares. Assim, em nosso primeiro artigo, realizamos a avaliação da função cardiovascular em animais de meia idade (12 meses), comparativamente aqueles considerados adultos jovens (6 meses). A seguir, em nosso segundo trabalho observamos as alterações cardiovasculares nos animais MPS II ao longo do tempo em 6, 8 e 10 meses de idade. Os animais de 12 meses não foram utilizados no estudo da MPS II, pois esta janela temporal sofre alterações devido a idade que poderiam ser fator de confusão para a análise da função cardiovascular.

3. OBJETIVOS

3.1 Objetivo geral

O objetivo da presente tese é descrever as alterações cardiovasculares presentes no modelo animal de Mucopolissacaridose II, sua progressão e potenciais mecanismos envolvidos na doença.

3.2 Objetivos específicos

- Realizar avaliações ecocardiográficas em animais wild type (normais) e com MPS II de diferentes idades;
- Descrever alterações histológicas no tecido cardíaco dos animais;
- Quantificar quebras de elastina na aorta e verificar se ocorre dilatação progressiva da mesma ao longo do tempo;
- Analisar a progressão da doença valvar no modelo murino;
- Realizar a dosagem da atividade de catepsinas no tecido cardíaco;
- Verificar o envolvimento do estresse oxidativo no processo fisiopatológico cardíaco da MPS II;

5. ARTIGOS

5.1 Artigo 1 – Manuscrito submetido - Anais da Academia Brasileira de Ciências

Age-related Changes in Cardiovascular Performance in Wild-type C57/Bl6 Mice

Angela Maria Vicente Tavares[1], Esteban Alberto Gonzalez [2,3], Luisa Pimentel[2,3], Cristina Campos Carraro[1], Adriane Belló Klein[1], Guilherme Baldo[1,2,3]

1. Programa de Pós-Graduação em Ciências Biológicas: Fisiologia - UFRGS, Rua Ramiro Barcelos, 2600, CEP 90035-003, Porto Alegre, RS, Brazil

2. Centro de Pesquisa Experimental - Hospital de Clínicas de Porto Alegre, Rua Ramiro Barcelos, 2350, CEP 90035-903, Porto Alegre, RS, Brazil

3. Programa de Pós-Graduação em Genética e Biologia Molecular - UFRGS, Av. Bento Gonçalves, 9500, CEP 91501-970, Porto Alegre, RS, Brazil

Key words: Aging, Cardiac function, C57/Bl6 mice, ejection fraction, myocardial contractility.

Cardiovascular System of Mice, Age-related Changes

AABC Section: HEALTH SCIENCES

Guilherme Baldo*

Centro de Terapia Gênica-HCPA Ramiro Barcelos, 2350 – CEP 90035-903, Porto Alegre, RS, Brazil

Fone (51) 999955677

E-mail: gbaldo@hcpa.edu.br

ABSTRACT

Background: Age-related changes in the human heart lead to gradual loss of its pumping function and cardiovascular system efficiency. The follow-up of age-related physiological changes in cardiovascular function in mice is critical to properly designed preclinical studies. Therefore, we aimed to describe the cardiovascular effects of aging in wild-type C57/Bl6 mice. **Materials and Methods:** Male, C57BL/6 mice were the subjects of the experiments. Transthoracic echocardiography was performed in 6- and 12-month-old animals (mature adult and middle-aged, respectively). Furthermore, we also evaluated aortic tissue histology and redox balance parameters in the heart tissue. **Results**: We observed reduction in contractile parameters as left ventricular ejection fraction in middle-aged mice ($p<0.01$). The end-diastolic volume increased with age ($P<0.01$). Flow capacity and pulmonary vascular resistance were not altered with age. We observed increase in elastin breaks in the aortic tissue, despite not having a significant difference in diameter. Reactive oxygen species levels in the heart 12-months-old were increased as well ($p<0.01$). **Conclusion:** At 12 months, wild-type mice already present mild dilation and a significant reduction in cardiac function. Furthermore, the middle-aged animals presented increase of ROS in cardiac tissue and reduced aortic artery elasticity. All these parameters are wisely hallmarks of the aging process.

INTRODUCTION

In humans, it is well-documented that a decrease in functional capacity occurs with age (Scalia et al. 2010). Aging is the dominant risk factor for development cardiovascular diseases, as the prevalence of cardiovascular diseases increases drastically with increasing age (Chiao & Rabinovitch 2015). Multiple alterations are described to occur in the myocardium, including structural and functional changes, which tends to lose quality as age progresses in human beings (Strait & Lakatta 2012). The entire cardiovascular system becomes less competent with age. There is reduction in the strength capacity of the cardiac muscle, with a decrease in systolic volume and, increase of peripheral vascular resistance. The outcome of these changes can lead to chronic diseases such as atherosclerosis, arterial hypertension, and heart failure (Nair 2020). The blood vessels also suffer with aging. The organization of collagen and elastin fibers in vascular tissue are essential for the mechanical stability, which provides strength and elasticity to vessels (Heinz 2021). Histologically, aging processes in elastic fibers are characterized by fragmentation and thinning of elastin structures and may result in impaired vascular tissue elasticity (Green et al. 2014). Other fundamental factor to health throughout life is oxidative metabolism. In this context, metabolic balance is critical to cells survival of an organism and the generation of free radicals is important for proper functioning, protection, and survival of cells within physiological limits (Phaniendra et al. 2015). On the other hand, an imbalance in the generation and neutralization of reactive oxygen species (ROS) may lead to the accumulation of ROS intermediate products inducing oxidative stress and damage

to tissues (OS). Redox signaling is a known mediator of cardiac adaptation to different physiological and pathological stimuli, that act both in the acute adaptation to damage and in cardiac remodeling (Santos et al. 2016). Oxidative stress is also associated with various chronic diseases and damages such as diabetes, neurodegenerative diseases, cardiovascular diseases, obesity, DNA damage, mitochondrial dysfunction, and aging of cells (Cesselli et al. 2017, Hajam et al. 2022). Despite that, there is no comprehensive study of the aging murine heart at a time point that would resemble middle-aged individuals. To describe these early alterations is particularly important to study disease processes that lead to heart failure at later time points. Considering that the adult life phases of mice are divided in three: mature adult (3-6 months), middle age (10-15 months) and old/older (18-24 months) depending on genotype (Flurkey K et al. 2007), we decided to perform histological, metabolic and, echocardiographic analyzes in 6- and 12-month-old C57BL/6 mice aiming to look for early changes in cardiovascular function.

MATERIALS AND METHODS

Animals and study design

Male isogenic wild-type (WT) C57BL/6 mice purchased from The Jackson Lab (USA) were the subjects for the experiments. The protocol was approved by our local Ethics committee (project #160442) and all experiments followed the Brazilian legislation (Lei 11794-CONCEA) and the Guide for the Care and Use of Laboratory Animals (2008) published by the National Research Council (Washington, DC, USA). At 3 weeks of age, offspring were separated from the dam and housed (2–4 per cage). Animals were maintained in conventional housing under

a 12 h light/12 h dark cycle with controlled temperature (19 ± 1 °C) and humidity (50 ± 10%) in the experimental unit from Hospital de Clínicas de Porto Alegre.

Echocardiography

Transthoracic two-dimensional, M-mode, and Doppler imaging were performed in all animals using an EnVisor HD System, Philips Medical (Andover, MA, USA), with a 12–4 MHz transducer at 3 cm depth. Animals were anesthetized with 2% isoflurane and trichotomized. Left ventricular (LV) dimensions from end-diastolic (ED) and end-systolic (ES) transverse diameter (D) (cm) were obtained by tracing the endocardial border at three levels: basal (at the tip of the mitral valve leaflets), middle (at the papillary muscle level) and apical (distal from the papillary muscle but before the final curve cavity). Also, LV anterior wall thickness (AWT), and posterior wall thickness (PWT) at end-diastole were measured from M-mode images at three planes. The final value for each animal was obtained by taking the average of all three planes (Gao S et al. 2011). The cardiac function was obtained by LV ejection fraction (LVEF), which is the central measure of LV systolic function. LVEF is the fraction of chamber volume ejected in systole (stroke volume) in relation to the volume of the blood in the ventricle at the end of diastole (EDV). Stroke volume (SV) is calculated as the difference between EDV and ES volume (ESV). LVEF (%) = [(EDV - ESV) / EDV] × 100 (Gao S et al. 2011). Two dimensional short-axis views were used for echocardiographic estimation of left ventricular volumes. The cavity volumes were calculated using modified Simpson's rule. Both ESV and EDV were calculated by the formula: $V = (Amv + Ap_1) \times (L/3 + Ap_2/2) \times (L/3 + \pi/6) \times (L/3)^3$; A = area; Am = area of short axis at the mitral valve level; Ap_1 = area of short axis at high papillary muscle level; Ap_2 = area of short axis at low papillary muscle level; L

= the longest length from the apical four-chamber view; MV = mitral valve; PM = papillary muscle; V = volume (Mercier et al. 1982). The contractile capacity of the heart was assessed by LV Fractional Shortening (LVFS), which was calculated using the cavity diameters. LVFS was calculated by the formula: LVFS (%) = [(EDD - ESD) / EDD] ×100 (Tavares et al. 2012). The pulmonary vascular resistance index (PVR) was calculated by pulmonary flow analysis using the ratio between acceleration time and ejection time (AT/ET). Acceleration time was measured from the time of onset of systolic flow to peak pulmonary outflow velocity. Ejection time was measured as the time from onset to completion of systolic pulmonary flow. The sample volume was placed proximal to the pulmonary valve leaflets and aligned to maximize laminar flow (Jones et al. 2002). Aortic diameter was measured during diastolic flow between aortic root and ascending aorta. LV mass of heart was calculated using an adapted standard cube formula, which assumes a spherical LV geometry according to the following equation: LV mass = 1.05 × [(AWTD + EDD + PWTD)^3 - EDD^3] (Gao S et al. 2011). All analyses were performed by a trained operator blinded for experimental groups. The number of mice in each group was eight for 6-month-old mice and six for 12-month-old mice.

Histological analysis

The aorta artery was processed and embedded in paraffin according to our hospital's routine. For paraffin-embedded sections, 3 μm-thick sections of ascending aorta were stained with Hematoxylin-Eosin. Breaks in elastin fiber structure from ascending aorta sections stained with Verhoeff-van Gieson (VVG) were analyzed for at least 3 different fields in at least 4 points each using Cell^F imaging systems

software (Olympus, Europe). They were quantified as the number of breaks per nm of aorta.

Reactive Oxygen Species – ROS

ROS concentration was quantified by measuring the fluorescence brought about through the oxidation of 2',7'-dichlorofluorescin (DFCH) by the ROS present in the sample. A standard curve with known concentrations of 2′,7′-dichlorofluorescein (DCF) was used. Fluorescence was measured using excitation (480nm) and emission (535 nm) wavelengths (LS 55 Fluorescence Spectrometer, Perkin Elmer, MA, USA). The results were expressed as pmol of ROS per milligram of protein (LeBel et al. 1992).

Determination of sulfhydryl levels

For the sulfhydryl assay, 0.1 mM of 5,5'-dithiobis-2-nitrobenzoic acid (DTNB) was added to left ventricular homogenate and incubated for 30 min at room temperature. The absorbance (measuring TNB formation) was measured spectrophotometrically at 412 nm (Anthos Zenyth 200 RT, Biochrom, UK) and the results were expressed in nmol/mg protein (Aksenov & Markesbery 2001).

Statistical analysis

The data were submitted to the Shapiro–Wilk normality test. Differences between younger and middle-aged mice were compared by student's t test. Data are expressed as mean ± SD, and $P<0.05$ was considered statistically significant.

RESULTS

The average heart rate at 6 months was 353 bpm. At 12 months, it was slightly lower (309 bpm) without being statistically significant (P = 0.092). Heart internal dimensions (ESD and EDD) were significantly increased at 12-month mice (0.210 ± 0.04 versus 0.274 ± 0.02 [P < 0.01] and 0.348 ± 0.05 versus 0.398 ± 0.02 [P < 0.05], respectively). In accordance, the cavitary volumes (EDV and ESV) were increased at 12-month-old C57BL/6 mice when compared to 6-month-old mice (0.062 ± 0.01 versus 0.083 ± 0.01 [P < 0.05] and 0.028 ± 0.01 versus 0.051 ± 0.00 [P < 0.01], respectively). These alterations invariably led to reduced LVEF at 12-month-old C57BL/6 mice when compared to 6-month-old mice (56.4 ± 8.1% versus 37.5 ± 5.8 [P < 0.01]), which was also confirmed by the results of LVFS (39.75± 6.6 versus 31.15 ± 3.2 [P < 0.01]) showing significant loss of contractility in the middle-aged animals. Myocardial mass was slightly elevated at 12 months, but not different from 6-month-old mice (P = 0.47). No differences were observed in PWT (P = 0.103) or AWT (P = 0.597) between groups. PVR was not significantly different between groups (P = 0.062), and age did not affect the aortic diameter as well (P = 0.501). All echocardiographic results are summarized in Table I.

Histological analysis performed in the ascending aorta artery showed increase in elastin breaks at 12-months compared to 6 months-old mice, evidencing loss vascular elasticity (2.88 ± 0.79 versus 7.66 ± 2.01 [P = 0.012]) (Figure 2). Finally, cardiac tissue ROS levels were increased at 12-months-old compared to 6-months-old mice (7.77 ± 1.09 versus 10.52 ± 1.27 [P = 0.027]) but no difference was found between groups in sulfhydryl content (P = 0.445) (Figure 3**)**.

DISCUSSION

During the aging process, the functions of various organs and systems are already somewhat restricted, which increases the risk of chronic diseases, mainly in the cardiovascular system (Wagner et al. 2019). The aging of this system implies in several morphological and functional changes (Nair 2020). Among the possible changes, the shape of the heart starts to change from elliptical to spheroid, which is associated with reduction in contractile efficiency (Strait & Lakatta 2012). In fact, the spheroid shape of the heart refers to development of myocardial dilation (Boyle et al. 2011), which is one of the features described during the aging process and could be observed in the present study by the increase in diastolic diameter (Figure 1). The ventricular dilation led to an increase of diastolic and residual volumes and, consequently to LVEF reduction. Despite that, interestingly, the ejected volume did not differ statistically between 6-months and 12-months groups (Table I). Thus, it was possible that cardiac dilation was not compensated, demonstrating that the myocardial muscle has lost some of its responsiveness at 12-months, evidencing impairment in ventricular function and the beginning of a heart failure process. In addition, LVFS, which is considered a good parameter of myocardial contractility (Schoensiegel et al. 2011), was also reduced in 12-month-old mice. All these findings are particularly important because it characterizes a heart failure (HF) process in middle-aged mice (Table 1).

Heart failure is defined as a loss of ability to supply adequate blood volume in response to systemic demands (Braunwald E, 2015). Considering the spectrum of HF, in the present study, the mice with 12 months of age presented a LVEF that

can be classified as being from mildly reduced (HFmrEF) to reduced (HFrEF) (Bozkurt et al. 2021). Previous studies have shown that, in humans, alterations in parameters of contractility such as LVEF and LVFS are inversely correlated with age but, at later stages they are usually accompanied by alteration in LV wall thickness and/or myocardial mass, which were not observed in the present study (Salmasi et al. 2013). These results agree with classical studies involving healthy subjects without cardiovascular disease, where it was shown that the prevalence of left ventricular hypertrophy increases with age and therefore cardiac dilation is considered a hallmark of cardiac aging (Paciaroni & Fraticelli 1995, Chiao & Rabinovitch 2015).

In addition, we evaluated some parameters in cardiac tissue related to redox balance. We observed an increase of total ROS at 12-months of age, but without alterations in sulfhydryl levels, although the sulfhydryl group is susceptible to reactive oxygen species action (Rudyk & Eaton 2014). Despite not having a significant correlation between sulfhydryl and reactive oxygen species levels (data not shown), ROS is capable of degrading sulfhydryl groups (Ortiz VD et al. 2019). We hypothesized that from a biochemical point of view in this time window in middle-aged animals, ROS is not able to cause sufficient redox imbalance to reduce sulfhydryl levels, as other antioxidants must be acting to maintain redox balance (Figure 2). Finally, we did not observe alterations in aortic diameter or pulmonary vascular resistance (PVR) in animals of 12-monsth of age, although other studies suggest that aortic dilation and increase of PVR may be age-dependent (Wolak et al. 2008, Heinz 2021). However, when we evaluated the histological structure of the artery, we observed that 12-month-old mice presented significatively more elastin breaks than at 6 months of age showing early loss of vascular elasticity (Figure 3).

Once again, our results suggest that in this particular mouse strain, studying mice at 12-months can reproduce most of the early findings related to myocardial aging alterations found in humans. This suggests that, at this time point, a still initial alteration of myocardial function and vascular structure can be detected, which then can progress to a more severe state, as previously reported in older mice (Boyle et al. 2011).

CONCLUSION

Altogether, our results suggest that 12-month-old C57Bl/6 mice present early aging myocardial alterations, with ventricular dilation, loss contractile capacity, and reduction in myocardial function. These data indicate that mice with this age can be used to study early myocardial and vascular alterations related to the heart aging process. In addition, early interventions can lead to best prognostics and, the time point where observed the start of progressive loss of cardiovascular function can be an excellent window to therapeutic approaches in preclinical studies involving research about aging.

Acknowledgments

The authors would like to thank Casa Hunter, Conselho Nacional de Desenvolvimento Científico, CAPES, FAPERGS and Fundo de Incentivo à Pesquisa do HCPA for financial support. The authors declare no conflict of interest regarding the content of this manuscript.

Author contributions

Angela Maria Vicente Tavares - Main author, echocardiographic and histological evaluations, data compilation, discussion of results and formulation of hypotheses.

Esteban Alberto Gonzalez – Histological evaluations and data compilation.

Luisa Pimentel – Histological evaluations and data compilation.

Cristina Campos Carraro – Analyzes of redox balance.

Adriane Belló Klein - Analyzes of redox balance.

Guilherme Baldo - Data compilation, discussion of results and formulation of hypotheses.

Declaration of interest.

The authors report no conflicts of interest. The authors alone are responsible for the content and writing of the paper.

REFERENCES

AKERBOOM T & SIES H. 1981. Assay of glutathione disulfide and glutathione mixed disulfides in biological samples. Methods Enzymol 77: 373–382.

AKSENOV MY & MARKESBERY WR. 2001. Changes in thiol content and expression of glutathione redox system genes in the hippocampus and cerebellum in Alzheimer's disease. Neurosci Lett 302(2-3): 141-145.

BOYLE AJ, SHIH H, HWANG J, YE J, LEE B, ZHANG Y, KWON D, JUN K, ZHENG D, SIEVERS R ET AL. 2011. Cardiomyopathy of aging in the mammalian heart is

characterized by myocardial hypertrophy, fibrosis and a predisposition towards cardiomyocyte apoptosis and autophagy. Exp Gerontol 46(7): 549-559.

BOZKURT B, COATS A & TSUTSUI H. 2021. Universal definition and classification of heart failure: a report of the Heart Failure Society of America, Heart Failure Association of the European Society of Cardiology, Japanese Heart Failure Society and Writing Committee of the Universal Definition of Heart Failure: Endorsed by the Canadian Heart Failure Society, Heart Failure Association of India, Cardiac Society of Australia and New Zealand, and Chinese Heart Failure Association. Eur Heart J 23(3): 352-380.

Braunwald E. 2015. The war against heart failure: The Lancet. Lancet 385(9970): 812-824.

CESSELLI D, ALEKSOVA A, SPONGA S, CERVELLIN C, DI LORETO C, TELL G & BELTRAMI AP. 2017. Cardiac Cell Senescence and Redox Signaling. Front Cardiovasc Med 4:38.

CHIAO YA & RABINOVITCH PS. 2015. The aging heart. Cold Spring Harb Perspect Med 5(9): a025148.

FLURKEY K, CURRER JM & HARRISON DE. 2007. "Mouse models in aging research". Faculty Research 1685: 2000-2009.

GAO S, HO D, VATNER DE & VATNER SF. 2011. Echocardiography in Mice. Curr Protoc Mouse Biol 1: 71-83.

GREEN EM, MANSFIELD JC, BELL JS & WINLOVE CP. 2014. The structure and micromechanics of elastic tissue. Interface Focus 4(2): 20130058–20130058.

HAJAM YA, RANI R, GANIE SY, SHEIKH TA, JAVAID D, QADRI SS, PRAMODH S, ALSULIMANI A, ALKHANANI MF, HARAKEH S ET AL. 2022. Oxidative Stress

in Human Pathology and Aging: Molecular Mechanisms and Perspectives. Cells 11(3): 552.

HEINZ A. Elastic fibers during aging and disease. 2021. Ageing Res Rev 66:101255.

HU ML, LOUIE S, CROSS CE, MOTCHNIK P & HALLIWELL B. 1993. Antioxidant protection against hypochlorous acid in human plasma. J Lab Clin Med 121(2): 257-262.

JONES JE, MENDES L, RUDD MA, RUSSO G, LOSCALZO J & ZHANG YY. 2002. Serial noninvasive assessment of progressive pulmonary hypertension in a rat model. Am J Physiol Heart Circ Physiol 283(1): H364-H371.

KUZNETSOVA T, HERBOTS L, LÓPEZ B, JIN Y, RICHART T, THIJS L, GONZÁLEZ A, HERREGODS M, FAGARD RH, DÍEZ J ET AL. 2009. Prevalence of left ventricular diastolic dysfunction in a general population. Circ Heart Fail 2(2): 105-112.

LEBEL, CP, ISCHIROPOULOS H & BONDY SC. 1992. Evaluation of the Probe 2′,7′-Dichlorofluorescin as an Indicator of Reactive Oxygen Species Formation and Oxidative Stress. Chem Res Toxicol 5: 227–231.

LOWRY OH, ROSEBROUGH NJ, FARR AL. & RANDALL RJ. 1951. Protein measurement with the Folin phenol reagent. J Biol Chem 193(1): 265-275.

MERCIER JC, DISESSA TG, JARMAKANI JM, NAKANISHI T, HIRAISHI S, ISABEL-JONES J & FRIEDMAN WF. 1982. Two-dimensional echocardiographic assessment of left ventricular volumes and ejection fraction in children. Circulation 65(5)962-969.

NAIR N. 2020. Epidemiology and pathogenesis of heart failure with preserved ejection fraction. Rev Cardiovasc Med 21(4): 531-540.

ORTIZ VD, TÜRCK P, TEIXEIRA R, LIMA-SEOLIN BG, LACERDA D, FRAGA SF, HICKMANN A, BELLÓ-KLEIN A, LUZ DE CASTRO A & DA ROSA ARAUJO AS. 2019. Carvedilol and thyroid hormones co-administration mitigates oxidative stress and improves cardiac function after acute myocardial infarction. Eur J Pharmacol 854: 159-166.

PACIARONI E & FRATICELLI A. 1995. Left Ventricular Hypertrophy. Drugs Aging 6(4): 301-311.

PHANIENDRA A, JESTADI DB & PERIYASAMY L. 2015. Free radicals: Properties, sources, targets, and their implication in various diseases. Indian J Clin Biochem 30: 11–26.

RUDYK O & EATON P. 2014. Redox Biology Biochemical methods for monitoring protein thiol redox states in biological systems. Redox Biol 2: 803–813.

SALMASI AM, ALIMO A, JEPSON E & DANCY M. 2003. Age-associated changes in left ventricular diastolic function are related to increasing left ventricular mass. Am J Hypertens 16(6): 473-477.

SANTOS CX, RAZA S & SHAH AM. 2016. Redox signaling in the cardiomyocyte: from physiology to failure. Int J Biochem Cell Biol 74: 145–51.

SCALIA GM, KHOO SK, O'NEILL S & LAW STUDY GROUP. 2010. Age-related changes in heart function by serial echocardiography in women aged 40-80 years. J Womens Health 19(9): 1741-1745.

SCHOENSIEGEL F, IVANDIC B, GEIS NA, SCHREWE A, KATUS HA & BEKEREDJIAN R. 2011. High Throughput Echocardiography in Conscious Mice: Training and Primary Screens. Ultraschall in der Medizin - Ultraschall Med 32(Suppl 1): S124-S129.

STRAIT J & LAKATTA E. 2012. Aging-associated cardiovascular changes, and their relationship to heart failure. Heart Fail Clin 8(1): 143-164.

TAVARES AM, DA ROSA ARAUJO AS, LLESUY S, KHAPER N, ROHDE LE, CLAUSELL N & BELLÓ-KLEIN A. 2012. Early loss of cardiac function in acute myocardial infarction is associated with redox imbalance. Exp Clin Cardiol 17(4): 263-267.

WAGNER J, KNAIER R, INFANGER D, ARBEEV K, BRIEL M, DIETERLE T, HANSSEN H, FAUDE O, ROTH R & HINRICHS T. 2019. Functional aging in health and heart failure: the COmPLETE Study. BMC Cardiovasc Disord 19(1): 180.

WOLAK A, GRANSAR H, THOMSON EJL, FRIEDMAN JD, HACHAMOVITCH R, GUTSTEIN A, SHAW LJ, POLK D, WONG ND, SAOUAF R ET AL. 2008. Aortic Size Assessment by noncontrast cardiac computed tomography: normal limits by age, gender, and body surface area. JACC Cardiovasc Imaging (2): 200-209.

Table and Figure Legends

Table I. Cardiac parameters in Wild-type C57BL/6 mice at different ages.

HR- heart rate; LV - left ventricle; ESD - end-systolic diameter; EDD - end-diastolic diameter; AWT - anterior wall thickness; PWT - posterior wall thickness; ESV - end-systolic volume; EDV - end-diastolic volume; SV - SV stroke volume; LVEF- LV ejection fraction; LVSF- LV shortening fraction. AoD - aortic diameter; AT/ET ratio - acceleration time and ejection time ratio; PVR - pulmonary vascular resistance. Data are expressed as mean ± SD and were analyzed using the Student's t test. $P<0.05$ was considered statistically significant. *$P<0.05$ and **$P<0.01$. Table I - Cardiac parameters in Wild-type C57BL/6 mice at different ages.

Figure 1. Echocardiographic evaluation.

Representative image of cardiac dilation shown by increasing left ventricular cavity diameters. Note the increase of end-systolic and end-diastolic diameters at 12-months compared to 6-months-old mice. Images were obtained by echocardiography in M-mode. ESD - end-systolic diameter; EDD - end-diastolic diameter.

Figure 2. Biochemical parameters in cardiac tissue

Analyzes of ROS and Sulfhydryl levels. (A) Total ROS (reactive oxygen species) (B) Sulfhydryl levels. Values are expressed as mean ± SD from 4 animals per group. *Significantly different ($P = 0.027$). Note the increase of Total ROS at 12-months compared to 6-months-old mice.

Figure 3. Elastin Breaks

Elastin breaks in ascending aortas. Representative images of characteristic abnormalities in elastic fiber using Verhoeff–Van Gieson (VVG) staining. (A) VVG stain of aortic tissues at 6 and 12 months, where elastin fibers stain in purple color. Representative histological sections of an aorta at 6 months (n = 3) and 12 months (n = 4). (B) Quantification of elastin breaks per nm was analyzed for at 3 different fields at least 4 points each and the mean value was recorded. P = 0.012 (1000x).

Table 1

Table 1. Cardiac parameters in Wild-type C57BL/6 mice at different ages.

Parameters	6 months (n=8)	12 months (n=6)
HR (bpm)	353 ± 26	309 ± 64
ESD (cm)	0.210 ± 0.04	0.274 ± 0.02**
EDD (cm)	0.348 ± 0.05	0.398 ± 0.02*
AWTD (cm)	0.129 ± 0.02	0.124 ± 0.02
PWTD (cm)	0.117 ± 0.01	0.107 ± 0.01
LV Mass (g)	0.176 ± 0.04	0.188 ± 0.02
ESV (mL)	0.028 ± 0.01	0.051 ± 0.00**
EDV (mL)	0.062 ± 0.01	0.083 ± 0.01*
SV (mL)	0.034 ± 0.00	0.032 ± 0.01
LVEF (%)	56.4 ± 8.1	37.5 ± 5.8**
LVSF (%)	39.75 ± 6.6	31.15 ± 3.2*
AoD (cm)	0.134 ± 0.01	0.139 ± 0.02
AT/ET ratio (PVR)	0.336 ± 0.03	0.303 ± 0.07

Figure 1

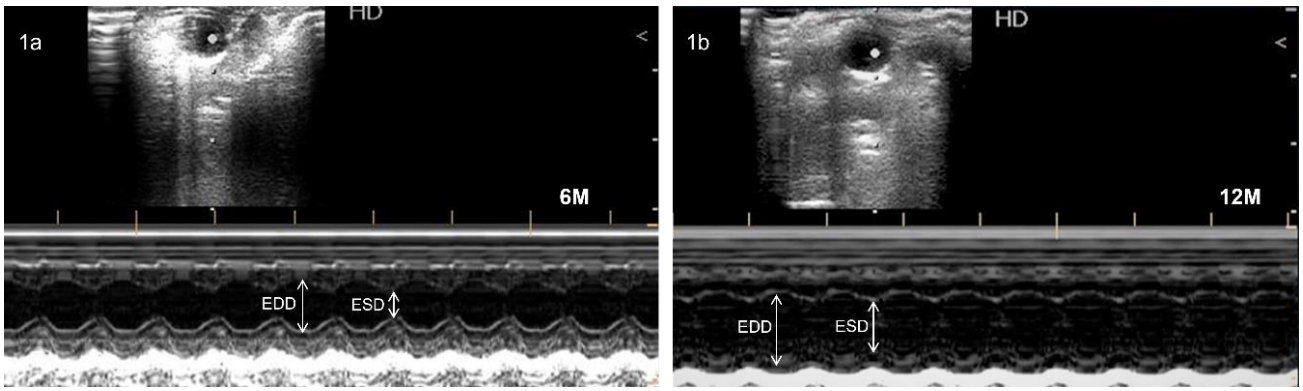

Figure 2

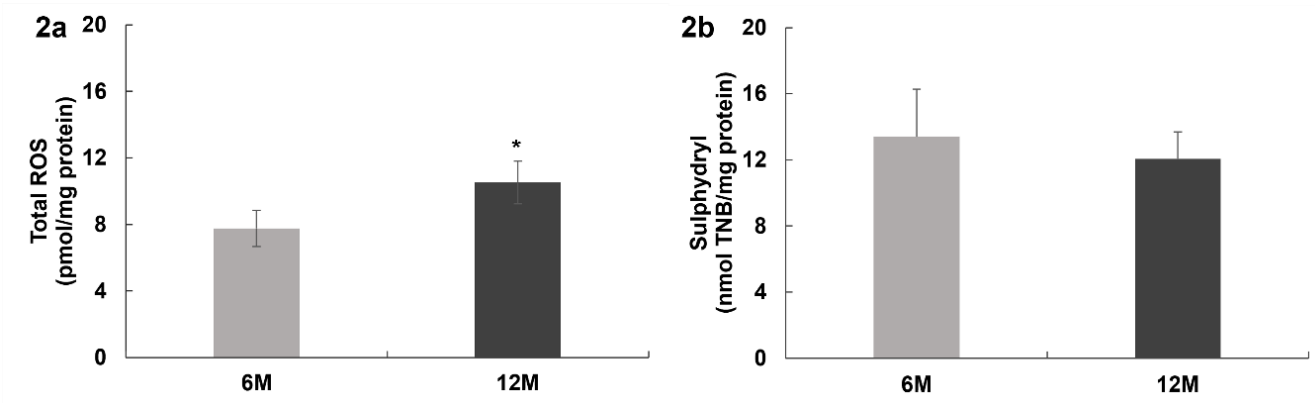

Figure 3

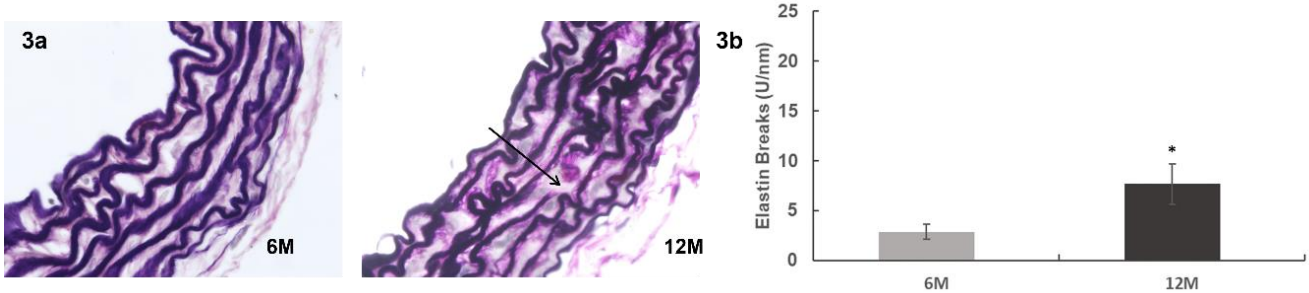

5.2 Artigo 2 - Manuscrito submetido – Cardiovascular Pathology

Characterization of heart disease in mucopolysaccharidosis type II mice

Angela Maria Vicente Tavares[1], Esteban Alberto Gonzalez [2,3], Luisa Pimentel[2,3], Guilherme Baldo[1,2,3]

1. Programa de Pós-Graduação em Ciências Biológicas: Fisiologia - UFRGS, Rua Ramiro Barcelos, 2600 - Porto Alegre, CEP: 90035-003 RS - Brazil

2. Centro de Pesquisa Experimental- Hospital de Clínicas de Porto Alegre, Rua Ramiro Barcelos, 2350 – Porto Alegre, CEP 90035-903 RS - Brazil

3. Programa de Pós-Graduação em Genética e Biologia Molecular – UFRGS Av. Bento Gonçalves, 9500 – Porto Alegre, CEP 91501970 RS - Brazil

Correspondence:

Guilherme Baldo

Centro de Terapia Gênica-HCPA

Ramiro Barcelos, 2350

90035-903

Porto Alegre, RS, Brazil

Email: gbaldo@hcpa.edu.br

Key words: Mucopolysaccharidosis type II, myocardial contractility, cardiovascular disease, glycosaminoglycans, Cathepsin.

Abstract

Mucopolysaccharidosis type II (MPSII) is a progressive lysosomal storage disease caused by mutations in the IDS gene that leads to iduronate 2-sulfatase (IDS) enzyme deficiency. The IDS enzyme catalyzes the first step of degradation of two glycosaminoglycans (GAGs), heparan sulfate (HS) and dermatan sulfate (DS). In the context of cardiovascular system, the consequences of MPSII are progressively harmful and can lead to death by cardiac heart failure. The aim of this study was to characterize the cardiovascular disease in MPSII mice. Thus, we evaluated the cardiovascular function of MPSII male mice at 6, 8 and 10 months of age, through functional, histological, and biochemical analyzes. Echocardiographic analyses showed that there is a progressive loss in cardiac function, observed through of parameters such as reduction in ejection fraction and fractional area change. Similar results were found in parameters of vascular competence, obtained by echo Doppler. Both aortic dilatation and increase of pulmonary resistance were observed at all time points in MPSII mice. The histological analyses showed increase in the thickness of the heart valves. Biochemical analyzes confirmed GAG storage on these tissues, with an elevation of dermatan sulphate in the myocardium. Furthermore, an important increase in the activity of proteases such as cathepsin B and S were found and could be related to the progressive loss of cardiac function observed in MPSII mice. Therefore, we consider that the IDS knockout mouse resembles cardiovascular abnormalities found in MPS II patients and can be used to evaluate new treatments.

1. Introduction

Mucopolysaccharidosis type II (MPSII), also known Hunter syndrome, is a rare, X-linked recessive disorder that affects predominantly males. This syndrome is characterized by iduronate-2-sulfatase (IDS) deficiency and storage of lysosomal undegraded glycosaminoglycans (GAGs). The IDS enzyme is responsible for cleaving dermatan sulfate (DS) and heparan sulfate (HS), and mutations that occur in *IDS* gene can reduce or abolish the IDS activity, leading to important clinical symptoms [1]. Approximately 600 pathogenic variants have been described in MPSII, with high genetic variation. As a result, patients may present severe or attenuated phenotypes of disease [2]. MPSII is characterized as a multisystemic disorder with a variable age of onset caused by progressive accumulation of HS and DS in most tissues and organs, such as liver, spleen, bones, joints, brain, and heart. It causes several abnormalities, including neurocognitive decline, skeletal abnormalities, hepatosplenomegaly, and cardiovascular disease. Among the most common cardiovascular alterations are valvular abnormalities, left ventricular hypertrophy, and hypertension [3]. Accumulation of GAGs progressively occurs in the ventricular muscle, artery aortic lumen and cardiac valves, mainly mitral and aortic ones. Progressive left ventricular hypertrophy and interventricular septal thickening can lead to loss cardiac function, affecting the life expectancy of patients and causing their premature death [4]. Histological abnormalities that are observed in the aortic artery wall include accumulation of GAGs, thickening, and disruption of elastin fibers. The result of these histological alterations may lead to constriction or dilation of large vessels, as the aortic artery, with aortic root dilatation (ARD) being frequently observed in MPSII patients [5]. The animal model develops most of disease features which suggests that the knockout mice (Ids-KO) may develop

cardiac abnormalities as well [6]. Different approaches have been used to treat MPSII, including enzyme replacement therapy (ERT), considered the standard of care. However, the treatment is little effective against some cardiovascular alterations, in particular the aortic and valvular abnormalities [7,8]. In the context, animal models are important tools to assess the progressive alterations of the disease. In previous studies using another MPS model (Mucopolysaccharidosis type I - MPSI) which accumulates the same GAGs as in MPSII, the decline of cardiac function could be observed only at six months of age, despite GAGs storage in the myocardium being visualized in histological sections as early as 2-month-old [9]. In other study we showed the involvement of proteases overexpression as one of the alterations that can lead to loss of cardiac function, as consequence of GAGs accumulation in MPSI [10]. Since the two disorders are very similar, we hypothesized that a somewhat similar process could happen in MPS II. Studies in the mouse model suggest that the treatment with recombinant enzyme often have limited impact on the cardiovascular aspect of the disease, corroborating the patient data's [4,11]. Garcia and colleagues conducted one of the most complete studies specifically on the murine model of MPSII, showing results about the outcome of disease, in several organs. Despite of showing histologic accumulation of GAGs in heart tissue, the study did not present data regarding loss of cardiac function of these animals, which is commonly observed in humans, possibly because of lack of data on the progression of heart alterations in the animal model [6]. Thus, the aim of this study was to perform a temporal assessment of cardiovascular function in Ids-KO animals and to look for possible mechanisms involved in the evolution of the disease.

2. Material and Methods

2.1 Experimental Groups – Animals

This study was approved by the authors' institutional ethics committee on animal experimentation (Comissão de Ética no Uso de Animais do Hospital de Clínicas de Porto Alegre - permit number #170562) and all experiments with animals were monitored by a veterinarian. Male *IDS*- mice (referred as the "MPSII") and their wild type littermate controls (*IDS*$^{+}$, referred to as the wild type, "WT" group hereafter) were the subjects for these experiments. All animals were genotyped at three weeks by PCR as previously described [12]. Animals were maintained in conventional housing under a 12-h light/12-h dark cycle with controlled temperature (19°C±1°C) and humidity (50%±10%). Mice were assessed at three different time points: 6, 8, and 10 months of age. The groups were evaluated by echocardiography, sacrificed by cervical dislocation, and its tissues collected immediately after death for further analysis. Part of ascending aorta and apical portion of the heart were flash frozen in liquid nitrogen and stored at −80°C for biochemical analysis; the basal portion of heart and other part of ascending aorta were fixed in buffered formalin 10% and processed to histologic analysis.

2.2 Echocardiographic analysis

The mice were anesthetized with isoflurane and positioned under a temperature-controlled bed. Animals were placed in the left lateral decubitus position (45° angle) to obtain the cardiac images. An EnVisor HD System (Philips Medical, Andover, MA, USA) medical ultrasound with a 12–4MHz linear transducer was used, and the images were captured by a trained operator with experience in small-animal echocardiography. To obtain better images was used at 3-4cm depth fundamental and harmonic imaging.

2.2.1 Left ventricular (LV) dimensions and functional parameters - LV diastolic and systolic transverse areas and diameters were obtained by two-dimensional tracing of the endocardial border at three levels: Basal (at the tip of the mitral valve leaflets), Medial (at the papillary muscle level), and Apical (distal from the papillary muscles, but before of the apical internal curve of LV cavity). The final value was obtained by taking the average of all three myocardial planes (**Figure 1**). The left ventricular ejection fraction (LVEF) is the central measure of LV systolic function. It is the fraction ejected volume in systole [stroke volume (SV)] in relation to the volume of the blood in the ventricle at end-diastole (EDV). Two dimensional short-axis views were used for echocardiographic estimation of left ventricular volumes. Both, residual volume [end-systolic volume (ESV)] and EDV were calculated by the formula: $V = (Amv + Ap_1) \times (L/3 + Ap_2/2) \times (L/3 + \pi/6) \times (L/3)3$; Amv – area of short axis at the mitral valve level (Basal); Ap_1 – area of short axis at high papillary muscle level (Medial); Ap_2 – area of short axis at low papillary muscle level (Apical); L – the longest length from the apical four-chamber view; mv – mitral valve; PM – papillary muscle; V – volume [13]. Stroke volume (SV) was obtained by difference between EDV and ES volume (ESV). LVEF (%) = [(EDV - ESV) / EDV] × 100 [14]. From the SV analysis it was possible to assess the cardiac output (CO), which was calculated using the equation: CO = SV × heart rate (HR) [15]. The contractile capacity of the heart was assessed by Fractional Area Change (FAC) and corroborated by CO and LVEF evaluations. To calculate the FAC, the difference between the areas at the end-diastole and end-systole was used. FAC was calculated by the formula: FAC (%) = [(EDA - ESA) / EDA] ×100. The pulmonary vascular resistance index was obtained by evaluating the blood flow through the pulmonary artery by echo-doppler. This parameter was calculated by equation: Acceleration time/ejection time (AT/ET)

[16]. Another analysis performed was the LV mass quantification, evaluated by echocardiography, that considered the anterior and posterior wall thicknesses (AWT and PWT, respectively) and was calculated using an adapted standard cube formula, which assumes a spherical LV geometry according to the following equation: LV mass = 1.05 × [(AWTD + EDD + PWTD)^3 - EDD^3] [14]. (**Table 1**).

2.3 Histopathologic analysis

The heart tissue and its valves (basal level of endocardial border) were fixed in buffered formalin and embedded in paraffin according to our hospital's routine processing methods. Thin sections (3µm) were stained with hematoxylin/eosin (H-E) and Alcian blue 1%, which stains GAGs blue. An adjacent slide was stained with Sirius red for the visualization of collagen content in the heart valves. Thin sections of ascending aorta were stained with Verhoeff-van Gieson (VVG), which stains elastin in purple. Breaks in elastin fiber structure from ascending aorta sections stained with VVG were analyzed for at least 3 different fields in at least 4 points each. They were quantified as the number of breaks per nm of aorta. Heart valve thickness was measured at 10 different points, and the average was taken and considered as the valve thickness value. Sections were analyzed by a trained researcher who was blinded to the groups. The thickness of the heart valves and breaks were measured using the computer software Cell^F.

2.4 Biochemical analyzes

2.4.1 GAG levels in heart tissue - Specific GAG levels were assessed by tandem mass spectrometry from heart tissue. GAGs were extracted after acetone precipitation. Dermatan sulphate (DS), heparan sulfate with O- or N-sulfation (HS–OS and HS–NS), disaccharides were obtained through digestion with chondroitinase B, heparitinase, and keratanase II followed by quantification through

liquid chromatography tandem mass spectrometry (LC/MS/MS) as previously described. Briefly, 10µL of extracted tissue was mixed with 90µL of 50mM Tris HCL (pH7) and added to Omega 10K filter plates (Pall Co, MI, USA) and centrifuged by 15 minutes. Samples were incubated in a shaker overnight at 37°C with 60µL of 50mM Tris HCL, 10µl of 5µg/ml of internal standard (chondrosine), 10µl of 0.6mU chondroitinase B (in BSA 1%), 10µl of 1mU heparitinase (in BSA 1%), and 10µl of 1mU keratanase II (in BSA 1%) (enzymes and IS were provided by Seikagaku Co, Tokyo, JPN) [17]. For detection, samples were injected into *Xevo TQ-S micro* Triple Quadrupole Mass Spectrometry (Waters Tech) operated in the negative ion mode with electrospray ionization. The mobile phase was a gradient elution of 148mM ammonia (solution A) to 100% acetonitrile (solution B). Specific precursor ion and product ion were 54 used to detect and quantify each disaccharide (138 HS-NS; 378.3, 175.1 HS-OS, DS) The concentration of each disaccharide was calculated using QQQ Quantitative Analysis software.

2.4.2 Elastase activity assay - For the elastase assay, samples were homogenized in buffer (100mM Tris HCl, pH 8 to 25 °C) at 0.2µg tissue/µl for heart samples or 50µl of solution for aortic samples. Elastase activity was measured using substrate N-Succinyl-Ala-Ala-Ala-p-nitroanilide (Sigma-Aldrich, USA) in a continuous spectrophotometric rate determination. Substrate solution (4.4mM SucAla3-pNA solution) was prepared in Tris-HCl buffer. The amount of product was determined by absorbance using kinetic reading and comparison with 0.02 units of elastase solution from the porcine pancreas (Sigma-Aldrich, USA). Readings were performed for 2h every 5 minutes at A410nm. The results were expressed as U/mg protein. One unit of elastase hydrolyzes 1µmol of N-Succinyl-Ala-Ala-Ala-p-nitroanilide per hour at pH 7.5 at 25°C.

2.4.3 Collagenase activity assay - For the collagenase assay, samples were homogenized in buffer (50mM Tricine with 10mM calcium chloride and 400nM sodium chloride, pH 7.5 to 25°C) at a concentration of 0.2µg/µl. Collagenase activity was measured using FALGPA substrate (1mM N-(3-[2Furyl]acryloyl)-Leu-Gly-Pro-Ala solution in buffer) (Sigma-Aldrich, USA) in a continuous spectrophotometric rate determination. The amount of product was determined by absorbance using kinetic reading and comparison with 0.2 units of collagenase solution from Clostridium histolyticum (Sigma-Aldrich, USA). Readings were performed by recording the decrease in 345nm for 2 hours every 5 minutes. The results were expressed as U/mg protein. One unit of collagenase hydrolyzes 1µmol of FALGPA per hour at 25°C, at pH 7.5 in the presence of calcium ions.

Caspase-3 activity assay – Caspase-3 activity was assessed using a fluorogenic assay. Samples were homogenized in acetate buffer and incubated with the Ac-YVAD-AMC substrate (Enzo Life Sciences, USA) at a final concentration of 25µM. Fluorescence was measured using Spectramax M3 every 5 min for 60 min at an excitation of 355 nm and an emission 460 nm using kinetic reading and comparison with 7-amino-4-methulcourmarin (AMC) standards. Results are expressed as nmol/h/mg protein.

2.4.4 Cathepsins activity assay - Twenty-four heart samples (from medial/apical portion; 6 animals per group) were homogenized (0.2mg/µL) in acetate buffer (100mM sodium acetate, 0.1% TritonX, EDTA 2.5 Mm, DTT 2.5 mM pH 7.4) for cathepsin assays. For the cathepsin B activity, 5µL of the sample was incubated with 95µL of assay buffer containing the specific substrate Z-Arg-Arg-AMC 50 µM (Enzo Life Sciences, USA - #BML-P137) in a microtiter plate at 37°C. Fluorescence was recorded using Spectramax M3 every 5 for 30 minutes at an excitation

wavelength of 355nm and an emission wavelength of 460nm. The increase in fluorescence intensity was proportional to the substrate hydrolysis, and then the total substrate consumption was calculated by comparison to the standard fluorescence of 7-amino-4-methylcourmarin (AMC), accordingly to manufacturer's instructions. Total cathepsin activity was measured using the Z-Phe-Arg substrate (Enzo Life Sciences, USA), 10 μM at pH 7.4, with the same buffer and parameters used for the CtsB assay. Inhibitors were from Calbiochem (San Diego, CA) and included CtsB inhibitor Ac-Leu-Val-Lysinal (#219385), CtsK inhibitor I [1,3-Bis (N-carbobenzoyloxy-L-leucyl) amino acetone; #219377] and CtsS Z-FL-COCHO (#219393). The inhibitors were added to some assays in final concentrations of 10, 100 or 1000nM, as indicated. The results were expressed as nmol/h/mg protein [10]. Protein content of each sample was measured by the Lowry technique for all assays [18].

2.5 Statistical analysis

Data were expressed as mean ± standard deviation (SD). Two-tailed parametric unpaired t-tests were applied for individual group comparisons between WT and MPSII mice. Two-way ANOVAs were performed for multi-group analysis followed by Tukey's multi-comparisons test. The normality test was calculated using the Shapiro-Wilk test. A $P<.05$ was considered statistically significant. All statistical analyses were performed with the Sigma Plot version 12.0 software (Systat Software Inc, USA).

3. Results

3.1 Characterization of cardiovascular function abnormalities in MPSII mice

Functional parameters were evaluated in WT (control animals) and MPSII groups at

6, 8 and 10 months of age, in 66 animals by echocardiography. Six (6) WT and four (4) MPSII mice participated of two evaluations, at 6 and 10 months, all the other animals were evaluated only once, within their specific group. The results are summarized in **Table 1**.

3.1.1 Cardiac function - In the context of MPSII disease we observed decreased ability of the cardiovascular system capacity to meet the body's demands. During echocardiographic evaluations, arrhythmogenic tracings were observed in MPSII animals at 8-months-old (n=4) and, at 10-months-old (n=5). Animals evaluated at 6-months-old did not present cardiac arrhythmia. The echocardiographic analyzes only were validated if the animals presented an intermittent arrhythmia, allowing stabilization of cardiac rhythm, during examination. After stabilization of arrhythmic phase, the exams were performed. Animals with severe arrhythmia were excluded of study (**Figure 2**). Despite there was variation in heart rate (HR) between groups, the difference was not statistically significant. Cardiac output (CO) was not altered at 6 months of age (P=0.325) but was decreased at 8 and 10 months in the MPSII groups [(P=0.001) and (P=0.005), respectively], when compared with WT groups at the corresponding time points. The increase in the dimensions of the left ventricular cavity (systolic and diastolic diameters) and consequent increase in residual volume (ESV) were determining factors for heart failure outcome observed in later times in MPSII groups. At 6 months it was observed cardiac dilation [Dd (P=0.049)]. In later times there was not statistical difference in diastolic diameter between WT and MPSII groups. The differences between WT and MPSII groups in systolic and diastolic diameters are represented in Figure 3. On the other hand, myocardial contractile capacity decreased progressively in the MPSII groups (6, 8 and 10 months), as observed in the FAC data [(P=0.023), (P=0.013) and (P=0.030)

respectively]. The LVEF is considered a gold standard measure in cardiac function evaluation. LVEF was reduced in MPSII groups at all time points evaluated. Although the animals presented decreased LVEF (P=0.023) at 6 months of age in the MPSII group, it was still considered preserved LVEF (LVEFp). The LVEF was considered reduced (LVEFr), with some degree of heart failure (HF), only at 8 and 10 months (P<0.001). The HF was a consequence of increase of residual volume (ESV) in cardiac cavity at 8 and 10 months in MPSII mice [(P<0.001) and (P=0.048), respectively]. When we evaluated the stroke volume (SV) we observed reduction this parameter only at 10 months in MPSII group (P=0.032). The EDV was not different between WT and MPSII groups, at 6, 8 or 10 months. Myocardial mass was not statistically different between groups at all evaluated time points.

3.1.2 Vascular function - Analyzes of aortic diameters showed that MPSII mice presented progressive dilation of aortic artery at 6, 8 and 10 months of age [(P=0.016), (P=0.000) and (P=0.001), respectively]. Pulmonary vascular resistance, assessed by AT/ET ratio, was increased at all time points [(P=0.038), (P=0.040) and (P=0.001), respectively] in MPSII groups (**Table 1**). Other parameters analyzed did not show important consistent alterations (data not shown).

3.2 Histological findings

3.2.1 Artery and Heart – The aorta arteries of MPSII groups were distended at 6, 8 and 10 months [average of 14μm (P=0.016) at 6 months, average of 29μm at 8 month (P=0.000) and average of 20μm at 10-month-old (P=0.001)] compared to its respective WT groups (**Figure 4: B and D**). In addition, the presence of vacuoles was observed in both tissues, artery, and heart, in the MPSII groups (**Figure 4: B, D, F and H**). Furthermore, also a loss of organization of cardiac fibers can be visualized in H–E staining. These findings were not observed in the WT groups in

the cardiac muscle and aorta artery, whose structures were intact (**Figure 4: A, C and G**).

3.2.2 Elastin breaks - Ascending aortas were stained with HE and VVG to identify and quantify elastin breaks. VVG staining showed the elastin fibers in purple and breaks were detected by its loss of continuity (**Figure 5A**). At 6 and 10 months, the MPSII groups showed significant increase in the number of breaks per nm, compared to WT groups (P=0.012 and P=0.010, respectively) (**Figure 5B**).

3.2.3 Heart Valve Thickness - The valve thickness was measured at 10 different points, and the average value was calculated. The result revealed that the cardiac valves were thickened at both time points, at 6 and 10 months evaluated in the MPSII mice (P=0.029 and P=0.015, respectively) (**Figure 6**).

3.3 Biochemical findings

3.3.1 Tissue GAGs storage - GAGs levels were assessed in the myocardium at 6 months of age (**Figure 7A**). Results show a massive increase of dermatan sulfate (DS) in MPSII group compared to WT group (P<0.001). Based on the result shown, we decided to evaluate DS at 8 months and the result was similar (P=0.006). For both time points, the dermatan was increased in MPSII group compared to its respective control group, but there was no difference in DS concentration over time when only MPSII groups were evaluated (P=0.524) (**Figure 7B**). Heparan sulphate levels were not different between groups.

3.3.2 Elastase and collagenase activity - Although we observed increased elastin breaks in MPSII mice, the total elastase activity in the ascendent aorta artery was not detectable in the conditions of this specific assay. Aortic tissue showed similar levels of collagenase activity at both time points and was not different between WT and MPSII groups [1.68±0.79 vs 1.11±0.23 (P=0.123) and 1.18±1.07 vs 1.00±0.32

(P=0.711), respectively].

3.3.3 Caspase-3 Activity - At 6 and 8 months, heart tissue had similar levels of Caspase-3 activity at both time points and was not different between WT and MPSII groups [0.27±0.07 vs 0.27±0.23 (P=0.937) and 0.14±0.04 vs 0.19±0.06 (P=0.126), respectively].

3.3.4 Cathepsins Activity - We observed that activity of total cathepsins in the cardiac tissue was substantially increased in MPSII groups to compared to its respective WT groups, at 6 and 8 months (P<0.001) (**Figure 8A**). Using the specific cathepsin B substrate we showed that its activity increased more than 200% in MPSII group at 6 months and around 500% in MPSII group at 8 months (**Figure 8B**). Aiming to identify other cathepsins that could be responsible for the increase in the activity observed using the Z-Phe-Arg substrate, we added specific inhibitors of CtsB, CtsS and CtsK to the reaction. Only the cathepsin S inhibitor was able to significantly reduce enzyme activity, showing elevation of this enzyme along with cathepsin B, which suggest elevation of multiple lysosomal cathepsins in the MPS II heart tissue (**Figure 8C** and **8D**).

4. Discussion

Absent or decreased activity of Iduronate 2-sulfatase results in excessive abnormal accumulation of GAGs dermatan (DS), and heparan sulfate (HS) in lysosomes, causing hypertrophy and increasing the number of lysosomes in the cells throughout the body [1]. In the cardiovascular system, this disease can progress to heart failure [19]. In the present work, we studied the progression of cardiovascular disease in MPSII mouse model (Ids-KO) and analyzed possible mechanisms involved in the evolution of the disease. Careful assessment of cardiac function was performed at

6, 8 and 10 months. We observed that the pump function of heart was progressively lost over time in MPS II mice, impairing the ability to meet the body's demands. The GAGs infiltration and its downstream effects are responsible for functional alterations of the valves, great vessels, conduction system and myocardium [20]. At 6 months, MPSII mice had loss of contractile capacity (FAC), presented cardiac dilation (Dd) and reduction of LVEF, but did not present cardiac arrhythmia, the CO was unchanged, and the ventricular residual volume (ESV) was not significantly altered (**Table 1 - Figure 3**). Although the LVEF has been relatively preserved (a small reduction, but within the normal range), other parameters analyzed in cardiovascular system showed deleterious alterations from 6 months of age in MPSII groups. In this time window, histological analysis showed intramyocardial vacuolization and infiltration of GAGs (pseudohypertrophy) (**Figure 4E-H**), which suggests that the initial dilation could be a compensatory response to deposition of GAGs in cardiac tissue to maintain CO at 6 months, although the myocardial thickness was not altered significatively (Data not shown) (**Table 1**). Therefore, we assume that 6 months can mark the initial phase of loss of cardiac function, in which the myocardial structure modifications not yet produced severe functional alterations. Worsened functional outcomes only appeared at later time points. At 8 and 10 months we observed that MPSII groups presented cardiac arrhythmia, impairment of CO, with consequent increase of ESV and LVEF reduction, characterizing a progressive process of heart failure (**Figure 2 and Table 1**). We also observed thickening of the heart valves (**Figure 6A and 6B**) and presence of vacuoles in valves and vessels (**Figure 4 A, B, C and D**). According to Hampe and colleagues, this finding is common in different types of MPS and about of 50% of patients with MPSII present this condition [21]. In addition, the reduced electrical

conductivity by cardiomyocytes and ventricular pseudohypertrophy were often associated with left valve defects [22]. Patients with MPSII develop thickened heart valves and regurgitation and often require valve replacement [23]. The cardiac valves were thickened in the MPSII mice from 6 months of age. We did not evaluate the pulmonary valve thickness due to their small size and difficulty of collection. However, since mitral and aortic valves were thickened in MPSII groups, we consider that a similar process could be happening at the pulmonary valve, since alterations in the PVR (AT/ET ratio reduction) were observed in MPSII groups at all time points evaluated (**Table 1**). The PVR development contributes to diastolic dysfunction and can lead to pulmonary hypertension, which was strongly associated with valvular dysfunction and accumulation of dermatan sulphate [20,24,25]. Total GAGs in cardiac tissue evaluated at 6 months showed that only DS was increased in MPSII mice compared to WT group (**Figure 7A**). From this result, we evaluated DS at 6 and 8 months and observed that DS was increased at both time points in MPSII mice (**Figure 7B**). These data are similar to results obtained in a study with MPS I mice [26]. The increase in DS levels can lead to severe impairment of cardiovascular system, usually observed in MPSII patients with the neuronopathic form of the disease [27,28]. In addition, the number of cardiovascular anomalies increases with age contributing to more serious pathophysiological consequence [29]. GAGs storage out of lysosomal environment led to dysregulation of the normal cellular processes of cardiovascular system and may lead to leakage of lysosomal enzyme to the cytoplasm [30]. Cathepsins are enzymes that primarily reside in the endosomes and lysosomes. Under conditions like inflammation, oxidative stress, and apoptosis can be localized also in other sites, as nuclear membrane, cytosol, plasma membrane, and extracellular space. Although cathepsins do not retain

optimal activity at the neutral pH of the cytosol, their proteolytic activity is known to be preserved by substrate binding and acidification of the cytosol in pathologic conditions [31,32]. We evaluated total cathepsins activity, which was markedly elevated in the heart tissue in MPSII groups at 6 and 8 months and confirmed that most of this activity was due to cathepsin B (**Figure 8A-B**). Cathepsin B was elected to analysis, despite not being a potent elastase or collagenase due to its previously demonstrated high activity in the MPS tissues and because it is active at neutral pH (although not as stable as in acidic pH) [10]. Cathepsins derived from cardiac cells can participate in the pathogenesis of cardiac injury in response to inflammation, apoptosis, and oxidative stress [33]. Our data suggest that the increase of cathepsins in cardiac tissue may also be outcomes of the highest concentration of GAG outside the lysosomal environment (**Figure 7A-B**). Studies that evaluated the role of cathepsins in cardiac tissue in MPS I mice obtained similar results [9,10]. Abnormal expression and/or activity of both lysosomal and extra-lysosomal cathepsins correlate with MPS major clinical manifestations such as neuropathology, bone and joint defects, and cardiovascular disease [34]. The inhibition assay of these enzymes demonstrated that cathepsin activity in MPSII cardiac tissue was also partially due to CtsS, another enzyme with activity at neutral pH. In the context of MPSs, the ubiquitous accumulation of GAGs also inflicts structural damage on vessels, with consequent loss of functionality. The aortic dilation (Aod) is another finding prevalent in severe MPS II patients [5]. At all time points evaluated, ascendent aorta dilation and elastin breaks were observed in MPSII mice (**Table 1**; **Figure 5A**). The elastic fiber depletion led to impairment in vascular function. Elastin breaks were found at both time points evaluated in MPSII groups, corroborating other studies of our research group that observed similar

results in MPS I disease (**Figure 5B**) [10,26]. To explain elastin breaks and aorta dilation we evaluated proteases activity (elastases and collagenases) that admittedly have contributed to degradation of vascular tissue in several disorders [9,10]. In our study there was no alteration in total elastase activity in the ascendent aorta artery, but this could be due to specific conditions for these assays (neutral pH, buffers and conditions used in the assay). In addition, both collagenase and caspase-3 activity showed no difference between the WT and MPSII groups, at 6 and 8 months, which suggests that there is no increase in apoptosis in these tissues. Previous studies demonstrated that the presence and activity (collagenolytic and/or elastolytic) of cathepsins in media conditioned by endothelial cells, smooth muscle cells, neonatal cardiomyocytes, and macrophages can be responsible for the elastin breaks and other damages that contributes to loss of vascular function [32,33]. From the literature findings and our data, we suggest that the cathepsins act on the cardiovascular system as part of mechanisms that contribute to the initiation and progression of structural damages that leads to heart failure in MPSII.

5. Conclusion

The knowledge about the cardiovascular outcomes of MPSII at different time points contributes to better understanding of disease pathogenesis and evaluation of potential treatments. In this work we demonstrated that loss of cardiac function in MPSII mice started at 6 months of age, although its global cardiac capacity was still preserved at this time. Disease progressed at later time points leading to heart failure. The MPSII mice at later times reproduces the cardiovascular events found in patients with Hunter's disease, showing the progress to heart failure and suggesting the possible mechanisms involved in this process.

Acknowledgements

This study was supported by research grants from the CNPq, FAPERGS and FIPE number #170562.

6. Bibliography

[1] Hashmi MS, Gupta V. Mucopolysaccharidosis Type II. 2022.

[2] Semyachkina AN, Voskoboeva EY, Zakharova EY, Nikolaeva EA, Kanivets I v., Kolotii AD, et al. Case report: A rare case of Hunter syndrome (type II mucopolysaccharidosis) in a girl. BMC Med Genet 2019;20. https://doi.org/10.1186/s12881-019-0807-x.

[3] Sohn YB, Choi EW, Kim SJ, Park SW, Kim SH, Cho SY, et al. Retrospective analysis of the clinical manifestations and survival of Korean patients with mucopolysaccharidosis type II: Emphasis on the cardiovascular complication and mortality cases. Am J Med Genet A 2012;158 A. https://doi.org/10.1002/ajmg.a.34371.

[4] Costa R, Urbani A, Salvalaio M, Bellesso S, Cieri D, Zancan I, et al. Perturbations in cell signaling elicit early cardiac defects in mucopolysaccharidosis type II. Hum Mol Genet 2017;26. https://doi.org/10.1093/hmg/ddx069.

[5] Poswar F de O, de Souza CFM, Giugliani R, Baldo G. Aortic root dilatation in patients with mucopolysaccharidoses and the impact of enzyme replacement therapy. Heart Vessels 2019;34. https://doi.org/10.1007/s00380-018-1242-1.

[6] Garcia AR, Pan J, Lamsa JC, Muenzer J. The characterization of a murine model of mucopolysaccharidosis II (Hunter syndrome). J Inherit Metab Dis 2007;30. https://doi.org/10.1007/s10545-007-0641-8.

[7] Fecarotta S, Gasperini S, Parenti G. New treatments for the mucopolysaccharidoses: from pathophysiology to therapy. Ital J Pediatr 2018;44. https://doi.org/10.1186/s13052-018-0564-z.

[8] Poswar F de O, Santos HS, Santos ABS, Berger SV, Souza CFM de, Giugliani R, et al. Progression of Cardiovascular Manifestations in Adults and Children With Mucopolysaccharidoses With and Without Enzyme Replacement Therapy. Front Cardiovasc Med 2022;8. https://doi.org/10.3389/fcvm.2021.801147.

[9] Baldo G, Tavares AMV, Gonzalez E, Poletto E, Mayer FQ, Matte UDS, et al. Progressive heart disease in mucopolysaccharidosis type I mice may be mediated by increased cathepsin B activity. Cardiovascular Pathology 2017;27. https://doi.org/10.1016/j.carpath.2017.01.001.

[10] Gonzalez EA, Martins GR, Tavares AMV, Viegas M, Poletto E, Giugliani R, et al. Cathepsin B inhibition attenuates cardiovascular pathology in mucopolysaccharidosis I mice. Life Sci 2018;196:102–9. https://doi.org/10.1016/j.lfs.2018.01.020.

[11] Baldo G, Mayer FQ, Martinelli BZ, de Carvalho TG, Meyer FS, de Oliveira PG, et al. Enzyme replacement therapy started at birth improves outcome in difficult-to-treat organs in mucopolysaccharidosis I mice. Mol Genet Metab 2013;109. https://doi.org/10.1016/j.ymgme.2013.03.005.

[12] Azambuja AS, Correa L, Gabiatti BP, Martins GR, de Oliveira Franco Á, Ribeiro MFM, et al. Aversive and non-aversive memory impairment in the

mucopolysaccharidosis II mouse model. Metab Brain Dis 2018;33. https://doi.org/10.1007/s11011-017-0110-5.

[13] Mercier JC, DiSessa TG, Jarmakani JM, Nakanishi T, Hiraishi S, Isabel-Jones J, et al. Two-dimensional echocardiographic assessment of left ventricular volumes and ejection fraction in children. Circulation 1982;65. https://doi.org/10.1161/01.CIR.65.5.962.

[14] Gao S, Ho D, Vatner DE, Vatner SF. Echocardiography in Mice. Curr Protoc Mouse Biol, John Wiley & Sons, Inc.; 2011. https://doi.org/10.1002/9780470942390.mo100130.

[15] Tavares AMV, da Rosa Araujo AS, Llesuy S, Khaper N, Rohde LE, Clausell N, et al. Early loss of cardiac function in acute myocardial infarction is associated with redox imbalance. Exp Clin Cardiol 2012;17.

[16] Jones JE, Mendes L, Audrey Rudd M, Russo G, Loscalzo J, Zhang YY. Serial noninvasive assessment of progressive pulmonary hypertension in a rat model. Am J Physiol Heart Circ Physiol 2002;283. https://doi.org/10.1152/ajpheart.00979.2001.

[17] Kubaski F, Osago H, Mason RW, Yamaguchi S, Kobayashi H, Tsuchiya M, et al. Glycosaminoglycans detection methods: Applications of mass spectrometry. Mol Genet Metab 2017;120. https://doi.org/10.1016/j.ymgme.2016.09.005.

[18] LOWRY OH, ROSEBROUGH NJ, FARR AL, RANDALL RJ. Protein measurement with the Folin phenol reagent. J Biol Chem 1951;193. https://doi.org/10.1016/s0021-9258(19)52451-6.

[19] D'avanzo F, Rigon L, Zanetti A, Tomanin R. Mucopolysaccharidosis type II: One hundred years of research, diagnosis, and treatment. Int J Mol Sci 2020;21. https://doi.org/10.3390/ijms21041258.

[20] Braunlin EA, Harmatz PR, Scarpa M, Furlanetto B, Kampmann C, Loehr JP, et al. Cardiac disease in patients with mucopolysaccharidosis: Presentation, diagnosis and management. J Inherit Metab Dis 2011;34. https://doi.org/10.1007/s10545-011-9359-8.

[21] Hampe CS, Yund BD, Orchard PJ, Lund TC, Wesley J, Scott Mcivor R. Differences in MPS I and MPS II disease manifestations. Int J Mol Sci 2021;22. https://doi.org/10.3390/ijms22157888.

[22] Sestito S, Rinninella G, Rampazzo A, D'Avanzo F, Zampini L, Santoro L, et al. Cardiac involvement in MPS patients: incidence and response to therapy in an Italian multicentre study. Orphanet J Rare Dis 2022;17. https://doi.org/10.1186/s13023-022-02396-5.

[23] Stapleton M, Kubaski F, Mason RW, Yabe H, Suzuki Y, Orii KE, et al. Presentation and treatments for Mucopolysaccharidosis Type II (MPS II; Hunter Syndrome). Expert Opin Orphan Drugs 2017;5. https://doi.org/10.1080/21678707.2017.1296761.

[24] Leal GN, de Paula AC, Leone C, Kim CA. Echocardiographic study of paediatric patients with mucopolysaccharidosis. Cardiol Young 2010;20. https://doi.org/10.1017/S104795110999062X.

[25] Selim L, Abdelhamid N, Salama E, Elbadawy A, Gamaleldin I, Abdelmoneim M, et al. Cardiovascular abnormalities in Egyptian children with mucopolysaccharidoses. Journal of Clinical and Diagnostic Research 2016;10. https://doi.org/10.7860/JCDR/2016/21135.8851.

[26] Schuh RS, Gonzalez EA, Tavares AMV, Seolin BG, Elias LS, Vera LNP, et al. Neonatal nonviral gene editing with the CRISPR/Cas9 system improves some cardiovascular, respiratory, and bone disease features of the

mucopolysaccharidosis I phenotype in mice. Gene Ther 2020;27. https://doi.org/10.1038/s41434-019-0113-4.

[27] Fesslová V, Corti P, Sersale G, Rovelli A, Russo P, Mannarino S, et al. The natural course and the impact of therapies of cardiac involvement in the mucopolysaccharidoses. Cardiol Young 2009;19:170–8. https://doi.org/10.1017/S1047951109003576.

[28] O'Toole D, Zaeri AAI, Nicklin SA, French AT, Loughrey CM, Martin TP. Signalling pathways linking cysteine cathepsins to adverse cardiac remodelling. Cell Signal 2020;76. https://doi.org/10.1016/j.cellsig.2020.109770.

[29] North BJ, Sinclair DA. The intersection between aging and cardiovascular disease. Circ Res 2012;110. https://doi.org/10.1161/CIRCRESAHA.111.246876.

[30] Fecarotta S, Tarallo A, Damiano C, Minopoli N, Parenti G. Pathogenesis of mucopolysaccharidoses, an update. Int J Mol Sci 2020;21. https://doi.org/10.3390/ijms21072515.

[31] Yadati T, Houben T, Bitorina A, Shiri-Sverdlov R. The Ins and Outs of Cathepsins: Physiological Function and Role in Disease Management. Cells 2020;9. https://doi.org/10.3390/cells9071679.

[32] Zhang X, Luo S, Wang M, Shi GP. Cysteinyl cathepsins in cardiovascular diseases. Biochim Biophys Acta Proteins Proteom 2020;1868. https://doi.org/10.1016/j.bbapap.2020.140360.

[33] Cheng XW, Shi GP, Kuzuya M, Sasaki T, Okumura K, Murohara T. Role for cysteine protease cathepsins in heart disease: Focus on biology and mechanisms with clinical implication. Circulation 2012;125. https://doi.org/10.1161/CIRCULATIONAHA.111.066712.

[34] de Pasquale V, Moles A, Pavone LM. Cathepsins in the Pathophysiology of Mucopolysaccharidoses: New Perspectives for Therapy. Cells 2020;9. https://doi.org/10.3390/cells9040979.

Table and Figures

Table

Table 1 – Echo findings in Wild type (control) and MPS II mice from 6 to 10 months of age

WT – Wild type group; LVEF - left ventricular ejection fraction; SV – stroke volume; EDV – end-diastolic volume; ESV - end-systolic volume; FAC – fractional area change; CO – cardiac output; Sd – systolic diameter; Dd – diastolic diameter; Aod – Aortic diameter; acceleration time and ejection time ratio; HR – heart rate. Data shown as mean ± SD for each group. $P<0.05$ was considered statistically significant.

Figures

Figure 1 - Plans used to cardiac function evaluation - schematic drawing LV diastolic and systolic transverse areas (A) (cm^2) and diameters (d) (cm) – M-mode; Basal, Medial, and Apical - endocardial border levels. The final value to systole and diastole was obtained by average of the three myocardial planes. LV – left ventricle; RV – right ventricle.

Figure 2 – Cardiac rhythm alterations in MPSII mice. Representative arrhythmogenic tracing was observed in MPSII mice from 8 to 10-months. Images were obtained by echocardiography in M-mode.

Figure 3. Cardiac diameters assessed using M-Mode. Cardiac diameters - difference between WT and MPSII groups, at all the time points evaluated.

Figure 4. Representation of arterial distention and presence of vacuoles in the ascending aorta and in the cardiac muscle. Representation of ascending aorta and cardiac tissue stained with HE. The figures show the intact tissue from an aortic artery (E and G) and heart muscle (A and C) presented in the wild type (WT) groups and the loss of organization of cardiac fibers and the presence of vacuoles observed in the MPSII groups in both tissues evaluated at 6- and 10-months-old (*400X*).

Figure 5 - Disruption of the aortic elastin. Elastin breaks in ascending aortas. Representative images of characteristic abnormalities in elastic fibers using Verhoeff–Van Gieson (VVG) staining. A) VVG stain of aortic tissues at 6 and 10 months, where elastin fibers stain in purple/dark color. Representative histological sections of an aorta at 6 months (WT, n = 3 and MPSII, n = 4) and 10 months (WT, n = 4 and MPSII, n = 9). B) Quantification of elastin breaks per nm was analyzed for at 3 different fields at least 4 points each and the mean value was recorded. P=0.012 at 6 months; P=0.010 at 10 months (*1000X*).

Figure 6 – **Heart valves**. Thickening of cardiac valves were assessed at 6-months-old and 10-months-old mice by histological analyses. A) representative images from WT and MPSII mice. B) Quantification of valve thickness at 6 months (WT, n = 3 and MPSII, n = 4) and 10 months (WT, n = 4 and MPSII, n = 3). P=0.029 at 6-months-old; P=0.015 at 10-months-old (*100X*).

Figure 7. Cardiac Tissue GAGs Storage. Cardiac tissue GAGs storage at 6 months of age (**7A**). Results show a massive increase of dermatan sulfate (DS) in

MPSII group compared to WT group (P=0.050). In evaluation of DS at 8 months the result was similar to 6 months (P=0.006). There was no difference in DS concentration over time when only MPSII groups were evaluated (P=0.524) (**7B**).

Figure 8. Activity and Inhibition of Cathepsins. Heart samples were homogenized in acetate buffer at pH 7.4 (n=6/group). Activity of total cathepsins was performed with the non-specific substrate Z-Phe-Arg-AMC. CtsB activity was determined using CtsB specific substrate Z-Arg-Arg-AMC. MPSII mice samples were incubated with inhibitor of CtsB, CtsK and CtsS at the indicated concentration (n=3). The activity is relative to the initial activity without adding inhibitor compared to uninhibited activity (P< 0.05). Cts – Cathepsins.

Table 1

Age	6 months			8 months			10 months		
Groups / Parameters	N (n=8)	MPSII (n=10)	P	N (n=9)	MPSII (n=8)	P	N (n=10)	MPSII (n=8)	P
LVEF (%)	56.43±9.1	46.09±8.3	.023	50.11±8.7	28.50±7.6	.000	45.91±4.7	28.27±6.0	.000
SV (mL)	0.034±0.0	0.029±0.0	.200	0.029±0.0	0.022±0.0	.099	0.032±0.0	0.019±0.0	.032
EDV (mL)	0.062±0.0	0.063±0.0	.881	0.059±0.0	0.074±0.0	.090	0.067±0.0	0.068±0.0	.783
ESV (mL)	0.028±0.0	0.034±0.0	.234	0.029±0.0	0.053±0.0	.000	0.035±0.0	0.049±0.0	.048
FAC (%)	34.44±8.0	24.78±8.1	.023	30.32±8.5	20.10±6.2	.013	31.39±8.2	23.40±5.2	.030
CO (mL/min)	12.09±2.7	10.52±2.9	.325	10.60±2.1	5.84±2.3	.001	10.95±3.7	5.70±1.1	.005
Sd (cm)	0.21±0.0	0.25±0.0	.060	0.25±0.0	0.27±0.0	.290	0.24±0.0	0.29±0.0	.036
Dd (cm)	0.35±0.0	0.39±0.0	.049	0.38±0.0	0.41±0.0	.325	0.38±0.0	0.40±0.0	.184
Mass (g)	0.18±0.0	0.14±0.0	.072	0.18±0.0	0.20±0.0	.473	0.17±0.0	0.20±0.0	.290
Aod (cm)	0.13±0.0	0.14±0.0	.016	0.12±0.0	0.15±0.0	.000	0.13±0.0	0.15±0.0	.001
AT/ET ratio	0.34±0.0	0.26±0.0	.038	0.34±0.0	0.28±0.0	.040	0.34±0.0	0.24±0.0	.001
HR (bpm)	353±25	372±35	.206	363±37	338±23	.175	364±58	341±50	.400

Figure 1

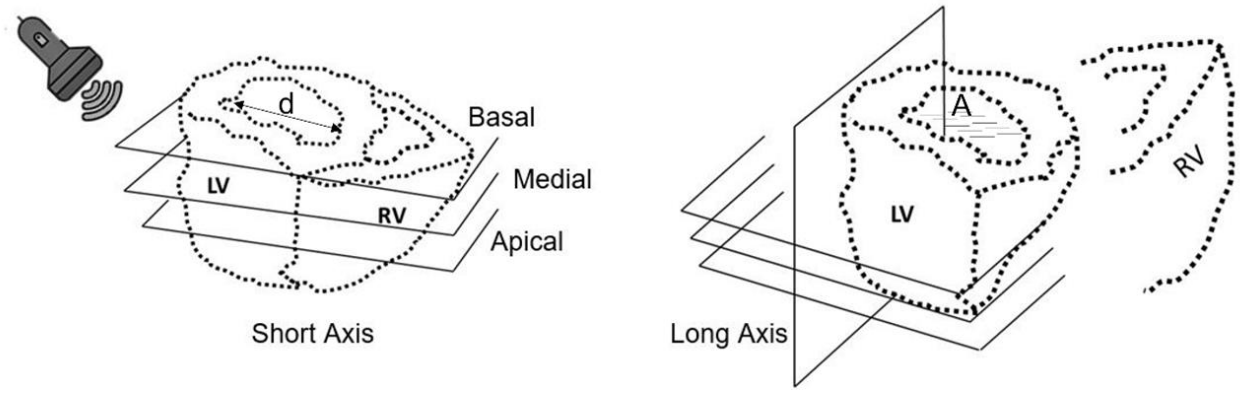

Figure 2

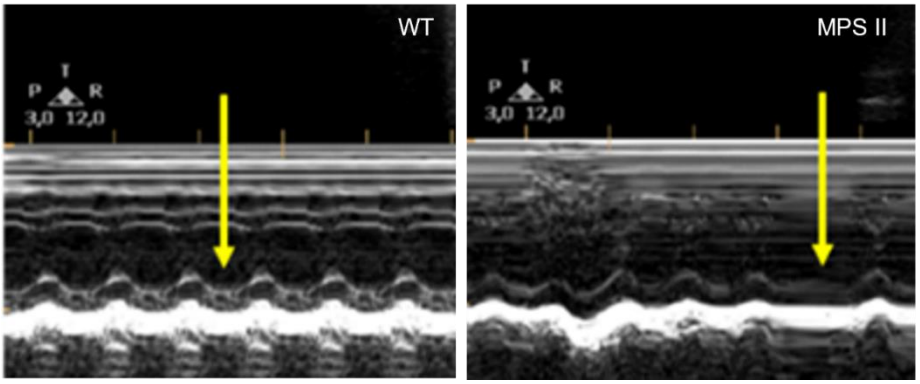

Figure 3

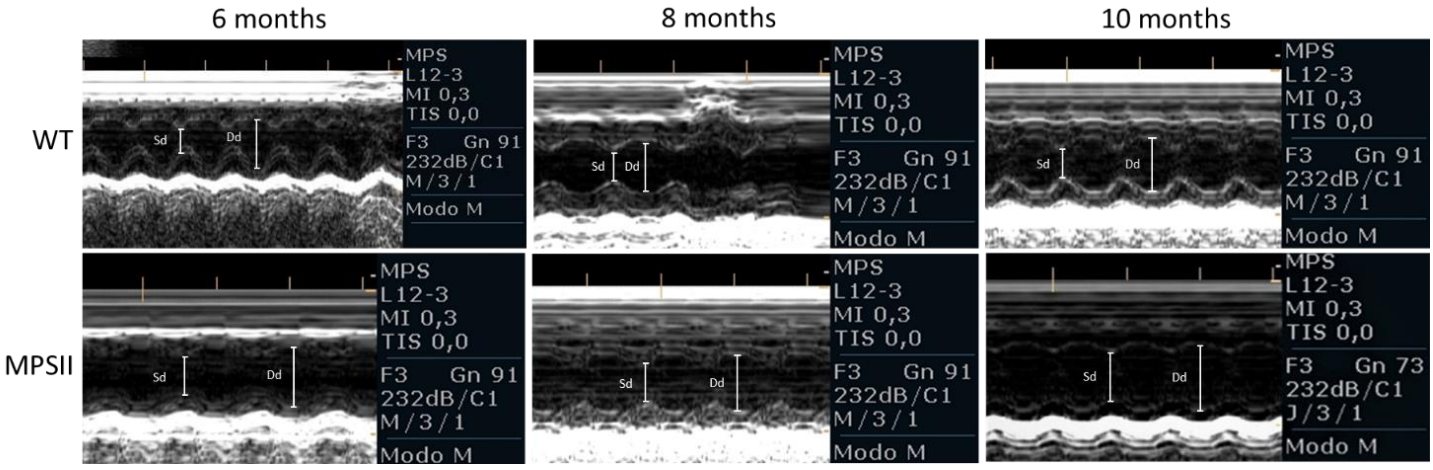

Figure 4

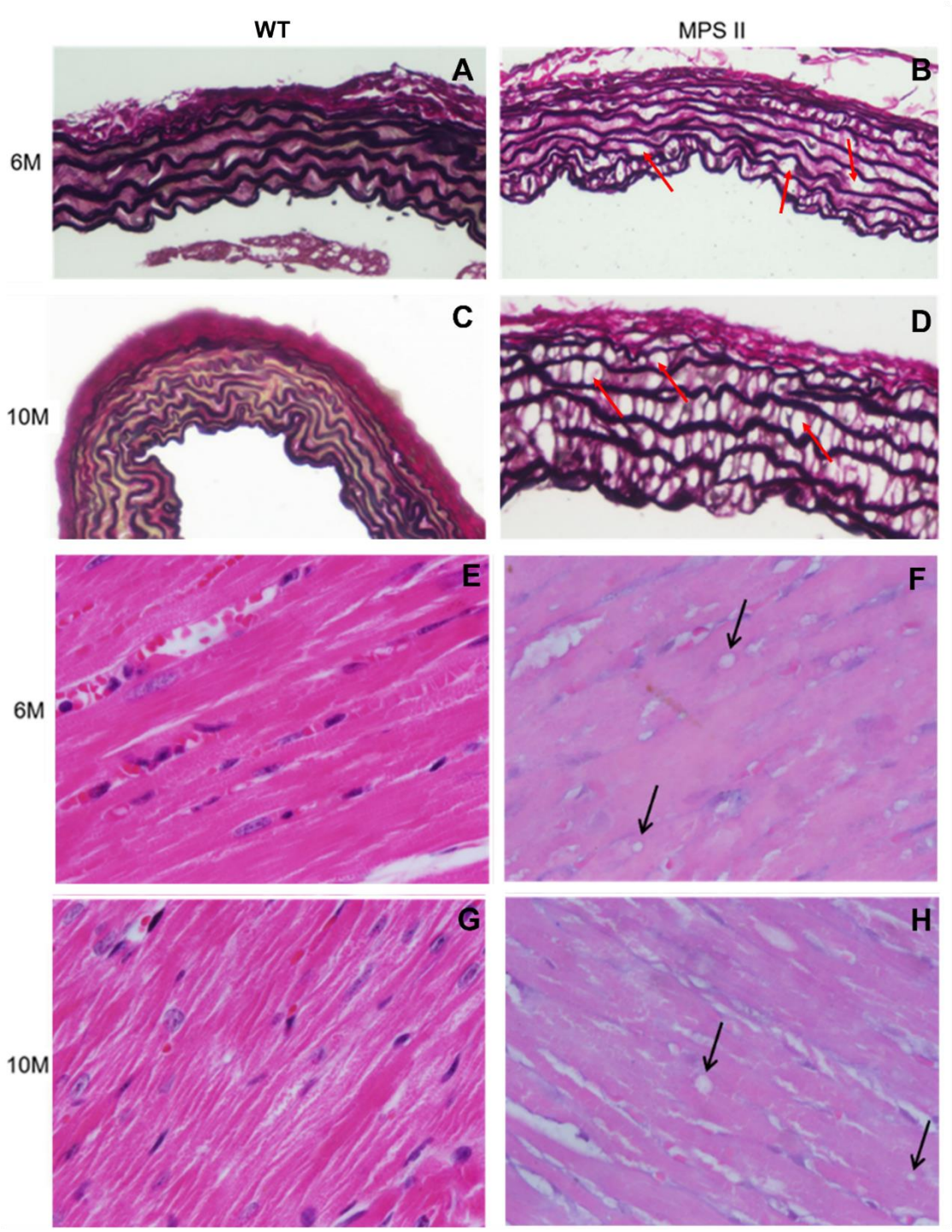

Figure 5

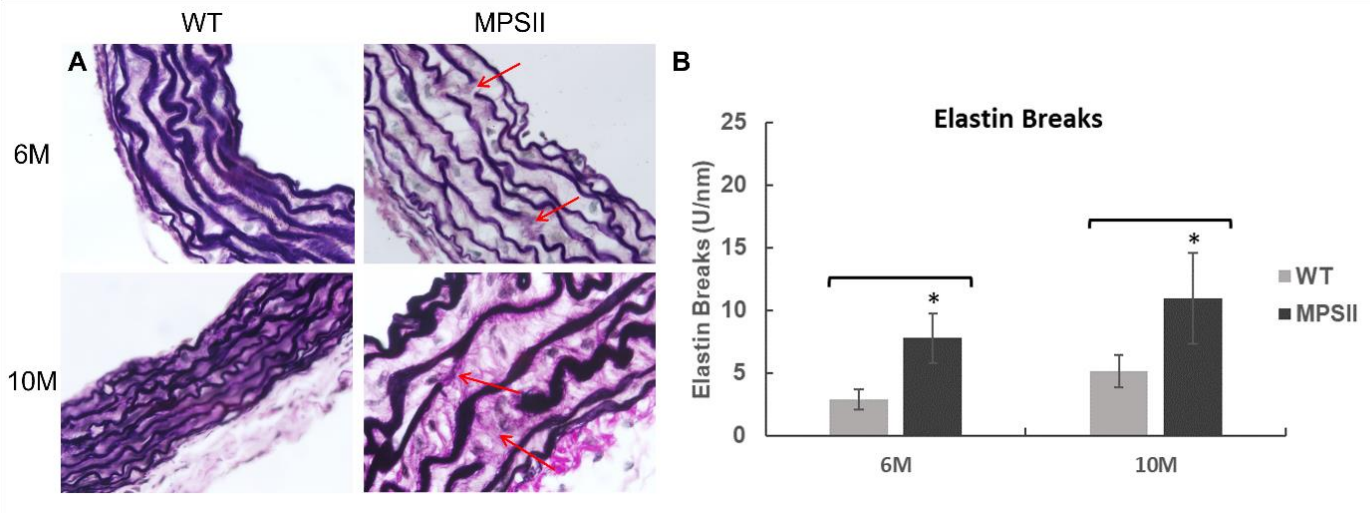

Figure 6

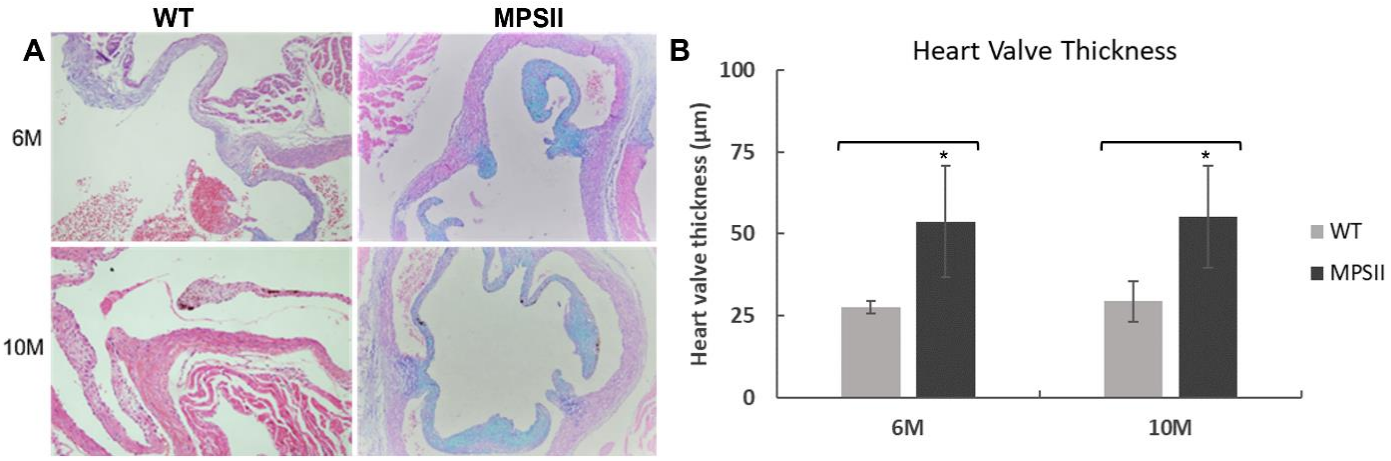

Figure 7

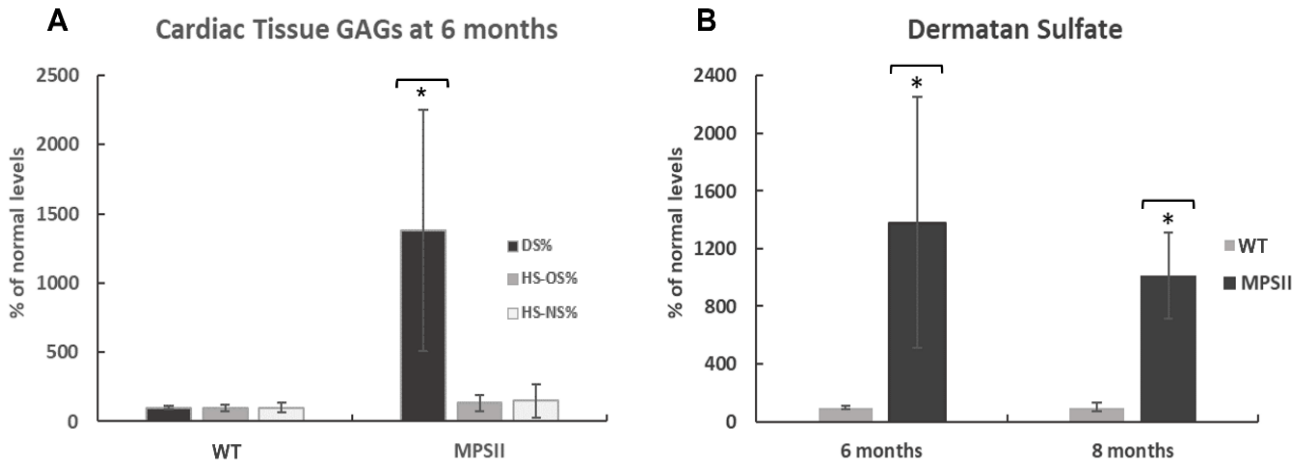

Figure 8

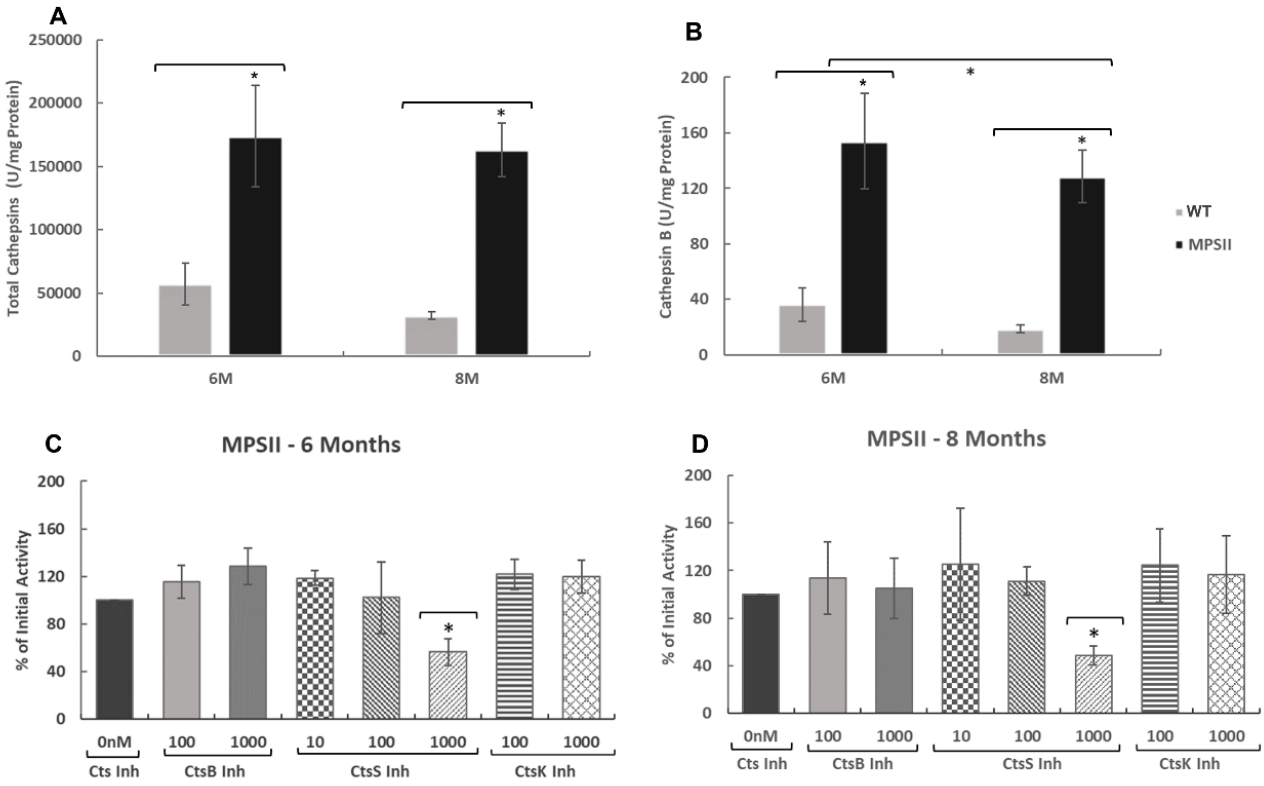

6. DISCUSSÃO GERAL

A presente tese foi concebida com o objetivo de avaliar os desfechos cardiovasculares ao longo do tempo em modelo murino de MPS II, e buscar possíveis mecanismos responsáveis pelos mesmos. Utilizando como base nossos estudos realizados com modelo de MPS I, no que tange à definição das janelas temporais, iniciamos este estudo com camundongos, a partir dos 6 meses de idade. A escolha deste tempo inicial se deu em função de um estudo onde avaliamos os animais a partir dos 2 meses de idade e observamos que os desfechos cardiovasculares funcionais se iniciavam apenas em tempos mais tardios (Baldo et al., 2017). A MPS II compartilha de muitas semelhanças com a MPS I, porém, também apresenta diferenças importantes.

O desenho experimental deste estudo previu o acompanhamento de 4 janelas temporais, compostas pelo grupo de animais MPS II e seus respectivos controles (Wild Type – WT) com 6, 8, 10 e 12 meses de idade (Flurkey K et al., 2007). O fato de termos os grupos WT avaliados em cada janela temporal, possibilitou analisarmos também os animais sem a doença. De fato, encontramos diferenças funcionais e morfológicas importantes, durante o processo de envelhecimento normal, quando comparamos animais considerados de meia-idade (12 meses) com adultos jovens (6 meses). Assim, com o objetivo de caracterizar alterações, ainda que precoces, observadas durante o processo de envelhecimento, descrevemos os achados mais relevantes da linhagem de camundongos C57/Bl6 de meia idade (Artigo 1).

A literatura tem mostrado que o envelhecimento implica em diversas alterações no sistema cardiovascular (Nandini, 2020). A modificação no formato do coração é associada à redução da eficiência da mecânica cardíaca e parece caracterizar o início do processo de envelhecimento do órgão (Strait & Lakatta, 2012). Em nosso estudo observamos uma mudança da geometria cardíaca, assim como uma redução na capacidade contrátil dos animais de meia idade, evidenciando um progressivo comprometimento da função cardíaca nestes animais. Curiosamente, o volume sistólico não foi diferente entre os grupos, provavelmente por causa do tamanho das estruturas cardíacas nos tempos

analisados. Esses achados são particularmente importantes porque caracterizam um processo inicial de IC, ainda que, com fração de ejeção considerada levemente reduzida (FEm) nos camundongos de meia-idade, sem doença preexistente (Bozkurt et al., 2021). Estudos em humanos tem reportado que para envelhecer de forma saudável, os níveis ideais dos principais fatores de saúde cardiovascular são importantes na redução do risco de morte prematura, relacionada à perda funcional, definida como o início de doenças cardiovasculares em indivíduos com menos de 60 anos (Andersson & Vasan, 2018). Intervenções precoces podem levar a melhores prognósticos; neste sentido, este pode ser considerado um momento de transição, o qual marca o início da perda da função cardíaca, e que pode ser estratégico para o estudo de abordagens terapêuticas envolvendo o retardo do envelhecimento deste sistema.

Embora tenhamos acompanhado os animais em quatro janelas temporais, para o estudo da doença, utilizamos apenas 3 tempos, 6, 8 e 10 meses, pois observamos que os animais MPS II começam a morrer aos 12 meses, tornando difícil a obtenção de dados. Esta definição também foi embasada nos desfechos de ritmicidade cardíaca. Diferente dos grupos de animais adultos jovens, os quais não apresentaram eventos arritmogênicos, todos os animais de meia idade avaliados apresentaram disritmia. Estas alterações dificultaram as avaliações ecocardiográficas, pois, embora fossem intermitentes, em alguns animais, foi necessário a interrupção do exame e, os mesmos tiveram seus dados descartados. Além disso, os animais WT também apresentaram redução da capacidade funcional, devido ao envelhecimento. Isto posto, entendemos que esta janela temporal apresentava um viés de confusão importante por causa da idade destes animais. Portanto, nosso trabalho sobre os desfechos da MPS II no sistema cardiovascular foi realizado em 3 janelas temporais, 6, 8 e 10 meses (Artigo 2).

O objetivo geral do nosso estudo foi descrever as alterações cardiovasculares presentes na MPS II, sua progressão e potenciais mecanismos envolvidos na doença. Semelhante aos desfechos cardíacos que encontramos em estudos prévios, nos animais MPS I, aos 6 meses de idade, os animais MPS II apresentaram redução da FE, embora preservada (FEp), o que representa uma capacidade funcional ainda responsiva às demandas corporais (Baldo et al., 2017; Gonzalez et al., 2021). Em ambos os modelos (MPS I e II), aos 8 meses, a FE foi reduzida a ponto de ser considerada IC. Neste sentido, os nossos dados

corroboram o caráter progressivo da doença, sugerindo ainda, que o grau de IC se estabiliza aos 8 meses de idade, pois a FE e outros parâmetros como DC e FAC dos animais MPS II, estabilizaram, pois mantiveram grau semelhante de comprometimento, aos 10 meses de idade.

Importante destacar que os estudos clínicos têm mostrado este grau de comprometimento funcional, com redução da FE (< 50%) em apenas em 2% dos pacientes (Lin et al., 2021). No entanto, entendemos que a maior responsividade cardíaca dos animais à doença, não diminui a sua contribuição para avaliação dos mecanismos de ação envolvidos nos vários desfechos observados, também em humanos, como doença valvar, arritmias cardíaca, hipertrofia concêntrica, disfunção diastólica, entre outros (Lin et al., 2021; Poswar et al., 2022).

Os dados obtidos nas avaliações histológicas e bioquímicas sugerem que os animais MPS II apresentaram a forma grave da doença (neuronopata). As características histológicas foram semelhantes entre MPS I e II, pela presença de vacúolos no tecido cardíaco e aorta, além da quebra de elastina neste mesmo vaso. Por outro lado, a MPS II possui uma resposta bioquímica menos semelhante no que se refere as enzimas responsáveis pelas quebras de elastina na artéria aorta. Para explicar estas quebras e também a dilatação da aorta avaliamos a atividade das proteases colagenase, elastase e caspase-3. Nossos dados mostraram não haver alteração na atividade destas enzimas, nas condições do teste realizadas. Isso acaba sugerindo que outras proteases possam estar envolvidas nos processos que levam a alterações como a perda da elastância deste vaso.

No tecido cardíaco, nossos dados sugerem um papel relevante das catepsinas (Cts), em particular, um aumento progressivo da atividade da CtsB, aos 6 e 8 meses, nos animais MPS II (200 e 500%, respectivamente). Curiosamente, este dado corresponde a perda progressiva da função cardíaca observada nestes tempos. Como limitação do nosso estudo, não avaliamos o extravasamento desta protease, a partir do lisossomo, ou quantificamos o número de macrófagos residentes neste tecido, porém, em estudos prévios com animais MPS I, observamos ambos os eventos (Baldo et al., 2017; Gonzalez et al., 2018). As Cts podem participar da patogênese da lesão cardíaca em resposta à inflamação, apoptose e estresse oxidativo (EO) (Cheng et al., 2012). A partir destes dados, uma das hipóteses do nosso estudo era de que o EO pudesse fazer parte dos mecanismos de ação envolvidos no aumento das catepsinas do tecido cardíaco.

Dosamos Tióis totais (defesa antioxidante), TBARS (marcador de lipoperoxidação) e ROS totais (estresse oxidativo) aos 6, 8 e 10 meses, mas nossos resultados não mostraram alterações significativas nestes parâmetros (dados não mostrados). Embora o EO e os marcadores de apoptose tenham se mostrado inalterados, o processo inflamatório ainda será investigado e pode ter papel importante na patogênese da doença cardiovascular na MPS II, conforme observado em outros órgãos (Azambuja et al, 2020).

O aumento da catepsina B e potencialmente outras proteases desta família pode ser o mecanismo responsável por alterações na matriz extracelular do tecido cardíaco, aorta e valvas, como as quebras de elastina observadas. Um estudo prévio do grupo mostrou que, em células SHSY-5Y nocautes para o gene IDS, existe extravasamento da catepsina B para o citoplasma em decorrência do acúmulo de GAG lisossomal (Azambuja et al, 2020). Estas enzimas, embora mais ativas em pH ácido, ainda retém certa atividade em pHs mais próximos da neutralidade, podendo degradar proteínas da matriz extracelular. O uso de inibidores nos ensaios *in vitro* permitem identificar potencialmente outras Cts, como a CtsS, que podem contribuir em conjunto com a CtsB para estas alterações.

O acúmulo específico de dermatan sulfato no tecido cardíaco também é um achado importante. O fato de haver pouca produção e conteúdo de heparan sulfato nos tecidos cardíacos ajudam a entender as razões pelas quais pacientes com outros tipos de MPS, onde apenas ocorre acúmulo de heparan sulfato (como as síndromes de Sanfilippo) tenham comprometimento cardíaco mais raro e em tempos muito mais tardios (Poswar et al, 2022).

Nosso estudo para o entendimento da patogênese dos desfechos cardiovasculares observados neste modelo, ao longo do tempo, deixa perspectivas de pesquisa importantes que podem contribuir, de sobremaneira, para o entendimento dos mecanismos de ação que permeiam as doenças cardiovasculares na MPS II. Em conjunto, nossos dados sugerem que este pode ser um modelo interessante para avaliar os mecanismos que atuam, secundariamente, ao acúmulo de GAGs no tecido cardiovascular na MPS II. Além disso, o fato de estudos mostrarem que 68% dos pacientes com MPS II apresentam algum dano cardíaco, corrobora a necessidade de estudos pré-clínicos em modelos animais (Sestito et al., 2022).

7. CONCLUSÃO

A partir dos dados obtidos na presente tese, pode-se concluir que:

- ✓ Os camundongos C57BL6 wild type possuem alterações importantes ao longo da vida, podendo ser utilizados como um modelo de envelhecimento;

- ✓ Animais com MPS II também possuem alterações na função cardiovascular, que aparecem a partir dos 6 meses de idades. Estas alterações incluem hipertrofia e perda da capacidade contrátil, assim como dilatação da aorta e aumento da resistência vascular pulmonar;

- ✓ Os animais MPS II apresentaram acúmulo de GAGs nos tecidos do sistema cardiovascular, confirmado pela dosagem de dermatan sulfato tecidual;

- ✓ Há um aumento nas quebras de elastina na aorta dos animais com MPS II;

- ✓ Os animais MPS II apresentaram acúmulo de GAGs e espessamento das valvas cardíacas;

- ✓ A atividade de catepsinas estava aumentada, em especial a catepsina B, nos animais com MPS II, sugerindo envolvimento desta protease na patogênese da doença cardíaca neste modelo;

- ✓ Não houve diferenças entre os grupos com relação aos parâmetros de estrese oxidativo avaliados, mesmo com o aumento na atividade da CtsB.

8. BIBLIOGRAFIA

Ayuna, Ahmed, Karolina M. Stepien, Christian J. Hendriksz, Matthew Balerdi, Anupam Garg, e Peter Woolfson. 2020. “Cardiac Rhythm Abnormalities - An Underestimated Cardiovascular Risk in Adult Patients with Mucopolysaccharidoses”. *Molecular Genetics and Metabolism* 130(2):133–39. doi: 10.1016/J.YMGME.2020.03.005.

Azambuja, A. S., L. N. Pimentel-Vera, E. A. Gonzalez, E. Poletto, C. v. Pinheiro, U. Matte, R. Giugliani, e Guilherme Baldo. 2020. “Evidence for Inflammasome Activation in the Brain of Mucopolysaccharidosis Type II Mice”. *Metabolic Brain Disease* 35(7):1231–36. doi: 10.1007/s11011-020-00592-5.

Azambuja, Amanda Stapenhorst, Lilian Correa, Bernardo Pappi Gabiatti, Giselle Renata Martins, Álvaro de Oliveira Franco, Maria Flávia Marques Ribeiro, e Guilherme Baldo. 2018. “Aversive and Non-Aversive Memory Impairment in the Mucopolysaccharidosis II Mouse Model”. *Metabolic Brain Disease* 33(1). doi: 10.1007/s11011-017-0110-5.

Bajaj, Lakshya, Parisa Lotfi, Rituraj Pal, Alberto di Ronza, Jaiprakash Sharma, e Marco Sardiello. 2019. “Lysosome Biogenesis in Health and Disease”. *Journal of Neurochemistry* 148(5):573–89. doi: 10.1111/JNC.14564.

Bajpai, Geetika, Caralin Schneider, Nicole Wong, Andrea Bredemeyer, Maarten Hulsmans, Matthias Nahrendorf, Slava Epelman, Daniel Kreisel, Yongjian Liu, Akinobu Itoh, Thirupura S. Shankar, Craig H. Selzman, Stavros G. Drakos, e Kory J. Lavine. 2018. “The Human Heart Contains Distinct Macrophage Subsets with Divergent Origins and Functions”. *Nature Medicine* 24(8):1234–45. doi: 10.1038/s41591-018-0059-x.

Baldo, G., F. Q. Mayer, B. Martinelli, F. S. Meyer, M. Burin, L. Meurer, A. M. V. Tavares, R. Giugliani, e U. Matte. 2012. “Intraperitoneal Implant of Recombinant Encapsulated Cells Overexpressing Alpha-l-Iduronidase Partially Corrects Visceral Pathology in Mucopolysaccharidosis Type i Mice”. *Cytotherapy* 14(7). doi: 10.3109/14653249.2012.672730.

Baldo, G., A. M. V. Tavares, E. Gonzalez, E. Poletto, F. Q. Mayer, U. D. S. Matte, e R. Giugliani. 2017. “Progressive Heart Disease in Mucopolysaccharidosis Type I Mice

May Be Mediated by Increased Cathepsin B Activity". *Cardiovascular Pathology* 27. doi: 10.1016/j.carpath.2017.01.001.

Berger, Kenneth I., Simone C. Fagondes, Roberto Giugliani, Karen A. Hardy, Kuo Sheng Lee, Ciarán McArdle, Maurizio Scarpa, Martin J. Tobin, Susan A. Ward, e David M. Rapoport. 2013. "Respiratory and Sleep Disorders in Mucopolysaccharidosis". *Journal of Inherited Metabolic Disease* 36(2):201–10. doi: 10.1007/S10545-012-9555-1.

Bleiziffer, Sabine, Hendrik Ruge, Jürgen Hörer, Andrea Hutter, Sarah Geisbüsch, Gernot Brockmann, Domenico Mazzitelli, Robert Bauernschmitt, e Rüdiger Lange. 2010. "Predictors for New-Onset Complete Heart Block after Transcatheter Aortic Valve Implantation". *JACC. Cardiovascular Interventions* 3(5):524–30. doi: 10.1016/J.JCIN.2010.01.017.

Blondelle, Jordan, Stephan Lange, Barry H. Greenberg, e Randy T. Cowling. 2015. "Cathepsins in Heart Disease-Chewing on the Heartache?" *American Journal of Physiology. Heart and Circulatory Physiology* 308(9):H974–76. doi: 10.1152/AJPHEART.00125.2015.

Boelens, Jaap Jan, Mieke Aldenhoven, Duncan Purtill, Annalisa Ruggeri, Todd DeFor, Robert Wynn, Ed Wraith, Marina Cavazzana-Calvo, Attilio Rovelli, Alain Fischer, Jakub Tolar, Vinod K. Prasad, Maria Escolar, Eliane Gluckman, Anne O'Meara, Paul J. Orchard, Paul Veys, Mary Eapen, Joanne Kurtzberg, Vanderson Rocha, H. Malech, E. Horwitz, J. Le-Rademacher, W. He, B. Gaspar, F. Porta, T. A. Driscoll, D. B. Landi, P. L. Martin, K. M. Page, e H. Parikh. 2013. "Outcomes of Transplantation Using Various Hematopoietic Cell Sources in Children with Hurler Syndrome after Myeloablative Conditioning". *Blood* 121(19):3981. doi: 10.1182/BLOOD-2012-09-455238.

Boffi, Lucia, Pierluigi Russo, e Giuseppe Limongelli. 2018. "Early Diagnosis and Management of Cardiac Manifestations in Mucopolysaccharidoses: A Practical Guide for Paediatric and Adult Cardiologists 11 Medical and Health Sciences 1102 Cardiorespiratory Medicine and Haematology". *Italian Journal of Pediatrics* 44. doi: 10.1186/s13052-018-0560-3.

Bolourchi, Meena, Pierangelo Renella, e Raymond Y. Wang. 2016. "Aortic Root Dilatation in Mucopolysaccharidosis I-VII". *International Journal of Molecular Sciences* 17(12). doi: 10.3390/IJMS17122004.

Braunlin, Elizabeth A., Paul R. Harmatz, Maurizio Scarpa, Beatriz Furlanetto, Christoph Kampmann, James P. Loehr, Katherine P. Ponder, William C. Roberts, Howard M. Rosenfeld, e Roberto Giugliani. 2011. “Cardiac Disease in Patients with Mucopolysaccharidosis: Presentation, Diagnosis and Management”. *Journal of Inherited Metabolic Disease* 34(6).

Braunwald, Eugene. 2013. “Heart Failure”. *JACC. Heart Failure* 1(1):1–20. doi: 10.1016/J.JCHF.2012.10.002.

Brusius-Facchin, Ana Carolina, Luiza Abrahão, Ida Vanessa Doederlein Schwartz, Charles Marques Lourenço, Emerson Santana Santos, Alessandra Zanetti, Rosella Tomanin, Maurizio Scarpa, Roberto Giugliani, e Sandra Leistner-Segal. 2013. “Extension of the Molecular Analysis to the Promoter Region of the Iduronate 2-Sulfatase Gene Reveals Genomic Alterations in Mucopolysaccharidosis Type II Patients with Normal Coding Sequence”. *Gene* 526(2):150–54. doi: 10.1016/J.GENE.2013.05.007.

Burke, Michael A., Stuart A. Cook, Jonathan G. Seidman, e Christine E. Seidman. 2016. “Clinical and Mechanistic Insights Into the Genetics of Cardiomyopathy”. *Journal of the American College of Cardiology* 68(25):2871–86.

Cheng, Xian Wu, Koji Obata, Masafumi Kuzuya, Hideo Izawa, Kae Nakamura, Eri Asai, Tetsuro Nagasaka, Masako Saka, Takahiro Kimata, Akiko Noda, Kohzo Nagata, Hai Jin, Guo Ping Shi, Akihisa Iguchi, Toyoaki Murohara, e Mitsuhiro Yokota. 2006. “Elastolytic Cathepsin Induction/Activation System Exists in Myocardium and Is Upregulated in Hypertensive Heart Failure”. *Hypertension (Dallas, Tex.: 1979)* 48(5):979–87. doi: 10.1161/01.HYP.0000242331.99369.2F.

Chi, Congwu, Andrew S. Riching, e Kunhua Song. 2020. “Lysosomal Abnormalities in Cardiovascular Disease”. *International Journal of Molecular Sciences* 21(3).

CHMP. [s.d.]. “ANNEX I SUMMARY OF PRODUCT CHARACTERISTICS”.

Cohn, Jay N., Roberto Ferrari, e Norman Sharpe. 2000. Cardiac Remodeling-Concepts and Clinical Implications: A Consensus Paper From an International Forum on Cardiac Remodeling.

Costa, Roberto, Andrea Urbani, Marika Salvalaio, Stefania Bellesso, Domenico Cieri, Ilaria Zancan, Mirella Filocamo, Paolo Bonaldo, Ildiko Szabo, Rosella Tomanin, e Enrico Moro. 2017. “Perturbations in Cell Signaling Elicit Early Cardiac Defects in Mucopolysaccharidosis Type II”. *Human Molecular Genetics* 26(9). doi: 10.1093/hmg/ddx069.

Coutinho, Maria Francisca, Juliana Inês Santos, e Sandra Alves. 2016a. “Less Is More: Substrate Reduction Therapy for Lysosomal Storage Disorders”. *International Journal of Molecular Sciences* 17(7). doi: 10.3390/IJMS17071065.

Coutinho, Maria Francisca, Juliana Inês Santos, e Sandra Alves. 2016b. “Less Is More: Substrate Reduction Therapy for Lysosomal Storage Disorders”. *International Journal of Molecular Sciences 2016, Vol. 17, Page 1065* 17(7):1065. doi: 10.3390/IJMS17071065.

Cross, Benjamin, Karolina M. Stepien, Chaitanya Gadepalli, Ahmed Kharabish, Peter Woolfson, Govind Tol, e Petra Jenkins. 2022. “Pre-Operative Considerations in Adult Mucopolysaccharidosis Patients Planned for Cardiac Intervention”. *Frontiers in Cardiovascular Medicine* 9. doi: 10.3389/FCVM.2022.851016.

Demydchuk, Mykhaylo, Chris H. Hill, Aiwu Zhou, Gábor Bunkóczi, Penelope E. Stein, Denis Marchesan, Janet E. Deane, e Randy J. Read. 2017. “Insights into Hunter Syndrome from the Structure of Iduronate-2-Sulfatase”. *Nature Communications* 8. doi: 10.1038/NCOMMS15786.

Doherty, Gary J., e Harvey T. McMahon. 2009. “Mechanisms of Endocytosis”. *Annual Review of Biochemistry* 78:857–902. doi: 10.1146/ANNUREV.BIOCHEM.78.081307.110540.

Dreyfuss, Juliana L., Caio v Regatieri, Thais R. Jarrouge, Renan P. Cavalheiro, Lucia O. Sampaio, e Helena B. Nader. 2009. “Heparan Sulfate Proteoglycans: Structure, Protein Interactions and Cell Signaling”. 81(3):409–29.

Elliott, Perry, Bert Andersson, Eloisa Arbustini, Zofia Bilinska, Franco Cecchi, Philippe Charron, Olivier Dubourg, Uwe Kühl, Bernhard Maisch, William J. McKenna, Lorenzo Monserrat, Sabine Pankuweit, Claudio Rapezzi, Petar Seferovic, Luigi Tavazzi, e Andre Keren. 2008. “Classification of the Cardiomyopathies: A Position Statement from the European Society Of Cardiology Working Group on Myocardial and Pericardial Diseases”. *European Heart Journal* 29(2):270–76. doi: 10.1093/EURHEARTJ/EHM342.

Farrugia, Brooke L., Megan S. Lord, James Melrose, e John M. Whitelock. 2018. “The Role of Heparan Sulfate in Inflammation, and the Development of Biomimetics as Anti-Inflammatory Strategies”. *The Journal of Histochemistry and Cytochemistry : Official Journal of the Histochemistry Society* 66(4):321–36. doi: 10.1369/0022155417740881.

Fecarotta, Simona, Antonietta Tarallo, Carla Damiano, Nadia Minopoli, e Giancarlo Parenti. 2020. “Pathogenesis of Mucopolysaccharidoses, an Update”. *International Journal of Molecular Sciences* 21(7). doi: 10.3390/ijms21072515.

Froissart, R., I. Moreira da Silva, N. Guffon, D. Bozon, e I. Maire. 2002. “Mucopolysaccharidosis Type II--Genotype/Phenotype Aspects”. *Acta Paediatrica (Oslo, Norway : 1992). Supplement* 91(439):82–87. doi: 10.1111/J.1651-2227.2002.TB03116.X.

Garcia, A. R., J. Pan, J. C. Lamsa, e J. Muenzer. 2007. “The Characterization of a Murine Model of Mucopolysaccharidosis II (Hunter Syndrome)”. *Journal of Inherited Metabolic Disease* 30(6). doi: 10.1007/s10545-007-0641-8.

Gatica, Damián, Mario Chiong, Sergio Lavandero, e Daniel J. Klionsky. 2022. “The Role of Autophagy in Cardiovascular Pathology”. *Cardiovascular Research* 118(4):934–50. doi: 10.1093/cvr/cvab158.

Gatica, Damián, e Daniel J. Klionsky. 2017. “New Insights into MTORC1 Amino Acid Sensing and Activation.” *Biotarget* 1:2–2. doi: 10.21037/biotarget.2017.04.01.

Gonzalez, E.A., G. R. Martins, A. M. V. Tavares, M. Viegas, E. Poletto, R. Giugliani, U. Matte, e G. Baldo. 2018. “Cathepsin B Inhibition Attenuates Cardiovascular Pathology in Mucopolysaccharidosis I Mice”. *Life Sciences* 196. doi: 10.1016/j.lfs.2018.01.020.

Gonzalez, E. A., A. M. V. Tavares, E. Poletto, R. Giugliani, U. Matte, e G. Baldo. 2017. “Losartan Improves Aortic Dilatation and Cardiovascular Disease in Mucopolysaccharidosis I”. *Journal of Inherited Metabolic Disease* 40(3). doi: 10.1007/s10545-017-0014-x.

Gonzalez, E. A., S. A. Tobar Leitão, D. D. S. Soares, A. M. V. Tavares, R. Giugliani, G. Baldo, e U. Matte. 2021. “Cardiac Pathology in Mucopolysaccharidosis I Mice: Losartan Modifies ERK1/2 Activation during Cardiac Remodeling”. *Journal of Inherited Metabolic Disease* 44(3). doi: 10.1002/jimd.12327.

Gonzalez, Esteban Alberto, Giselle Renata Martins, Angela Maria Vicente Tavares, Michelle Viegas, Edina Poletto, Roberto Giugliani, Ursula Matte, e Guilherme Baldo. 2018. “Cathepsin B Inhibition Attenuates Cardiovascular Pathology in Mucopolysaccharidosis I Mice”. *Life Sciences* 196:102–9. doi: 10.1016/j.lfs.2018.01.020.

Guffon, Nathalie, Yves Bertrand, Isabelle Forest, Alain Fouilhoux, e Roseline Froissart. 2009. “Bone Marrow Transplantation in Children with Hunter Syndrome: Outcome

after 7 to 17 Years". *The Journal of Pediatrics* 154(5):733–37. doi: 10.1016/J.JPEDS.2008.11.041.

Hampe, Christiane S., Brianna D. Yund, Paul J. Orchard, Troy C. Lund, Jacob Wesley, e R. Scott Mcivor. 2021. "Differences in MPS I and MPS II Disease Manifestations". *International Journal of Molecular Sciences* 22(15).

Hashmi, Mydah S., e Vikas Gupta. 2022. *Mucopolysaccharidosis Type II*.

Holt, Joshua B., Michele D. Poe, e Maria L. Escolar. 2011. "Natural Progression of Neurological Disease in Mucopolysaccharidosis Type II". *Pediatrics* 127(5):e1258–65. doi: 10.1542/PEDS.2010-1274.

Huynh, Minh Bao, Christophe Morin, Gilles Carpentier, Stephanie Garcia-Filipe, Sofia Talhas-Perret, Véronique Barbier-Chassefière, Toin H. van Kuppevelt, Isabelle Martelly, Patricia Albanese, e Dulce Papy-Garcia. 2012. "Age-Related Changes in Rat Myocardium Involve Altered Capacities of Glycosaminoglycans to Potentiate Growth Factor Functions and Heparan Sulfate-Altered Sulfation". *Journal of Biological Chemistry* 287(14):11363–73. doi: 10.1074/JBC.M111.335901.

Jones, Simon A., Z. Almássy, M. Beck, K. Burt, J. T. Clarke, R. Giugliani, C. Hendriksz, T. Kroepfl, L. Lavery, S. P. Lin, G. Malm, U. Ramaswami, R. Tincheva, e J. E. Wraith. 2009. "Mortality and Cause of Death in Mucopolysaccharidosis Type II—a Historical Review Based on Data from the Hunter Outcome Survey (HOS)". *Journal of Inherited Metabolic Disease* 32(4):534–43. doi: 10.1007/S10545-009-1119-7.

Jung, Christian, Georg Fuernau, Phillip Muench, Steffen Desch, Ingo Eitel, Gerhard Schuler, Volker Adams, Hans R. Figulla, e Holger Thiele. 2015. "Impairment of the Endothelial Glycocalyx in Cardiogenic Shock and Its Prognostic Relevance". *Shock (Augusta, Ga.)* 43(5):450–55. doi: 10.1097/SHK.0000000000000329.

Jung, Jennifer, Heide Marika Genau, e Christian Behrends. 2015. "Amino Acid-Dependent MTORC1 Regulation by the Lysosomal Membrane Protein SLC38A9". *Molecular and Cellular Biology* 35(14):2479–94. doi: 10.1128/MCB.00125-15.

Khan, Shaukat A., Hira Peracha, Diana Ballhausen, Alfred Wiesbauer, Marianne Rohrbach, Matthias Gautschi, Robert W. Mason, Roberto Giugliani, Yasuyuki Suzuki, Kenji E. Orii, Tadao Orii, e Shunji Tomatsu. 2017. "Epidemiology of Mucopolysaccharidoses". *Molecular Genetics and Metabolism* 121(3):227–40. doi: 10.1016/j.ymgme.2017.05.016.

Konstam, Marvin A., Daniel G. Kramer, Ayan R. Patel, Martin S. Maron, e James E. Udelson. 2011. "Left Ventricular Remodeling in Heart Failure: Current Concepts in

Clinical Significance and Assessment". *JACC. Cardiovascular Imaging* 4(1):98–108. doi: 10.1016/J.JCMG.2010.10.008.

Kosuga, Motomichi, Ryuichi Mashima, Asami Hirakiyama, Naoko Fuji, Tadayuki Kumagai, Joo Hyun Seo, Mari Nikaido, Seiji Saito, Kazuki Ohno, Hitoshi Sakuraba, e Torayuki Okuyama. 2016. "Molecular Diagnosis of 65 Families with Mucopolysaccharidosis Type II (Hunter Syndrome) Characterized by 16 Novel Mutations in the IDS Gene: Genetic, Pathological, and Structural Studies on Iduronate-2-Sulfatase". *Molecular Genetics and Metabolism* 118(3):190–97. doi: 10.1016/J.YMGME.2016.05.003.

Kubaski, Francyne, Harumi Osago, Robert W. Mason, Seiji Yamaguchi, Hironori Kobayashi, Mikako Tsuchiya, Tadao Orii, e Shunji Tomatsu. 2017. "Glycosaminoglycans Detection Methods: Applications of Mass Spectrometry". *Molecular Genetics and Metabolism* 120(1–2).

Kubaski, Francyne, Hiromasa Yabe, Yasuyuki Suzuki, Toshiyuki Seto, Takashi Hamazaki, Robert W. Mason, Li Xie, Tor Gunnar Hugo Onsten, Sandra Leistner-Segal, Roberto Giugliani, Vũ Chí Dũng, Can Thi Bich Ngoc, Seiji Yamaguchi, Adriana M. Montaño, Kenji E. Orii, Toshiyuki Fukao, Haruo Shintaku, Tadao Orii, e Shunji Tomatsu. 2017. "Hematopoietic Stem Cell Transplantation for Patients with Mucopolysaccharidosis II". *Biology of Blood and Marrow Transplantation : Journal of the American Society for Blood and Marrow Transplantation* 23(10):1795–1803. doi: 10.1016/J.BBMT.2017.06.020.

Li, J. P., e M. Kusche-Gullberg. 2016a. "Heparan Sulfate: Biosynthesis, Structure, and Function". *International Review of Cell and Molecular Biology* 325:215–73. doi: 10.1016/BS.IRCMB.2016.02.009.

Li, J. P., e M. Kusche-Gullberg. 2016b. "Heparan Sulfate: Biosynthesis, Structure, and Function". *International Review of Cell and Molecular Biology* 325:215–73. doi: 10.1016/BS.IRCMB.2016.02.009.

Lin, H. Y., S. P. Lin, C. K. Chuang, M. R. Chen, B. F. Chen, e J. E. Wraith. 2005. "Mucopolysaccharidosis I under Enzyme Replacement Therapy with Laronidase--a Mortality Case with Autopsy Report". *Journal of Inherited Metabolic Disease* 28(6):1146–48. doi: 10.1007/S10545-005-0211-X.

Lin, Hsiang Yu, Ming Ren Chen, Chung Lin Lee, Shan Miao Lin, Chung Lieh Hung, Dau Ming Niu, Tung Ming Chang, Chih Kuang Chuang, e Shuan Pei Lin. 2021. "Natural Progression of Cardiac Features and Long-Term Effects of Enzyme Replacement

Therapy in Taiwanese Patients with Mucopolysaccharidosis II". *Orphanet Journal of Rare Diseases* 16(1). doi: 10.1186/S13023-021-01743-2.

Lin, Hsiang Yu, Chih Kuang Chuang, Ming Ren Chen, Shan Miao Lin, Chung Lieh Hung, Chia Ying Chang, Pao Chin Chiu, Wen Hui Tsai, Dau Ming Niu, Fuu Jen Tsai, Shio Jean Lin, Wuh Liang Hwu, Ju Li Lin, e Shuan Pei Lin. 2016. "Cardiac Structure and Function and Effects of Enzyme Replacement Therapy in Patients with Mucopolysaccharidoses I, II, IVA and VI". *Molecular Genetics and Metabolism* 117(4):431–37. doi: 10.1016/j.ymgme.2016.02.003.

Lunde, Ida G., J. Magnus Aronsen, A. Olav Melleby, Mari E. Strand, Jonas Skogestad, Bård A. Bendiksen, M. Shakil Ahmed, Ivar Sjaastad, Håvard Attramadal, Cathrine R. Carlson, e Geir Christensen. 2022. "Cardiomyocyte-Specific Overexpression of Syndecan-4 in Mice Results in Activation of Calcineurin-NFAT Signalling and Exacerbated Cardiac Hypertrophy". *Molecular Biology Reports*. doi: 10.1007/S11033-022-07985-Y.

Luong, Hien, Sarojini Singh, Mallikarjun Patil, e Prasanna Krishnamurthy. 2021. "Cardiac Glycosaminoglycans and Structural Alterations during Chronic Stress-Induced Depression-like Behavior in Mice". *American Journal of Physiology. Heart and Circulatory Physiology* 320(5):H2044–57. doi: 10.1152/AJPHEART.00635.2020.

Lutgens, Suzanne P. M., Kitty B. J. M. Cleutjens, Mat J. A. P. Daemen, e Sylvia Heeneman. 2007. "Cathepsin Cysteine Proteases in Cardiovascular Disease". *FASEB Journal : Official Publication of the Federation of American Societies for Experimental Biology* 21(12):3029–41. doi: 10.1096/FJ.06-7924COM.

Luzio, J. Paul, Paul R. Pryor, e Nicholas A. Bright. 2007. "Lysosomes: Fusion and Function". *Nature Reviews. Molecular Cell Biology* 8(8):622–32. doi: 10.1038/NRM2217.

Maccari, Francesca, Laura Rigon, Veronica Mantovani, Fabio Galeotti, Marika Salvalaio, Francesca D'Avanzo, Alessandra Zanetti, Federica Capitani, Orazio Gabrielli, Rosella Tomanin, e Nicola Volpi. 2022. "Glycosaminoglycan Signatures in Body Fluids of Mucopolysaccharidosis Type II Mouse Model under Long-Term Enzyme Replacement Therapy". *Journal of Molecular Medicine* 100(8):1169–79. doi: 10.1007/s00109-022-02221-3.

Marques, André R A, Saftig, Paul. Lysosomal storage disorders – challenges, concepts, and avenues for therapy: beyond rare diseases. *Journal of Cell Science* 132(2), jcs221739–. doi:10.1242/jcs.221739.

Marunouchi, Tetsuro, e Kouichi Tanonaka. 1094. *Biol. Pharm. Bull. 38(8): 1094-1097 (2015)*. Vol. 38.

Mataveli, Fabio D. Aguiar, Sang Won Han, Helena Bonciani Nader, Aline Mendes, Rose Kanishiro, Paulo Tucci, Antonio Carlos Lopes, Jose Carlos Costa Baptista-Silva, Ana Paula Cleto Marolla, Leonardo Pinto de Carvalho, Priscila Martins Andrade Denapoli, e Maria Aparecida da Silva Pinhal. 2009. “Long-Term Effects for Acute Phase Myocardial Infarct VEGF165 Gene Transfer Cardiac Extracellular Matrix Remodeling”. *Growth Factors (Chur, Switzerland)* 27(1):22–31. doi: 10.1080/08977190802574765.

McBride, Kim L., Susan A. Berry, e Nancy Braverman. 2020. “Treatment of Mucopolysaccharidosis Type II (Hunter Syndrome): A Delphi Derived Practice Resource of the American College of Medical Genetics and Genomics (ACMG)”. *Genetics in Medicine* 22(11):1735–42. doi: 10.1038/s41436-020-0909-z.

Menkovic, Iskren, Pamela Lavoie, Michel Boutin, e Christiane Auray-Blais. 2019. “Distribution of Heparan Sulfate and Dermatan Sulfate in Mucopolysaccharidosis Type II Mouse Tissues Pre- and Post-Enzyme-Replacement Therapy Determined by UPLC-MS/MS”. *Bioanalysis* 11(8):727–40. doi: 10.4155/bio-2018-0306.

Minami, Kohtaro, Hideto Morimoto, Hiroki Morioka, Atsushi Imakiire, Masafumi Kinoshita, Ryuji Yamamoto, Tohru Hirato, e Hiroyuki Sonoda. 2022. “Pathogenic Roles of Heparan Sulfate and Its Use as a Biomarker in Mucopolysaccharidoses”. *International Journal of Molecular Sciences* 23(19).

Mizumoto, Shuji, e Shuhei Yamada. 2022. “The Specific Role of Dermatan Sulfate as an Instructive Glycosaminoglycan in Tissue Development”. *International Journal of Molecular Sciences* 23(13).

Mohamed, Shifaza, Qi Qi He, Arti A. Singh, e Vito Ferro. 2020. “Mucopolysaccharidosis Type II (Hunter Syndrome): Clinical and Biochemical Aspects of the Disease and Approaches to Its Diagnosis and Treatment”. *Advances in Carbohydrate Chemistry and Biochemistry* 77:71–117. doi: 10.1016/BS.ACCB.2019.09.001.

Muenzer, Joseph, James E. Wraith, Michael Beck, Roberto Giugliani, Paul Harmatz, Christine M. Eng, Ashok Vellodi, Rick Martin, Uma Ramaswami, Muge Gucsavas-Calikoglu, Suresh Vijayaraghavan, Suzanne Wendt, Antonio Puga, Brian Ulbrich, Marwan Shinawi, Maureen Cleary, Diane Piper, Ann Marie Conway, e Alan Kimura. 2006. “A Phase II/III Clinical Study of Enzyme Replacement Therapy with Idursulfase in Mucopolysaccharidosis II (Hunter Syndrome)”. *Genetics in Medicine :*

Official Journal of the American College of Medical Genetics 8(8):465–73. doi: 10.1097/01.GIM.0000232477.37660.FB.

Nagashima, Kazuo, Hisako Endo, Koko Sakakibara, Yumiko Konishi, Ko Miyachi, Jau Jinn Wey, Yoshiyuki Suzuki, e Jinichi Onisawa. 1976. “Morphological and Biochemical Studies of a Case of Mucopolysaccharidosis II (Hunter’s Syndrome)”. *Acta Pathologica Japonica* 26(1):115–32. doi: 10.1111/J.1440-1827.1976.TB03297.X.

Naseem, R. Harris, Wade Hedegard, Timothy D. Henry, Jennifer Lessard, Kathryn Sutter, e Stephen A. Katz. 2005. “Plasma Cathepsin D Isoforms and Their Active Metabolites Increase after Myocardial Infarction and Contribute to Plasma Renin Activity”. *Basic Research in Cardiology* 100(2):139–46. doi: 10.1007/S00395-004-0499-3.

Pahakis, Manolis Y., Jason R. Kosky, Randal O. Dull, e John M. Tarbell. 2007. “The Role of Endothelial Glycocalyx Components in Mechanotransduction of Fluid Shear Stress”. *Biochemical and Biophysical Research Communications* 355(1):228–33. doi: 10.1016/J.BBRC.2007.01.137.

Parenti, Giancarlo, Diego L. Medina, e Andrea Ballabio. 2021. “The Rapidly Evolving View of Lysosomal Storage Diseases”. *EMBO Molecular Medicine* 13(2). doi: 10.15252/EMMM.202012836.

Peters, C., e W. Krivit. 2000a. “Hematopoietic Cell Transplantation for Mucopolysaccharidosis IIB (Hunter Syndrome)”. *Bone Marrow Transplantation* 25(10):1097–99. doi: 10.1038/SJ.BMT.1702398.

Platt, Frances M., Alessandra d’Azzo, Beverly L. Davidson, Elizabeth F. Neufeld, e Cynthia J. Tifft. 2018. “Lysosomal Storage Diseases”. *Nature Reviews. Disease Primers* 4(1). doi: 10.1038/S41572-018-0025-4.

Poswar, Fabiano de Oliveira, Hallana Souza Santos, Angela Barreto Santiago Santos, Solano Vinicius Berger, Carolina Fischinger Moura de Souza, Roberto Giugliani, e Guilherme Baldo. 2022. “Progression of Cardiovascular Manifestations in Adults and Children With Mucopolysaccharidoses With and Without Enzyme Replacement Therapy”. *Frontiers in Cardiovascular Medicine* 8. doi: 10.3389/fcvm.2021.801147.

Poswar, Fabiano de Oliveira, Carolina Fischinger Moura de Souza, Roberto Giugliani, e Guilherme Baldo. 2019. “Aortic Root Dilatation in Patients with Mucopolysaccharidoses and the Impact of Enzyme Replacement Therapy”. *Heart and Vessels* 34(2). doi: 10.1007/s00380-018-1242-1.

Prydz, Kristian. 2015. “Determinants of Glycosaminoglycan (GAG) Structure”. *Biomolecules* 5. doi: 10.3390/biom5032003.

Radosinska, Jana, Miroslav Barancik, e Norbert Vrbjar. 2017. “Heart Failure and Role of Circulating MMP-2 and MMP-9”. *Panminerva Medica* 59(3). doi: 10.23736/S0031-0808.17.03321-3.

Raiman, Julian, Tony Rupar, John Mitchell, e Hanna Faghfoury. [s.d.]. *Canadian Consensus Position Statement for the Diagnosis and Management of MPS II*.

Ramírez-Hernández, M. A., L. E. Figuera, L. C. Rizo de la Torre, M. T. Magaña-Torres, S. C. Mendoza-Ruvalcaba, L. Arnaud-López, J. E. García-Ortiz, G. M. Zúñiga-González, A. M. Puebla-Pérez, B. C. Gómez-Meda, e M. P. Gallegos-Arreola. 2022. “Mutational Spectrum of the Iduronate-2-Sulfatase Gene in Mexican Patients with Hunter Syndrome”. *European Review for Medical and Pharmacological Sciences* 26(14):5115–27. doi: 10.26355/EURREV_202207_29300.

Rapoport, David M e J Mitchell, John J. 2017. “Pathophysiology, evaluation, and management of sleep disorders in the mucopolysaccharidoses” *Mol Genet Metab* 122S:49-54. doi: 10.1016/j.ymgme.2017.08.008.

Ravikumar, Brinda, Marie Futter, Luca Jahreiss, Viktor I. Korolchuk, Maike Lichtenberg, Shouqing Luo, Dunecan C. O. Massey, Fiona M. Menzies, Usha Narayanan, Maurizio Renna, Maria Jimenez-Sanchez, Sovan Sarkar, Benjamin Underwood, Ashley Winslow, e David C. Rubinsztein. 2009. “Mammalian Macroautophagy at a Glance”. *Journal of Cell Science* 122(Pt 11):1707–11. doi: 10.1242/JCS.031773.

Rebsamen, Manuele, Lorena Pochini, Taras Stasyk, Mariana E. G. de Araújo, Michele Galluccio, Richard K. Kandasamy, Berend Snijder, Astrid Fauster, Elena L. Rudashevskaya, Manuela Bruckner, Stefania Scorzoni, Przemyslaw A. Filipek, Kilian V. M. Huber, Johannes W. Bigenzahn, Leonhard X. Heinz, Claudine Kraft, Keiryn L. Bennett, Cesare Indiveri, Lukas A. Huber, e Giulio Superti-Furga. 2015. “SLC38A9 Is a Component of the Lysosomal Amino Acid Sensing Machinery That Controls MTORC1”. *Nature* 519(7544):477–81. doi: 10.1038/NATURE14107.

Riaz, Sadaf, Nabeel Abdulrahman, Shahab Uddin, Ayesha Jabeen, Alain P. Gadeau, Larry Fliegel, e Fatima Mraiche. 2020. “Anti-Hypertrophic Effect of Na+/H+ Exchanger-1 Inhibition Is Mediated by Reduced Cathepsin B”. *European Journal of Pharmacology* 888. doi: 10.1016/j.ejphar.2020.173420.

Rienks, Marieke, Anna Pia Papageorgiou, Nikolaos G. Frangogiannis, e Stephane Heymans. 2014. “Myocardial Extracellular Matrix: An Ever-Changing and Diverse Entity”. *Circulation Research* 114(5):872–88.

Schenke-Layland, Katja, Ulrich A. Stock, Ali Nsair, Jiansong Xie, Ekaterini Angelis, Carissa G. Fonseca, Robert Larbig, Aman Mahajan, Kalyanam Shivkumar, Michael C. Fishbein, e William R. MacLellan. 2009. “Cardiomyopathy Is Associated with Structural Remodelling of Heart Valve Extracellular Matrix”. *European Heart Journal* 30(18):2254–65. doi: 10.1093/eurheartj/ehp267.

Schuh, R. S., E. A. Gonzalez, A. M. V. Tavares, B. G. Seolin, L. S. Elias, L. N. P. Vera, F. Kubaski, E. Poletto, R. Giugliani, H. F. Teixeira, U. Matte, e G. Baldo. 2020. “Neonatal Nonviral Gene Editing with the CRISPR/Cas9 System Improves Some Cardiovascular, Respiratory, and Bone Disease Features of the Mucopolysaccharidosis I Phenotype in Mice”. *Gene Therapy* 27(1–2). doi: 10.1038/s41434-019-0113-4.

Sciarretta, Sebastiano, Maurizio Forte, Giacomo Frati, e Junichi Sadoshima. 2018. “New Insights into the Role of Mtor Signaling in the Cardiovascular System”. *Circulation Research* 122(3):489–505.

Semyachkina, A. N., E. Y. Voskoboeva, E. Y. Zakharova, E. A. Nikolaeva, I. v. Kanivets, A. D. Kolotii, G. v. Baydakova, M. N. Kharabadze, R. G. Kuramagomedova, e N. v. Melnikova. 2019. “Case Report: A Rare Case of Hunter Syndrome (Type II Mucopolysaccharidosis) in a Girl”. *BMC Medical Genetics* 20(1). doi: 10.1186/s12881-019-0807-x.

Sestito, Simona, Giada Rinninella, Angelica Rampazzo, Francesca D’Avanzo, Lucia Zampini, Lucia Santoro, Orazio Gabrielli, Agata Fiumara, Rita Barone, Nicola Volpi, Maurizio Scarpa, Rosella Tomanin, e Daniela Concolino. 2022. “Cardiac Involvement in MPS Patients: Incidence and Response to Therapy in an Italian Multicentre Study”. *Orphanet Journal of Rare Diseases* 17(1). doi: 10.1186/s13023-022-02396-5.

Silbert, Jeremiah E., e Geetha Sugumaran. 2002. “Biosynthesis of Chondroitin/Dermatan Sulfate”. *IUBMB Life* 54(4):177–86. doi: 10.1080/15216540214923.

Sohn, Young Bae, Sung Yoon Cho, Sung Won Park, Su Jin Kim, Ah Ra Ko, Eun Kyung Kwon, Sun Ju Han, e Dong Kyu Jin. 2013. “Phase I/II Clinical Trial of Enzyme Replacement Therapy with Idursulfase Beta in Patients with Mucopolysaccharidosis

II (Hunter Syndrome)". *Orphanet Journal of Rare Diseases* 8(1). doi: 10.1186/1750-1172-8-42.

Sohn, Young Bae, Eun Wha Choi, Su Jin Kim, Sung Won Park, Se Hwa Kim, Sung Yoon Cho, Soo In Jeong, June Huh, I. Seok Kang, Heung Jae Lee, Kyung Hoon Paik, e Dong Kyu Jin. 2012. "Retrospective Analysis of the Clinical Manifestations and Survival of Korean Patients with Mucopolysaccharidosis Type II: Emphasis on the Cardiovascular Complication and Mortality Cases". *American Journal of Medical Genetics, Part A* 158 A(1). doi: 10.1002/ajmg.a.34371.

Song, Wenyu, Fujian Lu, Zequan Ding, Liqi Huang, Kui Hu, Jinmiao Chen, e Lai Wei. 2022. "Identification of Heparan Sulfate in Dilated Cardiomyopathy by Integrated Bioinformatics Analysis". *Frontiers in Cardiovascular Medicine* 9. doi: 10.3389/fcvm.2022.900428.

Tollefsen, Douglas M. 2010. "Vascular Dermatan Sulfate and Heparin Cofactor II". P. 351–72 em *Progress in Molecular Biology and Translational Science*. Vol. 93. Elsevier B.V.

Tomatsu, Shunji, Isabella Azario, Kazuki Sawamoto, Alice Silvia Pievani, Andrea Biondi, e Marta Serafini. 2016. "Neonatal Cellular and Gene Therapies for Mucopolysaccharidoses: The Earlier the Better?" *Journal of Inherited Metabolic Disease* 39(2):189–202. doi: 10.1007/S10545-015-9900-2.

Trownbridge, Janet M., e Richard L. Gallo. 2002. "Dermatan Sulfate: New Functions from an Old Glycosaminoglycan". *Glycobiology* 12(9). doi: 10.1093/GLYCOB/CWF066.

Tulebayeva, Assel, Maira Sharipova, e Riza Boranbayeva. 2020. "Respiratory Dysfunction in Children and Adolescents with Mucopolysaccharidosis Types I, II, IVA, and VI". *Diagnostics (Basel, Switzerland)* 10(2). doi: 10.3390/DIAGNOSTICS10020063.

Valenzano, Kenneth J., Richie Khanna, Allan C. Powe, Robert Boyd, Gary Lee, John J. Flanagan, e Elfrida R. Benjamin. 2011. "Identification and Characterization of Pharmacological Chaperones to Correct Enzyme Deficiencies in Lysosomal Storage Disorders". *Assay and Drug Development Technologies* 9(3):213–35. doi: 10.1089/ADT.2011.0370.

Wang, Shuyu, Zhi Yang Tsun, Rachel L. Wolfson, Kuang Shen, Gregory A. Wyant, Molly E. Plovanich, Elizabeth D. Yuan, Tony D. Jones, Lynne Chantranupong, William Comb, Tim Wang, Liron Bar-Peled, Roberto Zoncu, Christoph Straub, Choah Kim, Jiwon Park, Bernardo L. Sabatini, e David M. Sabatini. 2015. "Metabolism.

Lysosomal Amino Acid Transporter SLC38A9 Signals Arginine Sufficiency to MTORC1". *Science (New York, N.Y.)* 347(6218):188–94. doi: 10.1126/SCIENCE.1257132.

Wang, Xuejun, e Jeffrey Robbins. 2014. "Proteasomal and Lysosomal Protein Degradation and Heart Disease". *Journal of Molecular and Cellular Cardiology* 71:16–24. doi: 10.1016/J.YJMCC.2013.11.006.

Wu, Yuling, Nana Pan, Yi An, Mengyuan Xu, Lijuan Tan, e Lijuan Zhang. 2021. "Diagnostic and Prognostic Biomarkers for Myocardial Infarction". *Frontiers in Cardiovascular Medicine* 7:617277. doi: 10.3389/fcvm.2020.617277

Wuopio, Jonas, Jørgen Hilden, Carl Bring, Jens Kastrup, Ahmad Sajadieh, Gorm Boje Jensen, Erik Kjøller, Hans Jørn Kolmos, Anders Larsson, Janus Christian Jakobsen, Per Winkel, Christian Gluud, Axel C. Carlsson, e Johan Ärnlöv. 2018. "Cathepsin B and S as Markers for Cardiovascular Risk and All-Cause Mortality in Patients with Stable Coronary Heart Disease during 10 Years: A CLARICOR Trial Sub-Study". *Atherosclerosis* 278:97–102. doi: 10.1016/J.ATHEROSCLEROSIS.2018.09.006.

Yoshizawa, Takahiro, Shuji Mizumoto, Yuki Takahashi, Shin Shimada, Kazuyuki Sugahara, Jun Nakayama, Shin'Ichi Takeda, Yoshihiro Nomura, Yuko Nitahara-Kasahara, Takashi Okada, Kiyoshi Matsumoto, Shuhei Yamada, e Tomoki Kosho. 2018. "Vascular Abnormalities in the Placenta of Chst14-/- Fetuses: Implications in the Pathophysiology of Perinatal Lethality of the Murine Model and Vascular Lesions in Human CHST14/D4ST1 Deficiency". *Glycobiology* 28(2):80–89. doi: 10.1093/glycob/cwx099.

Zech, Antonia T. L., Sonia R. Singh, Saskia Schlossarek, e Lucie Carrier. 2020. "Autophagy in Cardiomyopathies". *Biochimica et Biophysica Acta - Molecular Cell Research* 1867(3).

9. ANEXOS

9.1 Produção do Período - Artigos relacionados com a TESE

Received: 3 August 2020 | Revised: 28 October 2020 | Accepted: 2 November 2020

DOI: 10.1002/jimd.12327

ORIGINAL ARTICLE

JIMD SSIEM WILEY

Cardiac pathology in mucopolysaccharidosis I mice: Losartan modifies ERK1/2 activation during cardiac remodeling

Esteban Alberto Gonzalez[1,2] | Santiago Alonso Tobar Leitão[3,4] | Douglas dos Santos Soares[3,4] | Angela Maria Vicente Tavares[2] | Roberto Giugliani[1,2,5] | Guilherme Baldo[1,2,5] | Ursula Matte[1,2,5]

[1]Postgraduate Program in Genetic and Molecular Biology, UFRGS, Porto Alegre, Brazil

[2]Cells, Tissues, and Genes Laboratory, Experimental Research Center, Hospital de Clínicas de Porto Alegre, Porto Alegre, Brazil

[3]Cardiovascular Research Laboratory, Experimental Research Center, Hospital de Clínicas de Porto Alegre, Porto Alegre, Brazil

[4]Postgraduate Program in Health Science: Cardiology and Cardiovascular Science, UFRGS, Porto Alegre, Brazil

[5]Department of Genetics, UFRGS, Porto Alegre, Brazil

Correspondence
Guilherme Baldo, Centro de Pesquisa Experimental – HCPA, Ramiro Barcelos, 2350, 90035-903, Porto Alegre, RS, Brazil.
Email: gbaldo@hcpa.edu.br

Funding information
Conselho Nacional de Desenvolvimento Científico e Tecnológico; Coordenação de Aperfeiçoamento de Pessoal de Nível Superior; Fundação de Amparo à Pesquisa do Estado do Rio Grande do Sul; Hospital de Clínicas de Porto Alegre

Communicating Editor: Areeg El-Gharbawy

Abstract

Mucopolysaccharidosis type I (MPS I) is a lysosomal storage disorder caused by mutations in the *IDUA* gene, that codifies the alpha-L-iduronidase enzyme, which deficiency leads to storage of glycosaminoglycans, with multiple clinical manifestations. One of the leading causes of death in MPS I patients are cardiac complications such as cardiac valve thickening, conduction abnormalities, myocardial dysfunction, and cardiac hypertrophy. The mechanism leading to cardiac dysfunction in MPS I is not entirely understood. In a previous study, we have demonstrated that losartan and propranolol improved the cardiac function in MPS I mice. Thus, we aimed to investigate whether the pathways influenced by these drugs may modulate the cardiac remodeling process in MPS I mice. According to our previous observation, losartan and propranolol restore the heart function, without altering valve thickness. MPS I mice presented reduced activation of AKT and ERK1/2, increased activity of cathepsins, but no alteration in metalloproteinase activity was observed. Animals treated with losartan showed a reduction in cathepsin activity and restored ERK1/2 activation. While both losartan and propranolol improved heart function, no mechanistic evidence was found for propranolol so far. Our results suggest that losartan or propranolol could be used to ameliorate the cardiac disease in MPS I and could be considered as adjuvant treatment candidates for therapy optimization.

KEYWORDS

AKT, cardiac disease, cardiac remodeling, ERK1/2, losartan, mucopolysaccharidosis type I, propranolol

1 | INTRODUCTION

Mucopolysaccharidosis type I (MPS I) is a lysosomal storage disorder caused by mutations in the *IDUA* gene, leading to the deficiency of the lysosomal hydrolase alpha-L-iduronidase (IDUA, EC 3.2.1.76), which is involved in the catabolism of the glycosaminoglycans (GAGs) heparan and dermatan sulfate. GAG storage is progressive and results in a subsequent multi-organ dysfunction.[1,2] Due to high variability, patients may present a

Gene Therapy
https://doi.org/10.1038/s41434-019-0113-4

ARTICLE

Neonatal nonviral gene editing with the CRISPR/Cas9 system improves some cardiovascular, respiratory, and bone disease features of the mucopolysaccharidosis I phenotype in mice

Roselena Silvestri Schuh[1,2] · Esteban Alberto Gonzalez[1,3] · Angela Maria Vicente Tavares[1,4] · Bruna Gazzi Seolin[4] · Lais de Souza Elias[1] · Luisa Natalia Pimentel Vera[1,3] · Francyne Kubaski[3] · Edina Poletto[1,3] · Roberto Giugliani[1,3] · Helder Ferreira Teixeira[2] · Ursula Matte[1,3] · Guilherme Baldo[1,3,4]

Received: 30 October 2018 / Revised: 9 October 2019 / Accepted: 19 November 2019

Abstract

Mucopolysaccharidosis type I (MPS I) is caused by deficiency of alpha-L-iduronidase (IDUA), leading to multisystemic accumulation of glycosaminoglycans (GAG). Untreated MPS I patients may die in the first decades of life, mostly due to cardiovascular and respiratory complications. We previously reported that the treatment of newborn MPS I mice with intravenous administration of lipossomal CRISPR/Cas9 complexes carrying the murine *Idua* gene aiming at the *ROSA26* locus resulted in long-lasting IDUA activity and GAG reduction in various tissues. Following this, the present study reports the effects of gene editing in cardiovascular, respiratory, bone, and neurologic functions in MPS I mice. Bone morphology, specifically the width of zygomatic and femoral bones, showed partial improvement. Although heart valves were still thickened, cardiac mass and aortic elastin breaks were reduced, with normalization of aortic diameter. Pulmonary resistance was normalized, suggesting improvement in respiratory function. In contrast, behavioral abnormalities and neuroinflammation still persisted, suggesting deterioration of the neurological functions. The set of results shows that gene editing performed in newborn animals improved some manifestations of the MPS I disorder in bone, respiratory, and cardiovascular systems. However, further studies will be imperative to find better delivery strategies to reach "hard-to-treat" tissues to ensure better systemic and neurological effects.

Introduction

Mucopolysaccharidosis type I (MPS I) is an autosomal recessive disease caused by deficiency of the lysosomal enzyme alpha-L-iduronidase (IDUA, EC 3.2.1.76), which is involved in the catabolism of the glycosaminoglycans (GAGs) heparan and dermatan sulfate (DS). Enzyme replacement therapy (ERT) and hematopoietic stem cell transplantation (HSCT) are the two treatments currently available for MPS I. However, these therapies are not completely effective, as ERT is not capable of crossing the blood–brain barrier (BBB) and reach the brain, joints, heart valves, or bones, while HSCT shows to be mostly effective if performed before cognitive decline [1–3].

MPS I clinical spectrum varies from the severe Hurler syndrome (OMIM #67014) to the attenuated Scheie syndrome (OMIM #67016), with intermediate disease phenotypes classified as Hurler–Scheie syndrome (OMIM#67015) [1, 4]. Multisystemic manifestations as organomegaly, corneal clouding, heart and valve diseases, pulmonary

Supplementary information The online version of this article (https://doi.org/10.1038/s41434-019-0113-4) contains supplementary material, which is available to authorized users.

✉ Ursula Matte
umatte@hcpa.edu.br

1 Centro de Terapia Gênica, Serviço de Pesquisa Experimental - Hospital de Clinicas de Porto Alegre, R. Ramiro Barcelos 2350, 90035-903 Porto Alegre, RS, Brazil

2 Programa de Pós-Graduação em Ciências Farmacêuticas da Universidade Federal do Rio Grande do Sul (UFRGS), Faculdade de Farmácia, Av. Ipiranga 2752, 90610-000 Porto Alegre, RS, Brazil

3 Programa de Pós-Graduação em Genética e Biologia Molecular da Universidade Federal do Rio Grande do Sul (UFRGS), Campus do Vale, Av. Bento Gonçalves 9500, 91501-970 Porto Alegre, RS, Brazil

4 Programa de Pós-Graduação em Fisiologia da Universidade Federal do Rio Grande do Sul (UFRGS), Instituto de Ciências Básicas da Saúde, R. Sarmento Leite 500, 90035-190 Porto Alegre, RS, Brazil

Published online: 11 December 2019

Life Sciences 196 (2018) 102–109

Contents lists available at ScienceDirect

Life Sciences

journal homepage: www.elsevier.com/locate/lifescie

Cathepsin B inhibition attenuates cardiovascular pathology in mucopolysaccharidosis I mice

Esteban Alberto Gonzalez[a,b], Giselle Renata Martins[a], Angela Maria Vicente Tavares[c,e], Michelle Viegas[a], Edina Poletto[a,b], Roberto Giugliani[a,b,d], Ursula Matte[a,b], Guilherme Baldo[a,b,c,*]

[a] Gene Therapy Center, Hospital de Clínicas de Porto Alegre, Porto Alegre, Brazil
[b] Post-Graduation Program in Genetics and Molecular Biology, UFRGS, Porto Alegre, Brazil
[c] Post-Graduation Program in Physiology, UFRGS, Porto Alegre, Brazil
[d] Medical Genetics Service, Hospital de Clínicas de Porto Alegre, Porto Alegre, Brazil
[e] Ritter dos Reis University Center, UniRitter, Porto Alegre, Brazil

ARTICLE INFO

Keywords:
Mucopolysaccharidosis type I
Cardiovascular disease
Cathepsin B
Ca-074 Me

ABSTRACT

Mucopolysaccharidosis type I (MPS I) is a lysosomal storage disorder with multisystemic features, including heart enlargement, heart valve dysfunction, and aortic stiffness and dilatation. Previous studies have shown that MPS I mice overexpress cathepsin B (CtsB) in multiple tissues, including those from the cardiovascular system. Here, we hypothesized that inhibition of CtsB could ameliorate cardiac function parameters, as well as aorta and valve abnormalities found in MPS I.

First, we found that total elastase activity in an MPS I aorta is elevated. Following that, we demonstrated that CtsB leaks from the lysosome in MPS I human fibroblasts, possibly acting as a degradative agent of extracellular matrix components from the aorta, cardiac muscle, and heart valves. We then used a CtsB inhibitor in vivo in the MPS I mouse model. After 4 months of treatment, partial inhibition of CtsB activity in treated mice reduced aortic dilatation, as well as heart valve thickening, and led to improvements in cardiac function parameters, although none of these were completely normalized. Based on these results, we conclude that lysosomal alterations in this disease promote leakage of CtsB to outside the organelle, where this protein can have multiple pathological roles. CtsB inhibition improved cardiovascular parameters in MPS I mice and can have a potential benefit in this disease.

1. Introduction

Mucopolysaccharidosis type I (MPS I) is an autosomal recessive disorder caused by deficiency of lysosomal enzyme alpha-L-iduronidase (IDUA), which is involved in the catabolism of glycosaminoglycans (GAG), heparan and dermatan sulfate. The disease is characterized by multiple organ dysfunction, which includes organomegaly, bone and joint deformities, short stature, abnormal facial features and, in severe cases, mental retardation. There is a spectrum of severity, ranging from the severe Hurler phenotype to the more attenuated Scheie phenotype. Death can occur from multiple causes in the first decades of life [1].

Heart and valve disease are present in all MPS types, and death from heart failure is common. MPS I patients suffer from heart enlargement [2], heart valve thickening and regurgitation, and aortic stiffness and dilatation [3,4]. Studies in animal models (both dogs and mice) have shown that MPS I animals have dilated hearts with reduced contractility, dilated ascending aortas with increased elastin breaks, and heart valve thickening and regurgitation [5–7].

The extracellular matrix (ECM) plays many roles in the cardiovascular wall and valve homeostasis [8]. Elastin and collagen are the main compounds of the cardiovascular ECM and play a vital role in biomechanical and functional properties in the myocardium, aorta and heart valves. Although the proportions of elastin and collagen vary considerably in these tissues, distribution and properties of these connective tissue proteins are important for structural integrity and function. An imbalance in the turnover of ECM proteins in the myocardium and vasculature can lead to cardiovascular disorders such as stenosis, left ventricular hypertrophy, heart failure and aortic aneurysm [9–11]. These changes have been attributed to the lack of control of proteolytic enzymes that degrade the major components of the ECM. The increase in protease activity (especially in Cathepsin B) subsequent to the primary defect has been described as a possible pathological mechanism present in different types of MPS [5,7,12–14].

Cathepsin B (CtsB) is a pH-dependent lysosomal protease

* Corresponding author at: Gene Therapy Center, Hospital de Clínicas de Porto Alegre, Ramiro Barcelos, 2350, 90035-903, RS, Brazil.
E-mail address: gbaldo@hcpa.edu.br (G. Baldo).

https://doi.org/10.1016/j.lfs.2018.01.020
Received 31 October 2017; Received in revised form 12 January 2018; Accepted 19 January 2018

Journal of Controlled Release 288 (2018) 23–33

Contents lists available at ScienceDirect

Journal of Controlled Release

journal homepage: www.elsevier.com/locate/jconrel

In vivo genome editing of mucopolysaccharidosis I mice using the CRISPR/Cas9 system

Roselena Silvestri Schuh[a,b], Édina Poletto[a,d], Gabriela Pasqualim[a,d], Angela Maria Vicente Tavares[a,c], Fabíola Shons Meyer[a], Esteban Alberto Gonzalez[a,d], Roberto Giugliani[a,d], Ursula Matte[a,d], Helder Ferreira Teixeira[b], Guilherme Baldo[a,c,d,*]

[a] Centro de Terapia Gênica do Hospital de Clínicas de Porto Alegre, R. Ramiro Barcelos 2350, 90035-903 Porto Alegre, RS, Brazil
[b] Programa de Pós-Graduação em Ciências Farmacêuticas da Universidade Federal do Rio Grande do Sul (UFRGS), Faculdade de Farmácia, Av. Ipiranga 2752, 90610-000 Porto Alegre, RS, Brazil
[c] Programa de Pós-Graduação em Fisiologia da Universidade Federal do Rio Grande do Sul (UFRGS), Instituto de Ciências Básicas da Saúde, R. Sarmento Leite, 500, 90035-190 Porto Alegre, RS, Brazil
[d] Programa de Pós-Graduação em Genética e Biologia Molecular da Universidade Federal do Rio Grande do Sul (UFRGS), Departamento de Genética, Campus do Vale, Av. Bento Gonçalves, 9500, 91501-970 Porto Alegre, RS, Brazil

ARTICLE INFO

Keywords:
CRISPR/Cas
Genome editing
Liposome
Lysosomal storage disease
Mucopolysaccharidosis type I
Nonviral vector

ABSTRACT

Mucopolysaccharidosis type I (MPS I) is a multisystemic disorder caused by the deficiency of alpha-L-iduronidase (IDUA) that leads to intracellular accumulation of glycosaminoglycans (GAG). In the present study we aimed to use cationic liposomes carrying the CRISPR/Cas9 plasmid and a donor vector for *in vitro* and *in vivo* MPS I gene editing, and compare to treatment with naked plasmids. The liposomal formulation was prepared by microfluidization. Complexes were obtained by the addition of DNA at +4/−1 charge ratio. The overall results showed complexes of about 110 nm, with positive zeta potential of +30 mV. The incubation of the complexes with fibroblasts from MPS I patients led to a significant increase in IDUA activity and reduction of lysosomal abnormalities. Hydrodynamic injection of the liposomal complex in newborn MPS I mice led to a significant increase in serum IDUA levels for up to six months. The biodistribution of complexes after hydrodynamic injection was markedly detected in the lungs and heart, corroborating the results of increased IDUA activity and decreased GAG storage especially in these tissues, while the group that received the naked plasmids presented increased enzyme activity especially in the liver. Furthermore, animals treated with the liposomal formulation presented improvement in cardiovascular parameters, one of the main causes of death observed in MPS I patients. We conclude that the IDUA production in multiple organs had a significant beneficial effect on the characteristics of MPS I disease, which may bring hope to gene therapy of Hurler patients.

1. Introduction

Mucopolysaccharidosis type I (MPS I, OMIM #607014 #607015 #607016) is an autosomal recessive lysosomal storage disease (LSD) caused by the widespread accumulation of the glycosaminoglycans (GAGs) heparan and dermatan sulfate, which are partially degraded or not degraded due to a deficiency of alpha-L-iduronidase enzyme (IDUA, EC 3.2.1.76). This abnormal GAG storage interferes with normal functioning of cells, tissues, and organs, leading to multiple abnormalities, including organomegaly, skeletal deformities, and developmental delay. Severe untreated patients die in the first decades of life, mostly due to respiratory and cardiovascular problems [1,2]. Among the MPS I *IDUA* variants, Trp402* is the most prevalent mutation in patients, which produces no IDUA protein, and is associated with very severe clinical manifestations in homozygotes [3,4].

Enzyme replacement therapy (ERT) and hematopoietic stem cell transplantation (HSCT) are the two treatments currently available for MPS I. However, these therapies are not completely effective as ERT is not capable of crossing the blood–brain barrier (BBB) or has difficulty to reach some tissues such as aorta, heart valves, and bones, while HSCT shows to have a considerable morbimortality, being effective to prevent the neurological regression only if performed in early years [5–7]. In this sense, novel and alternative therapies are required, and one of the most promising is gene therapy. Ideally, this treatment would

* Corresponding author at: Centro de Terapia Gênica do Hospital de Clínicas de Porto Alegre, R. Ramiro Barcelos 2350, 90035-903 Porto Alegre, RS, Brazil.
E-mail address: gbaldo@hcpa.edu.br (G. Baldo).

https://doi.org/10.1016/j.jconrel.2018.08.031
Received 19 April 2018; Received in revised form 3 July 2018; Accepted 22 August 2018
Available online 28 August 2018
0168-3659/

J Inherit Metab Dis
DOI 10.1007/s10545-017-0014-x

LETTER TO THE EDITORS

Losartan improves aortic dilatation and cardiovascular disease in mucopolysaccharidosis I

Esteban Alberto Gonzalez[1,2] · Angela Maria Vicente Tavares[1,3,4] · Edina Poletto[1,2] · Roberto Giugliani[2,5] · Ursula Matte[1,2] · Guilherme Baldo[1,2,3]

Received: 8 November 2016 / Revised: 2 January 2017 / Accepted: 5 January 2017

To the Editor,

We read with great interest the manuscript titled "Angiotensin receptor blockade mediated amelioration of mucopolysaccharidosis type I cardiac and craniofacial pathology" recently published in the *Journal of Inherited Metabolic Disorders* (Osborn et al., 2016). Simultaneously, we have been conducting a similar study, with results that are partially in accordance, and we thus have some additional important considerations concerning the content of their paper.

We treated juvenile (8-week-old) *Idua*$^{-/-}$ mice with losartan or other antihypertensive drug (propranolol) as an additional control (Suppl. Material and Methods) to determine the benefit of angiotensin receptor blockade (ARB) in mucopolysaccharidosis I (MPS I) and if this effect was specific to losartan. Mice were sacrificed at 6 months of age.

Our data showed an increase in aortic diameter measured by a digital caliper in untreated *Idua*$^{-/-}$ mice without significant gender differences (Suppl. Fig. 1). Treatment analysis was performed according to gender and without differentiation (Suppl. Fig. 2). Unlike Osborn et al.'s results, our data indicate that losartan is effective in decreasing aortic dilatation in MPS I at a similar rate for both genders (~20%). As a comparison, we also treated female mice with propranolol (a beta-blocker), which was not able to reduce aortic dilatation.

In agreement with Osborn et al., our echocardiographic analysis showed that losartan also improves ventricular contraction, expressed through left ventricular fraction shortening (LVSF) and suggesting an improved heart-pumping ability. It also prevented enlargement of left ventricular chamber dimensions (Suppl. Table 1). However, it is important to point out that propranolol also improved cardiac function, which suggests that heart dysfunction may be independent from angiotensin receptor (AT-1R) activation. Propranolol might have its beneficial effect by reducing hemodynamic stress on the aortic vasculature. In contrast, we believe that losartan targets the underlying pathophysiology in MPS possibly by antagonism of transforming growth factor (TGF)-β or other pathways, which will be investigated. Aortic diameter was also measured by echo, which confirmed that only losartan prevented abnormalities in the aorta.

The authors highlight the possibility that matrix metalloproteinase-12 (MMP-12) increase via AT-1R activation is one of the mechanisms involved in the pathogenesis of cardiovascular disease in MPS. Nonetheless, in a previous study, MPS I and VII mice developed aortic dilatation by similar mechanisms, and knocking out MMP-12 in MPS VII mice did not prevent aortic abnormalities (Baldo et al. 2011). This probably suggestst that multiple mechanisms and genes are responsible for this effect.

Communicated by: Carla E. Hollak

Electronic supplementary material The online version of this article (doi:10.1007/s10545-017-0014-x) contains supplementary material, which is available to authorized users.

✉ Ursula Matte
umatte@hcpa.edu.br

[1] Gene Therapy Center, Hospital de Clínicas de Porto Alegre, Ramiro Barcelos, 2350, 90035-903 Porto Alegre, Brazil

[2] Postgraduate Program in Genetics and Molecular Biology, UFRGS, Porto Alegre, Brazil

[3] Postgraduate Program in Physiology-UFRGS, Porto Alegre, Brazil

[4] Ritter dos Reis University Center-UniRitter, Porto Alegre, Brazil

[5] Medical Genetics Service, Hospital de Clínicas de Porto Alegre, Porto Alegre, Brazil

Published online: 03 February 2017

Cardiovascular Pathology 27 (2017) 45–50

Contents lists available at ScienceDirect

Cardiovascular Pathology

Original Article

Progressive heart disease in mucopolysaccharidosis type I mice may be mediated by increased cathepsin B activity☆

Guilherme Baldo [a,b], Angela Maria Vicente Tavares [a], Esteban Gonzalez [a], Edina Poletto [a], Fabiana Quoos Mayer [a,*], Ursula da Silveira Matte [a], Roberto Giugliani [a,b]

[a] Gene Therapy Center-Hospital de Clínicas de Porto Alegre, RS, Brazil
[b] Post-Graduation Program in Genetics and Molecular Biology, UFRGS, RS, Brazil

ARTICLE INFO

Article history:
Received 20 October 2016
Received in revised form 22 December 2016
Accepted 3 January 2017
Available online xxxx

Keywords:
Mucopolysaccharidosis type I
Glycosaminoglycan
Cathepsin B
lysosomal storage disorder
Heart dilatation

ABSTRACT

Mucopolysaccharidosis type I (MPS I) is a lysosomal disorder characterized by a deficiency of alpha-L-iduronidase and storage of undegraded glycosaminoglycans (GAGs). Clinical findings of the disease include heart failure, and patients often need valve replacement. It has been shown that, later in life, MPS I mice develop those abnormalities, but to date, there have not been studies on the progression and pathogenesis of the disease. Therefore, in the present study, we evaluated heart function in normal and MPS I male mice from 2 to 8 months of age. Echocardiographic analysis showed left ventricular enlargement with progressive reduction in ejection fraction, fractional area change, and left ventricular fractional shortening in the MPS I hearts at 6 and 8 months of age and a reduction in acceleration time/ejection time ratio of the pulmonary artery starting at 6 months of age, which suggests pulmonary vascular resistance. Histological and biochemical analysis confirmed progressive GAG storage from 2 months of age and onwards in the myocardium and heart valves, which had also increased in thickness. Additionally, macrophages were present in the MPS I heart tissue. Collagen content was reduced in the MPS I mouse valves. Cathepsin B, an enzyme that is known to be able to degrade collagen and is involved in heart dilatation, displayed a marked elevation in activity in the MPS I mice and could be responsible for the heart dilatation and valves alterations observed. Our results suggest that the MPS I mice have progressive heart failure and valve disease, which may be caused by cathepsin B overexpression.

1. Introduction

Mucopolysaccharidosis type I (MPS I) is an autosomal recessive disorder characterized by a deficiency of alpha-L-iduronidase (IDUA), a lysosomal enzyme involved in the degradation of glycosaminoglycans (GAGs), heparan sulfate, and dermatan sulfate [1]. The disease spectrum varies from the severe Hurler syndrome (OMIM #67014) to the attenuated Scheie syndrome (OMIM #67016), with intermediate disease phenotypes classified as Hurler–Scheie syndrome (OMIM #67015). Patients with Hurler syndrome present with severe mental retardation in addition to other systemic manifestations (dysostosis multiplex, hepatosplenomegaly, corneal clouding, and joint stiffness), which are also found in the more attenuated forms of the disease [2].

Heart and valve diseases are present in all forms of MPS I. It generally develops earlier in patients with Hurler syndrome [3] compared to patients with the more attenuated forms of MPS I [4]. Accurate data on the frequency of heart disease in patients with MPS I are hard to obtain due to early death in some cases, but it is estimated that at least 60% of patients with MPS I develop cardiac and valve abnormalities [5]. Myocardial and heart valve thickening is common in all forms of MPS I, with some patients also developing systemic or pulmonary hypertension [6,7]. Death by congestive heart failure is frequent in patients with Hurler syndrome, and both Hurler and Scheie phenotypes usually undergo valve replacement [5]. The MPS I hearts are often dilated, and patients with increased left ventricle dimensions usually have a very poor prognosis [3,8,9].

In the MPS I mouse model, myocardium alterations were observed at 6 and 10 months of age, and enlarged heart and valves as well as mitral and aortic valve regurgitation were observed at the latest studied time point [10]. Additionally, there were reduced elasticity and increased breaks in the elastin structure of the aorta with an associated increase of matrix metalloproteinase and cathepsin [11] activities. This model was created in 2003 by the disruption of the *Idua* gene with the neomycin resistance gene [12] and has proven to be a useful model for studying the pathogenesis of the disease as well as for the development of treatment options [13,14]. As the mechanism of heart dilatation and valve abnormalities in MPS I is unknown, we evaluated mice at different ages to verify the onset of myocardium and heart valve abnormalities and to look for mechanisms potentially responsible for them. Based on echocardiographic and histological findings, we hypothesized that a protease could be degrading the extracellular matrix (ECM) and

☆ This work was funded by grants from CNPq, PPGBM-UFRGS, and FIPE-HCPA.
* Corresponding author.

http://dx.doi.org/10.1016/j.carpath.2017.01.001
1054-8807/

Original Article

Effects of Copaiba Oil in Peripheral Markers of Oxidative Stress in a Model of Cor Pulmonale in Rats

Cristina Campos,[1] Patrick Turck,[1] Angela Maria Vicente Tavares,[1] Ciana Corssac,[1] Denise Lacerda,[1] Alex Araujo,[1] Susana Llesuy,[2] Adriane Bello Klein[1]

Universidade Federal do Rio Grande do Sul,[1] Porto Alegre, RS – Brazil
Hospital Italiano de Buenos Aires,[2] Buenos Aires – Argentina

Abstract

Background: To date, copaiba oil's systemic effects have never documented in Cor pulmonale induced by monocrotaline.

Objectives: To investigate copaiba oil's effects in peripheral markers of oxidative stress in rats with Cor pulmonale.

Methods: Male Wistar rats (170±20g, n=7/group) were divided into four groups: control (CO), monocrotaline (MCT), copaiba oil (O), and monocrotaline+copaiba oil (MCT-O). MCT (60 mg/kg i.p.) was administered, and after one week, treatment with copaiba oil (400 mg/kg/day-gavage-14 days) was begun. Echocardiography was performed and, later, trunk blood collection was performed for oxidative stress evaluations. Statistical analysis: two-way ANOVA with Student-Newman-Keuls post-hoc test. P values<0.05 were considered significant.

Results: Copaiba oil reduced pulmonary vascular resistance and right ventricle (RV) hypertrophy (Fulton index (mg/mg): MCT-O=0.39±0.03; MCT=0.49±0.01), and improved RV systolic function (RV shortening fraction, %) in the MCT-O group (17.8±8.2) as compared to the MCT group (9.4±3.1; p<0.05). Moreover, in the MCT-O group, reactive oxygen species and carbonyl levels were reduced, and antioxidant parameters were increased in the peripheral blood (p<0.05). Conclusions: Our results suggest that copaiba oil has an interesting systemic antioxidant effect, which is reflected in the improvements in function and RV morphometry in this Cor pulmonale model. Cor pulmonale attenuation promoted by copaiba oil coincided with a reduction in systemic oxidative stress.

Keywords: Cor Pulmonale; Monocrotaline,Rats; Oxidative Stress; Fabaceae; Phytotherapy; Hypertrophy, Right Ventricular; Copaiba Oil

Introduction

The Amazon forest could be considered a natural laboratory, since it has a wide diversity of plants with medicinal properties. The great majority of these plants have not yet been fully studied, as it is the case of copaiba.[1] Copaiba is a large tree that grows abundantly in the northern region of Brazil. Since the 16th century, copaiba oil has been used by the native indigenous people of the country in the treatment of various diseases. These traditional uses have motivated some researchers to study this oil.[2]

According to some reports, copaiba oil presents antioxidant and anti-lipoperoxidative properties.[3,4] The antioxidant properties of copaiba oil could be very useful in the treatment of some cardiovascular diseases associated with oxidative stress. However, only two studies were found in the literature demonstrating the beneficial effects of copaiba oil on cardiovascular diseases, such as pulmonary arterial hypertension (PAH).[5,6]

PAH is a chronic and fatal disease that is associated with progressive increases in pulmonary vascular resistance and pressure. These changes impair the performance of the right ventricle (RV) and result in RV failure, and ultimately death.[7] To study the physiopathological mechanisms involved in RV dysfunction and PAH development, a monocrotaline (MCT) model was used.[8] The active metabolite of MCT causes damage in the pulmonary endothelium, leading to PAH.[9]

The MCT model mimics aspects of human PAH, including *Cor pulmonale*, which is a term used to describe pathological RV hypertrophy induced by lung dysfunction.[10] In fact, multiple studies in animal models and patients implicate oxidative stress in the development of *Cor pulmonale* and PAH.[11-13] Oxidative stress can cause damage to pulmonary endothelial cells,[14] as well as contribute to RV dysfunction and failure.[11] However, no study has explored the impact of PAH on oxidative stress markers in peripheral blood by analyzing copaiba oil's effects. It was reported that oxidative stress measured in the blood of patients with a neurodegenerative disease could represent a reflection of the oxidative brain damage in those patients.[15] In this sense, evaluating peripheral markers of oxidative stress could have clinical applicability, since obtaining a blood sample represents a minimally invasive procedure.[16] This

Mailing Address: Adriane Bello Klein •
Universidade Federal do Rio Grande do Sul - Sarmento Leite, 500. Postal Code 90040-060, Porto Alegre, RS - Brazil
E-mail: bellklein@ufrgs.br
Manuscript received August 20, 2020, revised manuscript December 07, 2020, accepted January 27, 2021

DOI: https://doi.org/10.36660/abc.20200929

ARCHIVES OF PHYSIOLOGY AND BIOCHEMISTRY
https://doi.org/10.1080/13813455.2020.1779752

Taylor & Francis
Taylor & Francis Group

ORIGINAL ARTICLE

Cardioprotective doses of thyroid hormones improve NO bioavailability in erythrocytes and increase HIF-1α expression in the heart of infarcted rats

Alexandre Luz de Castro, Rafael Oliveira Fernandes, Vanessa D. Ortiz, Cristina Campos, Jéssica H. P. Bonetto, Tânia Regina G. Fernandes, Adriana Conzatti, Rafaela Siqueira, Angela Vicente Tavares, Adriane Belló-Klein and Alex Sander da Rosa Araujo

Laboratório de Fisiologia Cardiovascular, Departamento de Fisiologia, Instituto de Ciências Básicas da Saúde, Universidade Federal do Rio Grande do Sul, Porto Alegre, Brazil

ABSTRACT

Context: Infarction leads to a decrease in NO bioavailability in the erythrocytes. Thyroid hormones (TH) present positive effects after infarction. However, there are no studies evaluating the effects of cardioprotective doses of TH in the erythrocytes after infarction.

Objective: This study aimed to evaluate the effects of TH in NO bioavailability and oxidative stress parameters in the erythrocytes of infarcted rats.

Material and methods: Wistar rats were allocated into the three groups: Sham-operated (SHAM), infarcted (AMI) and infarcted + TH (AMIT). AMIT rats received T4 and T3 for 12days by gavage. Subsequently, the animals were evaluated by echocardiography and the LV and erythrocytes were collected.

Results: TH improved NO bioavailability and increased catalase activity in the erythrocytes. Besides that, TH increased HIF-1α in the heart.

Conclusion: TH seems to be positive for erythrocytes preventing a decrease in NO bioavailability and increasing antioxidant enzymatic defense after infarction.

ARTICLE HISTORY
Received 7 February 2020
Revised 26 May 2020
Accepted 3 June 2020BAD DATE

KEYWORDS
T3; T4; nitric oxide; reactive oxygen species; oxidative stress

Introduction

Acute myocardial infarction is an ischaemic pathology of the heart that involves an irreversible loss of cardiomyocytes, leading to a decrease in cardiac function (Schenkel *et al.* 2010). This condition is a leading cause of morbidity and mortality (Hong *et al.* 2019). Besides that, myocardial infarction is also associated with a decrease in nitric oxide (NO) bioavailability in the heart and in the red blood cells (Eligini *et al.* 2013, De Castro *et al.* 2015). The maintenance of NO levels in the cardiac tissue is important, mainly after the ischaemic injury, since this molecule can upregulate the expression of the hypoxia inducible factor-1α (HIF-1α) by activating the phosphatidylinositol 3-kinase (PI3K)-Akt pathway (Sandau *et al.* 2000, Kasuno *et al.* 2004). Activation and upregulation of HIF-1α has been recently found to be a protective mechanism against ischemia-reperfusion injury in the heart (Alchera *et al.* 2008, Zhong *et al.* 2008).

In relation to NO bioavailability, this parameter can be evaluated by the balance between reactive oxygen species (ROS) and NO levels (Bauersachs *et al.* 1999, Heusch *et al.* 2000). In fact, previous studies have shown that erythrocytes can be an important source of this vasodilator molecule in the circulation (Jia *et al.* 1996, Yang *et al.* 2013). In erythrocytes, NO production is derived from inorganic nitrite, which is converted to NO by the deoxygenated haemoglobin, and also by the activity of the enzyme nitric oxide synthase presented in these cells (Cosby *et al.* 2003, Gladwin *et al.* 2003, Yang *et al.* 2013). In relation to this, a study from Yang and colleagues demonstrated that erythrocytes derived-NO is an important molecule in terms of cardioprotection (Yang *et al.* 2013). In fact, the decrease in circulating NO was shown to be detrimental in an acute model of myocardial isquemia-reperfusion (Merx *et al.* 2014). In this context, high levels of ROS are detrimental to NO bioavailability in erythrocytes (Araujo *et al.* 2011). The red blood cells are susceptible to reactive species, because of its high levels of polyunsaturated fatty acids, iron and oxygen. In view of that, enzymatic and non-enzymatic antioxidants in these cells are very relevant to prevent oxidative stress (Araujo *et al.* 2011).

In relation to cardioprotection, recent studies have shown that thyroid hormones present positive effects in the infarcted heart (De Castro *et al.* 2015). In fact, it is well described that, after myocardial infarction, T3 plasma levels and/or the expression of thyroid hormone receptors in the heart are decreased (Gerdes and Iervasi 2010). In view of that, studies demonstrated that thyroid hormones administration is beneficial for the left and the right ventricles, as well as for the aorta of infarcted rats (Corssac *et al.* 2016, De Castro *et al.* 2015, Ortiz *et al.* 2016). In fact, previous studies from our group showed that cardioprotective doses of T3

CONTACT Alexandre Luz de Castro alexluzcastro@gmail.com Laboratório de Fisiologia Cardiovascular, Departamento de Fisiologia, Instituto de Ciências Básicas da Saúde, Universidade Federal do Rio Grande do Sul, Rua Sarmento Leite 500, sala 01, Porto Alegre CEP 90050170, Brazil

Biochimie 156 (2019) 33–46

Contents lists available at ScienceDirect

Biochimie

journal homepage: www.elsevier.com/locate/biochi

Research paper

Chronic whole-body heat treatment relieves atherosclerotic lesions, cardiovascular and metabolic abnormalities, and enhances survival time restoring the anti-inflammatory and anti-senescent heat shock response in mice

Maciel Alencar Bruxel, Angela Maria Vicente Tavares, Luiz Domingues Zavarize Neto, Victor de Souza Borges, Helena Trevisan Schroeder, Patricia Martins Bock, Maria Inês Lavina Rodrigues, Adriane Belló-Klein, Paulo Ivo Homem de Bittencourt Jr. *

Department of Physiology, Institute of Basic Health Sciences, Federal University of Rio Grande do Sul, Porto Alegre, RS, Brazil

ARTICLE INFO

Article history:
Received 14 July 2018
Accepted 26 September 2018
Available online 28 September 2018

Keywords:
Atherosclerosis
Heat shock response
HSF1
HSP70
HSP27
Sirtuin-1

ABSTRACT

Unhealthy lifestyle persistently feeds forward inflammation in metabolic organs thus imposing senescence-associated secretory phenotype (SASP), as observed in obesity and type 2 diabetes. However, SASP blocks physiological resolution of inflammation by suppressing the anti-inflammatory and anti-senescent heat shock (HS) response, *i.e.*, the gene program centered in heat shock factor-1 (HSF1)-dependent expression heat shock proteins (HSPs). As SASP-inducing factors are not removed, leading to the perpetuation of inflammation, we argued that SIRT1-HSF1-HSP axis might also be suppressed in atherosclerosis, which could be reversible by heat treatment (HT), the most powerful HS response trigger. $LDLr^{-/-}$ adult mice were fed on high-fat/high-cholesterol diet from the age of 90 days until the end of study (age of 270 days). After 120 days under atherosclerotic diet, the animals were submitted to either whole-body HT ($n = 42$; 40 °C) or sham ($n = 59$; 37 °C) treatment (15 min/session), under anesthesia, once a week, for 8 weeks, being echographically and metabolically monitored. Aortic expressions of SIRT1, HSF1, HSP27, HSP72 and HSP73 were progressively depressed in atherosclerotic animals, as compared to normal ($LDLr^{+/+}$; $n = 25$) healthy counterparts, which was paralleled by increased expression of NF-κB-dependent VCAM1 adhesion molecule. Conversely, HT completely reversed suppression of the above HS response proteins, while markedly inhibiting both VCAM1 expression and NF-κB DNA-binding activity. Also, HT dramatically reduced plasma levels of TG, total cholesterol, LDL-cholesterol, oxidative stress, fasting glucose and insulin resistance while rising HDL-cholesterol levels. HT also decreased body weight gain, visceral fat, cellular infiltration and aortic fatty streaks, and heart ventricular congestive hypertrophy, thereby improving aortic blood flow and myocardial performance (Tei) indices. Remarkably, heat-treated mice stopped dying after the third HT session (~ 8 human years), suggesting a curative effect. Therefore, evolution of atherosclerosis is associated with suppression of the anti-inflammatory and anti-senescent SIRT1-HSF1-HSP molecular axis, which is refreshed by chronic heat treatment.

Non-standard abbreviations: HS, heat shock; HSF1, heat shock transcription factor-1; HSP, heat shock protein; HT, heat treatment; NF-κB, nuclear factor transcription factors of the kappa light chain enhancer of activated B cells (κB) family; NLRP3, NLR [nucleotide-binding oligomerization domain (NOD)-leucine-rich repeat- and pyrin-domain (LRP) containing protein]-3 inflammasome; NO, nitric oxide; eNOS, endothelial NO synthase; SASP, senescence-associated secretory phenotype; SIRT1, nicotinamide adenosine dinucleotide (NAD^+)-dependent histone deacetylase of class III family sirtuin-1; VCAM1, vascular cell adhesion molecule-1.

* Corresponding author. Laboratory of Cellular Physiology, Department of Physiology, Institute of Basic Health Sciences, Federal University of Rio Grande do Sul, Rua Sarmento Leite 500, ICBS, 2nd floor, suite 350, Porto Alegre, RS, 90050-170, Brazil.
E-mail address: pauloivo@ufrgs.br (P.I. Homem de Bittencourt).

https://doi.org/10.1016/j.biochi.2018.09.011
0300-9084/

Journal of Cardiovascular Pharmacology Publish Ahead of Print
DOI: 10.1097/FJC.0000000000000617

CARDIAC

Copaiba oil attenuates right ventricular remodeling by decreasing myocardial apoptotic signaling in monocrotaline-induced rats

Cristina Campos-Carraro PhD[a], Patrick Turck MSc[a], Bruna Gazzi de Lima-Seolin MSc[a], Angela Maria Vicente Tavares PhD[a], Denise dos Santos Lacerda MSc[a]; Giana Blume Corssac MSc[a]; Rayane Brinck Teixeira PhD[a], Alexandre Hickmann BSc[a]; Susana Llesuy PhD[b]; Alex Sander da Rosa Araujo PhD[a]; Adriane Belló-Klein PhD[a].

[a]Universidade Federal Do Rio Grande Do Sul, Porto Alegre - RS - Brasil, [b]Universidad de Buenos Aires – Argentina.

Short title: Copaiba oil reduces myocardial apoptosis

Corresponding author:

Adriane Belló-Klein Ph.D.

E-mail address: bellklein@ufrgs.br

Universidade Federal do Rio Grande do Sul

Sarmento Leite, 500 – Bairro Farroupilha - Porto Alegre, Brasil - CEP: 90050-170

Telephone number: +55 (51) 3308-3621

Conflicts of Interest

The authors declare that they have no conflict of interest.